https://ntrs.nasa.gov/search.jsp?R=19690029234 2020-02-29T19:22:29+00:00Z

escribed above may be processed by Code UST in accordance with the abc

Name and Office Code

ECHNICAL MONITOR

E REVERSE SIDE OF GREEN COPY FOR GENERAL POLICY REGARDINC

UST USE ONLY

er 101932 NASA - TMX Number

NASA CR 101932

THE Marquardt CORPORATION VAN NUYS, CALIFORNIA

A-1080

FINAL REPORT

VOLUME 4

APOLLO SM-LM RCS ENGINE DEVELOPMENT PROGRAM SUMMARY REPORT

Contract NAS 9-7281

EDITED BY:

J. F. Foote
Project Engineer

APPROVED BY:

D. C. Sund
Senior Project Engineer

L. R. Bell, Jr.
Chief Engineer

C. A. Kerner
Program Manager

TABLE OF CONTENTS

VOLUME 1

Preface

Chapter 1 Marquardt R-4D Engine Development

VOLUME 2

Chapter 2 Thermal Management

Chapter 3 Space Ignition Characteristics

Chapter 4 Gas Pressurization Effects

Chapter 5 Contamination Control

Chapter 6 System Dynamic Effects

VOLUME 3

Chapter 7 Structural Design

Chapter 8 Material Selection

Chapter 9 Propellant Valve Design

Chapter 10 Injector Design

Chapter 11 Thrust Chamber Design

VOLUME 4

Chapter 12 Test Facilities and Instrumentation

Chapter 13 Test Data Analysis

Chapter 14 Flight Test Experience

Chapter 15 Reliability

CHAPTER 12

TEST FACILITIES & INSTRUMENTATION

BY

C. F. WATSON

TABLE OF CONTENTS

		Page
I.	INTRODUCTION	12-1
II.	SUMMARY	12-3
III.	ENGINE FIRING TEST FACILITIES	12-7
	Altitude Performance Test Cells	12-7
	Multi-Altitude Space Ignition Facility	12-15
	System Test Cells	12-22
IV.	COMPONENT AND ENGINEERING FUNCTION TEST AREAS	12-31
	Controlled Area No. 1 (CA-1)	12-31
	Controlled Area No. 2 (CA-2)	12-31
	Space Simulator Environmental Chamber	12-33
	AF-MJL Vibration Laboratory	12-33
	General Services	12-40
V.	MEASUREMENTS	12-43
	Thrust Measurement	12-43
	Propellant Flow Measurement	12-52
	Temperature Measurement	12-54
	Pressure Measurement	12-56
VI.	TEST PROCESS CONTROL AND DOCUMENTATION	12-57

LIST OF ILLUSTRATIONS

Figure Number	Title	Page
1	AF Marquardt Jet Laboratory, Van Nuys	12-2
2	R-4D Engine Firing Activity Chart	12-4
3	Test Sequence	12-6
4	Facility Schematic Altitude Engine Performance Test Cell	12-9
5	Cell No. 1	12-10
6	Engine Installation	12-11
7	Oxidizer Propellant System	12-12
8	Cell No. 1	12-13
9	Cell No. 1	12-16
10	Pad G Exhaust Flow Schematic	12-18
11	TMC Multi-Altitude Space Simulation Facility	12-19
12	Pad G Engine Installation	12-20
13	ATL Pad "G" Performance	12-21
14	Test Cell 9	12-23
15	Cell 9 Schematic	12-24
16	Cell 9 Predicted Performance	12-25
17	Magic Mountain Laboratory	12-26
18	Test Stand M-3	12-27
19	Signal Conditioning and Recording Equipment	12-28
20	Controlled Area No. 1-Engine Thrust Stand Build-up	12-32
21	Facility Schematic Controlled Area No. 2	12-34
22	Controlled Area No. 2	12-35
23	CA-2 Stand 2.3 Flow Collector	12-36
24	CA-2 Laminar Flow Stand	12-37
25	Lunar Orbiter Qualification Test Cold Soak Test Installation	12-38
26	Vibration Laboratory Equipment Schematic	12-39
27	Vibration Laboratory Ling 335 and MBS-100 Shakers	12-41
28	Vibration Laboratory Sine Wave & Random Control Console	12-42
29	Qualification Engine Build-up	12-45
30	Pulse Thrust Measurement System Block Diagram	12-48
31	Thrust Stand Frequency Response Compensator	12-49
32	Thrust Stand System Frequency Response with Compensator	12-50
33	Columbium Chamber Evaluation Using XR Film	12-55
34	Typical Controls Established for Engine Cell Firing Acceptance Test	12-59

I. INTRODUCTION

The successful flight performance of the Marquardt R-4D, 100# thrust bi-propellant rocket engine in space applications is the result of exhaustive ground test programs. The proper simulation of space environment and engine performance measurements in the ground test programs made it possible to accurately predict the engine space performance and engine reliability. Telemetry and tracking data from the 100% successful Lunar Orbiter space flights showed that the R-4D engine produced space thrust and specific impulse within one percent of the ground test values. The R-4D engine, used on the Apollo Service Module, Lunar Module and the Lunar Orbiter vehicle, has fired in space more than 5.68 hours with over 373,418 starts with complete success. During the Lunar Orbiter mission, the engine was restarted after a period of 127 days in the vacuum space environment. The above actual successful space operation of the R-4D engine verifies the quality of the ground test facilities, the measurement technique, and the test methods and controls used in the ground test programs.

The R-4D engine ground test programs, development, qualification and acceptance tests, were conducted exclusively within the Air Force-Marquardt Jet Laboratory at Van Nuys, California (AF-MJL-VN), see Figure 1. Within this Van Nuys test complex is one of the largest power systems test facilities of its kind in the world. Extensive laboratories for the development of materials, structures, controls, instrumentation and space power systems are in everyday use. The liquid rocket portion of this laboratory consists of a $21 million investment spread over a 10-acre test site. This portion of the laboratory includes rocket engine altitude test cells, the ultra high altitude engine ignition test cell, the space environmental simulation test chamber, the simulated fluid flow benches and the vibration, acceleration, shock, structures, electronics, chemistry and standards laboratories. The well equipped Air Force-Marquardt Jet Laboratory, together with the trained operating test personnel and the nedessary testing controls are responsible for the success of the R-4D engine program to date.

The ground test facilities, measurement technique and Test Process Control methods used in the development, qualification and production acceptance tests of the R-4D engine are described on the following pages.

NEG. 4404-64

AF-Marquardt Jet Laboratory - Van Nuys

Figure 1

II. SUMMARY

The history of the test facilities used on the Apollo Program is directly related to the history of the engine. The initial development tests were run in a sea level test stand in the North Test Area at Van Nuys using basic minimum measurement equipment. As the development program progressed and the spacecraft and engine environmental condition were better defined, the test requirements and test facilities became more sophisticated. The need for precise measurement of thrust, flow and other parameters at a wide variety of engine operating conditions and environmental conditions required the development of facilities along with new and unique test equipment, new test techniques and more rigid test controls and documentation than were required in the past for less precision propulsion devices. Much has been learned about the propellants, the effects of pressurant gas saturation on combustion, the products of combustion, the effects of altitude and other space environments on ignition, and cleanliness requirements and the facilities today reflect this knowledge. A brief history of the major facilities used on the program in calendar sequence is discussed below and shown on a schedule in Figure 2.

A major facilitiy refurbishment effort preceded the sea level development testing of the Apollo engine which started in July, 1962 in the North Test Area facility. This facility was renovated and set up with new propellant system, thrust measuring systems and instrumentation for this test program. The North Test Area was used for testing until December, 1962. Additional sea level tests in Test Cell 1 were running concurrently with the NTA testing. Direct connect altitude testing started in Precision Rocket Laboratory, Pad "G", in July 1962.

A completely new altitude test facility, Cell 6, was placed in operation in January, 1963 and a major portion of the development tests accomplished here. To meet the heavy load, an additional test cell, Cell 1, was set up for altitude testing and placed in operation in December, 1963.

To investigate the problems associated with space engine ignition, a third stage steam ejector was installed in Pad G to produce simulated altitude pressures at ignition of 0.008 psia (195,000 feet). Testing at this altitude pressure started in February, 1966. To further evaluate the space ignition characteristics, a large (9000 CFM) blower and liquid nitrogen cold trap were added to the three stages of steam ejector to produce simulated altitude pressure to 0.0002 psia (257,000 feet) during July, 1966. The multi-attitude capability, firing the engine in the up, horizontal, or down position, was also added to Pad G at this time.

The capabilities of all test facilities are continually being upgraded and added to. Equipment for saturating the propellant with pressurant gas was installed in Cell 1 in June, 1966 and in Pad G in July of 1966. Larger propellant pulse tanks (10 gallon) with saturation equipment and temperature conditioning, were installed in Cell 1 in November of 1966.

ENGINE FIRING ACTIVITY CHART

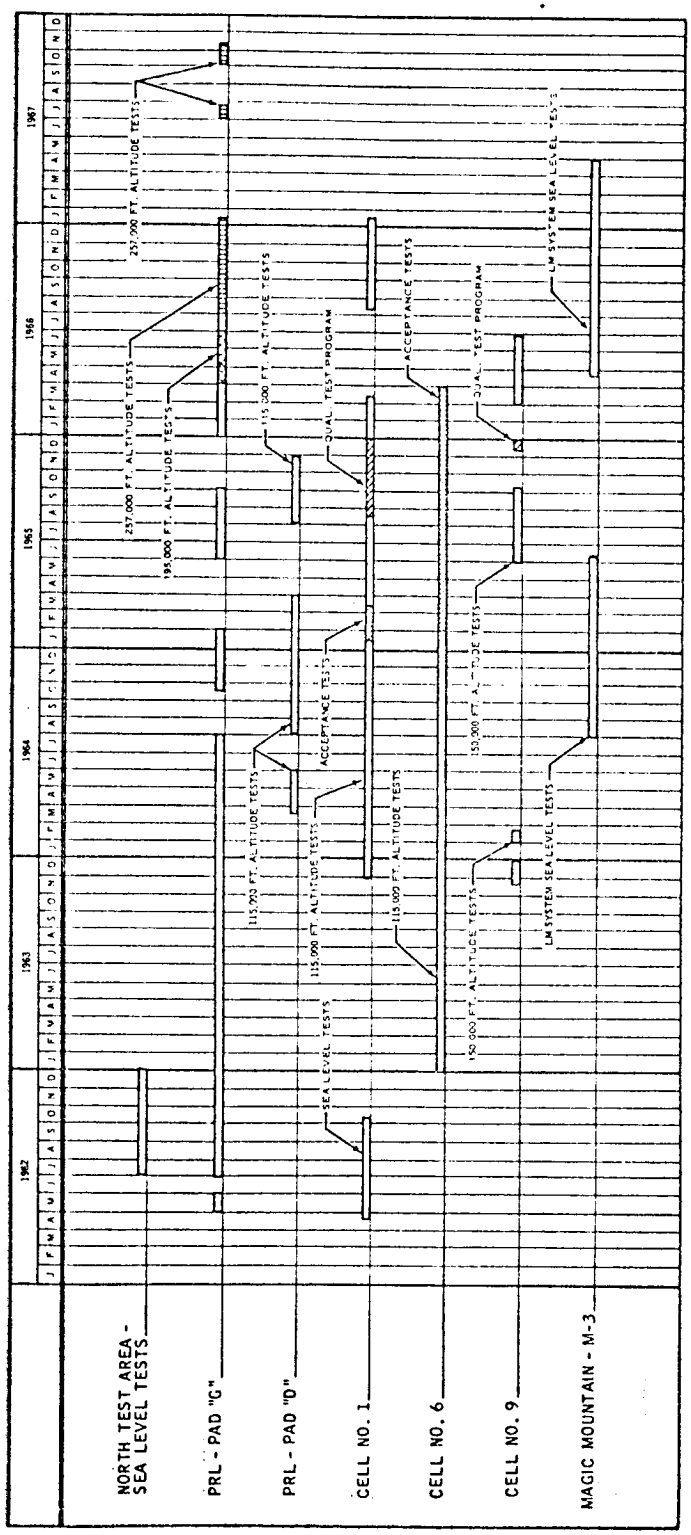

Figure 2

In September, 1964, all simulated propellant testing was centralized in a 1200 square foot test area called Controlled Area No. 2. As it is necessary to bring engines which have been fired into this room, engines which are dirty in the clean room context, the area was constructed and is maintained as a Federal Standard, Class 100,000 clean room. Individual work stations located within this area are maintained at the Federal Standard 209, Class 100 cleanliness levels. These individual work stations are used for flow and leak checking and trimming critical engine components, subassemblies and complete engines. In all, three types of work stations were provided; (1) a flow and leak check station for testing engine components and subassemblies; (2) flow distribution test stand for testing head and valve subassemblies and stations for installing filters on the engine inlet and accomplishing miscellaneous mechanical work.

Figure 3 lists the component, subassembly and engine tests which were initially performed in the area. With experience, it was learned that three of the six tests were unnecessary and actually resulted in rejection of satisfactory parts. Today, the only tests performed are the solenoid valve test, the pre-firing test of the head and valve assembly and the post firing test of the engine assembly. In operation today are two Class 100 laminar flow test stands for flow and pressure tests, one flow distribution stand, one Class 100 work bench and peripheral equipment. With this equipment, approximately 25 engines per week can be processed through the area.

In the early stages of testing, many propellant simulating fluids were considered. Distilled water is now being used because of its basic advantages of easy handling, safety, known and consistent characteristics, low cost and ready availability. Its major disadvantage is that it is not completely compatible with the current generation of fuels and oxidizers. This has been overcome by introducing into the test sequence a thorough purging and vacuum drying operation following each water flow test. The water flow systems, of which there are two, are supplied from stainless steel tanks, coated internally with a proprietary nylon material. The tanks are pressurized with high purity, filtered, gaseous nitrogen. To minimize nitrogen entrainment, pressure is applied only during actual test periods and a vacuum pressure of about 0.5 psia is maintained at all other times. The water is obtained in bulk from a commercial vendor in stainless steel tank trucks and transferred to the system tanks through a nominal 5 micron stainless steel filter. All systems are stainless steel throughout and are internally cleaned to LOX standards. Final filtration as low as one micron, depending upon requirements, is provided. As originally constructed, several components in the system caused trouble, primarily from corrosion and leakage. It was difficult to locate precision gages and regulators which were completely non-corroding and these are now purchased on special order. The usual difficulties in assembling dry stainless steel fittings were encountered. Solutions have included the elimination of pipe fittings, polishing flare fittings and the use of crush washers. In general, it has been found that assembling and operating water flow systems require the same care and rigid quality control as propellant systems if valid data are to be obtained and engine contamination minimized.

APOLLO R-4D TEST SEQUENCE SIMULATED PROPELLANTS

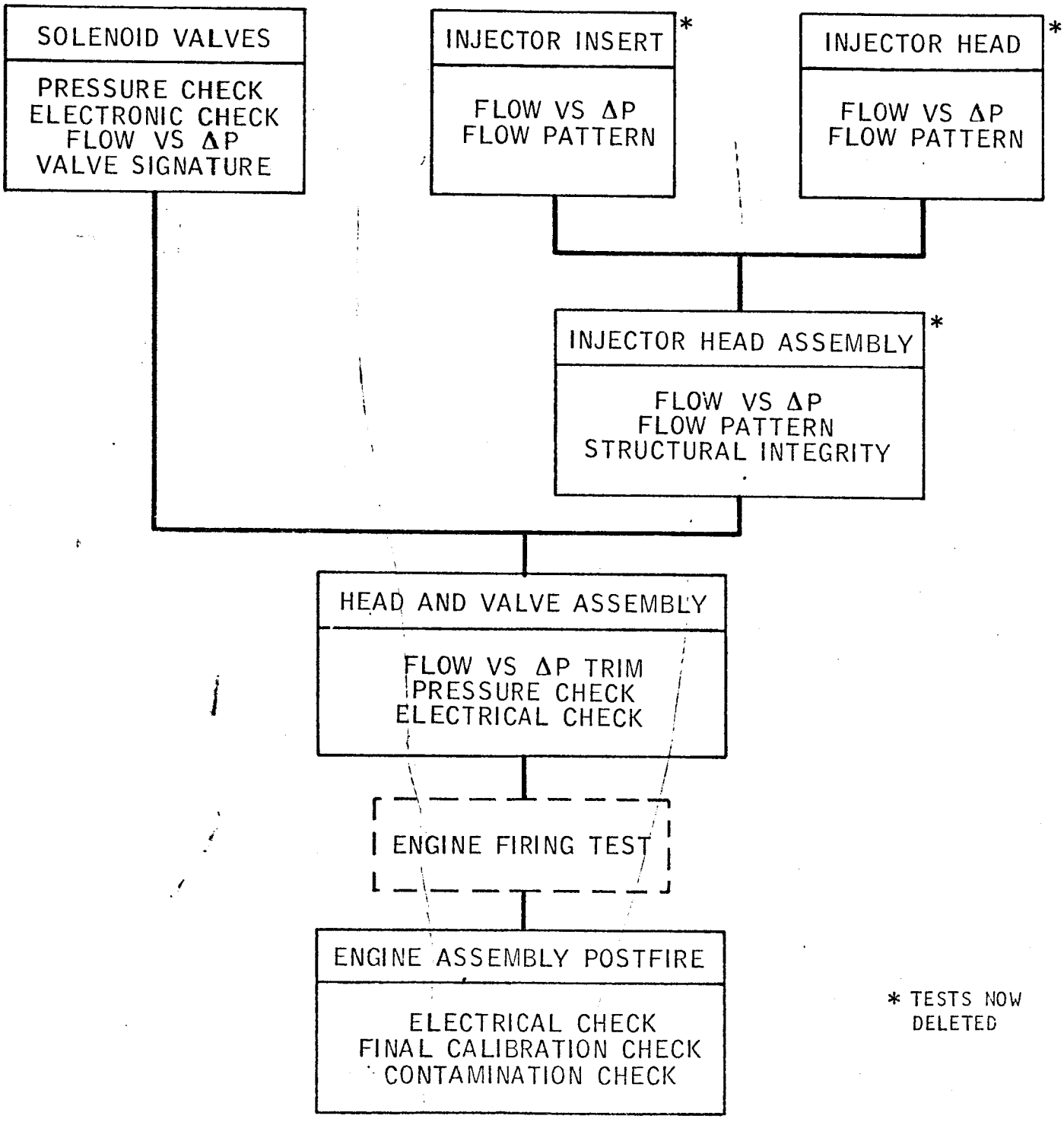

* TESTS NOW DELETED

Figure 3

Also in September, 1964, Controlled Area No. 1 was placed in operation. This Federal Standard 209, Class 100,000 room is used for installation of the R-4D engine on the thrust stand prior to engine firing and for purging the engine of residual propellants and removal from the thrust stand following an engine firing.

Testing Philosophy

A maximum amount of functional testing of the components and the engine is performed using distilled water as a substitute for propellants in the manufacture of the R-4D engine, as previously described. Critical engine components, subassemblies and complete engines are water flow tested and trimmed during the engine assembly process. The actual performance of the engine is determined by firing the engine at simulated space conditions; altitude pressure propellant inlet pressure and engine and propellant temperatures. In many of the performance tests the propellants are saturated with pressurant gas.

Each testing process on the R-4D engine is closely controlled. All elements of the test, test personnel, test facilities or test setups, and test procedures, are certified prior to the test. Certification consists of writing a detailed test procedure, training and testing the operating personnel on the (particular) requirements and facility operation and by actually running a test on a referee test item. If all elements of the test function as previously specified, the facility is certified and ready for testing.

Engine cleanliness is a prime requisite in the manufacture of the R-4D engine and is rigidly controlled. The components and engine are immaculately cleaned during the engine fabrication and this cleanliness maintained during all phases of testing. All materials which flow through the engine, propellant, helium, nitrogen, distrilled water, Freon, etc., are procured to rigid standards and pass through a nominal 5 micron filter prior to passing through the engine. In addition, a "piggyback" filter, nominally 15 micron, is installed directly on the engine inlets for all testing not conducted in a Class 100 clean area.

III. ENGINE FIRING TEST FACILITIES

Altitude Performance Test Cells

The altitude engine performance test cell, Cell 1, Cell 6, and Pad D are designed specifically for performance testing of the R-4D engine operating in both steady state and pulsing modes. In addition to an altitude simulation in excess of 115,000 feet, the propellant is supplied to the engine at precisely controlled pressure and temperature conditions. Cell 1 also has the capability of supplying propellant saturated with pressurant gas.

Each test cell is a self-contained test complex with all of the various systems, controls and data gathering equipment completely integrated to produce precise, reliable, meaningful data on the performance of the R-4D engine. A

reinforced concrete structure houses the altitude test chamber, the propellant system, the environmental temperature control system and the altitude system. The control room, containing the engine and facility controls and the recording instrumentation, is located adjacent to the concrete structure. A schematic of the major elements of the altitude engine performance test cell is shown in Figure 4. Figure 5 is a picture of the Cell 1 complex.

The test engine is installed on a thrust stand in a Class 100,000 clean room. This thrust stand engine assembly is then installed on a large seismic mass, which is mounted on vibration isolation pads, within the 5' diameter altitude chamber, refer to Figure 6, which is connected to the ejector system to produce the simulated altitude pressure.

The simulated altitude pressure is obtained by using a water cooled no flow diffuser, a tandem steam ejector and a single stage steam ejector as shown on Figure 4. The no flow diffuser, test engine combination provides one stage of the exhauster system. The tandem ejector provides this stage of exhauster when the engine is not firing. The exhaust products from the altitude producing system are scrubbed of contaminant prior to release into the atmosphere.

Propellant is normally supplied to the engine from the pulse tank or sight tube assembly, reference Figure 7 for schematic of oxidizer system. The pulse tank is used for steady state engine firings and the sight tube assembly for pulse firings. Both of these systems supply temperature conditioned propellants. Ambient temperature propellants can also be supplied to the engine from the propellant storage tanks. The storage tanks are normally used to fill the pulse tanks. The basic propellant system parameters are:

	Cell 1	Cell 6	Pad "D"
Pulse tank capacity, gallons.	10	2	2
Propellant supply pressure, psia.	1440 max.	1440 max.	1440 max.
Propellant temperature range, °F.	20 to 130	20 to 130	20 to 130
Propellant storage capacity, gallons of each propellant.	110	110	30

The pressurant gas content of the propellant influences the performance of the engine. Marquardt has pioneered the effects of propellants saturated with pressurant gas and has established procedures for degassing and saturating the propellants. Extensive tests have been conducted to determine the gas content of the propellants at various temperature conditions, stirrer speed, and stirring time for the particular tank design used at TMC. The stirring method of saturating the propellants was selected to allow the pressurant gases to diffuse into the

FACILITY SCHEMATIC

ALTITUDE ENGINE PERFORMANCE TEST CELL

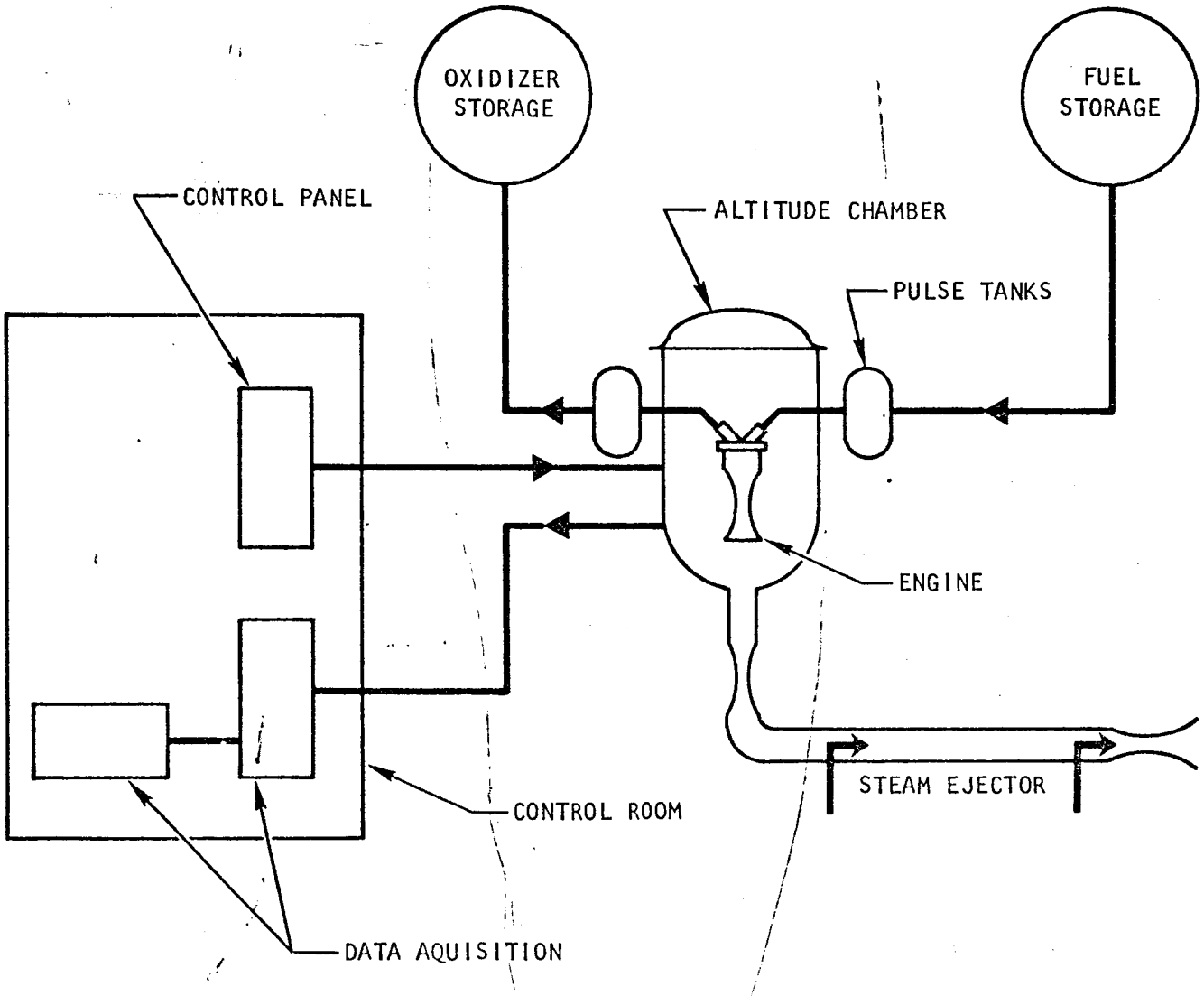

Figure 4

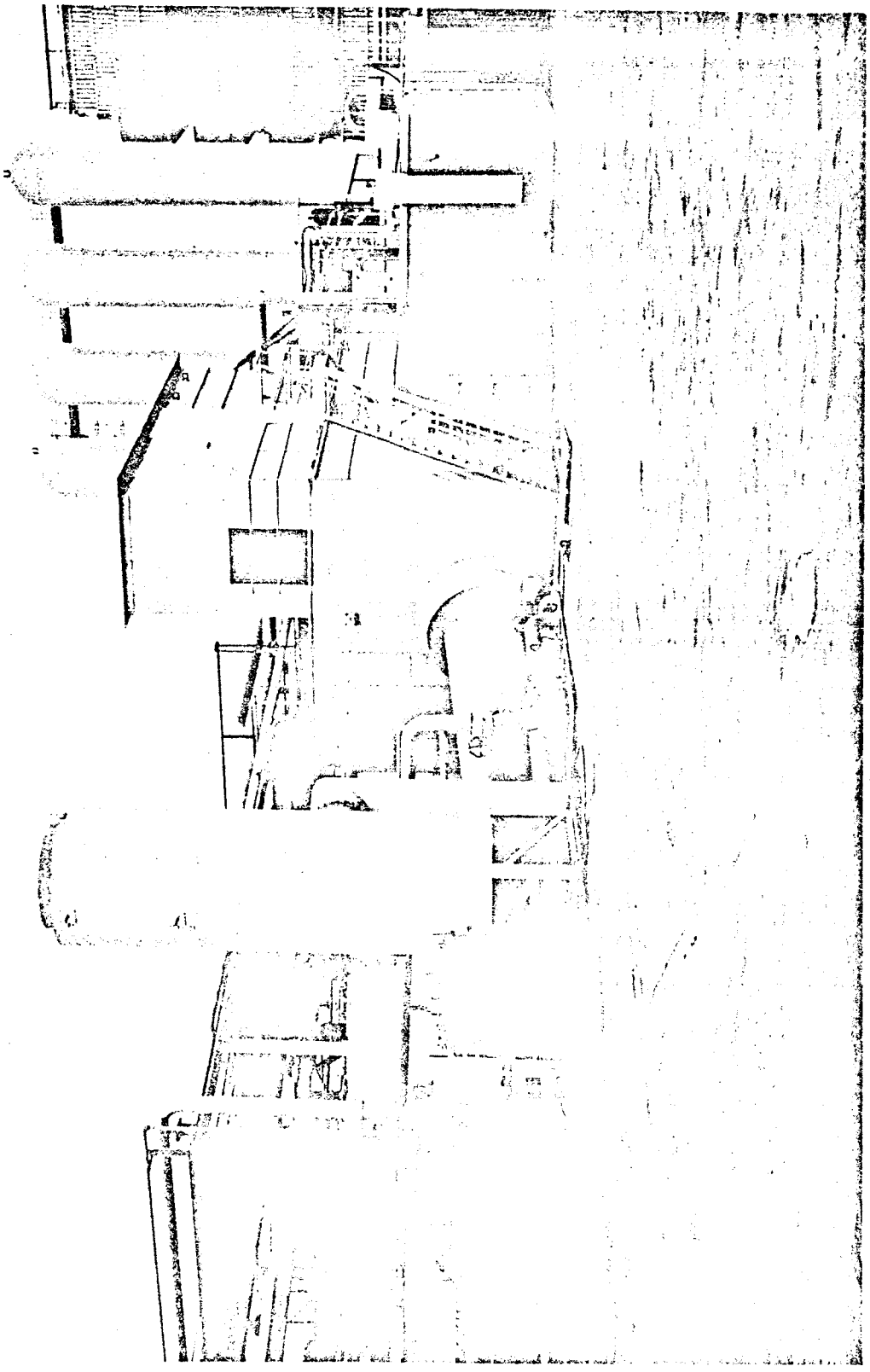

NEG. 8364-1

Cell No. 1

Figure 5

ENGINE INSTALLATION

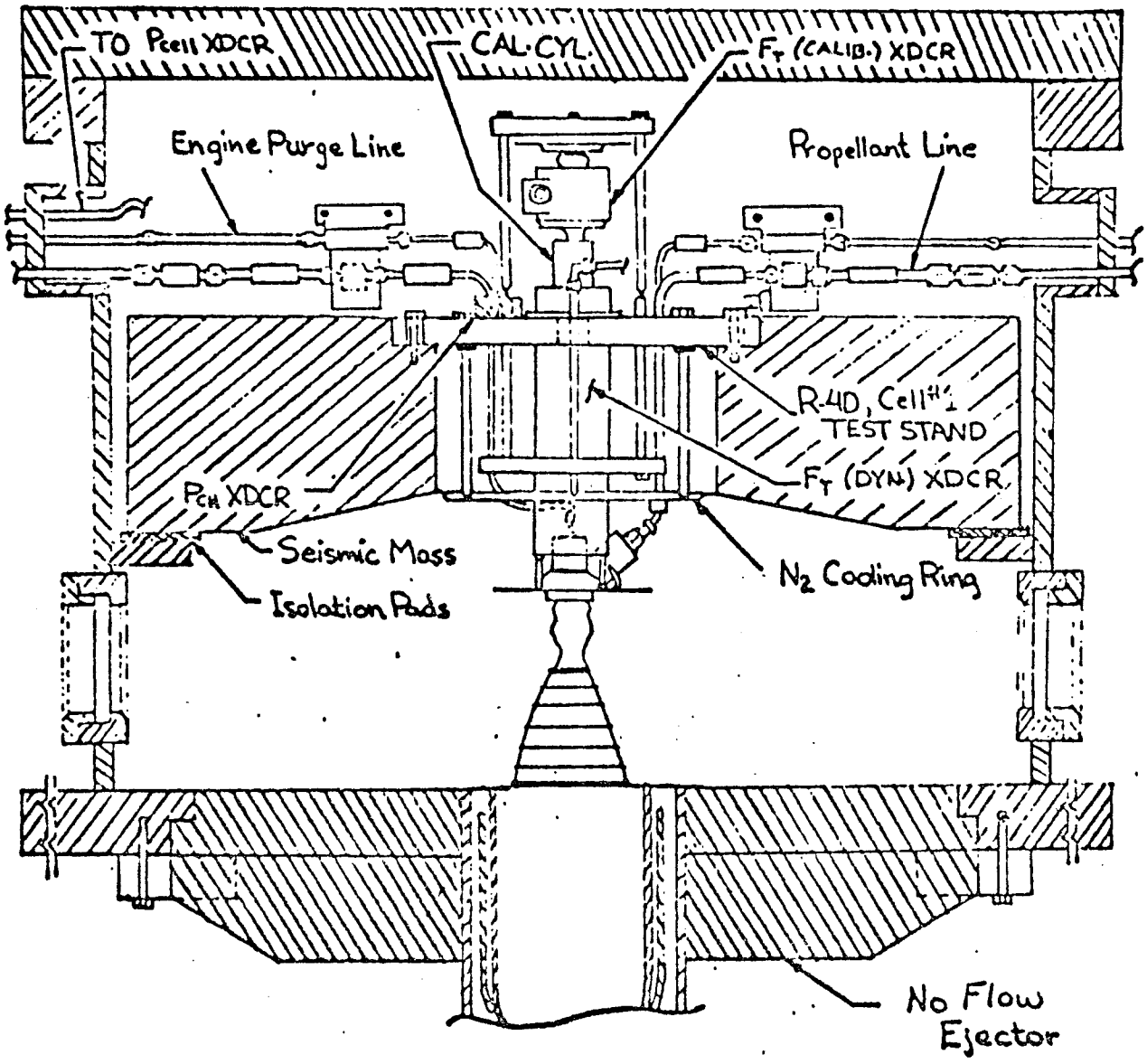

Figure 6

BASIC ALTITUDE ENGINE PERFORMANCE TEST CELL

OXIDIZER SYSTEM

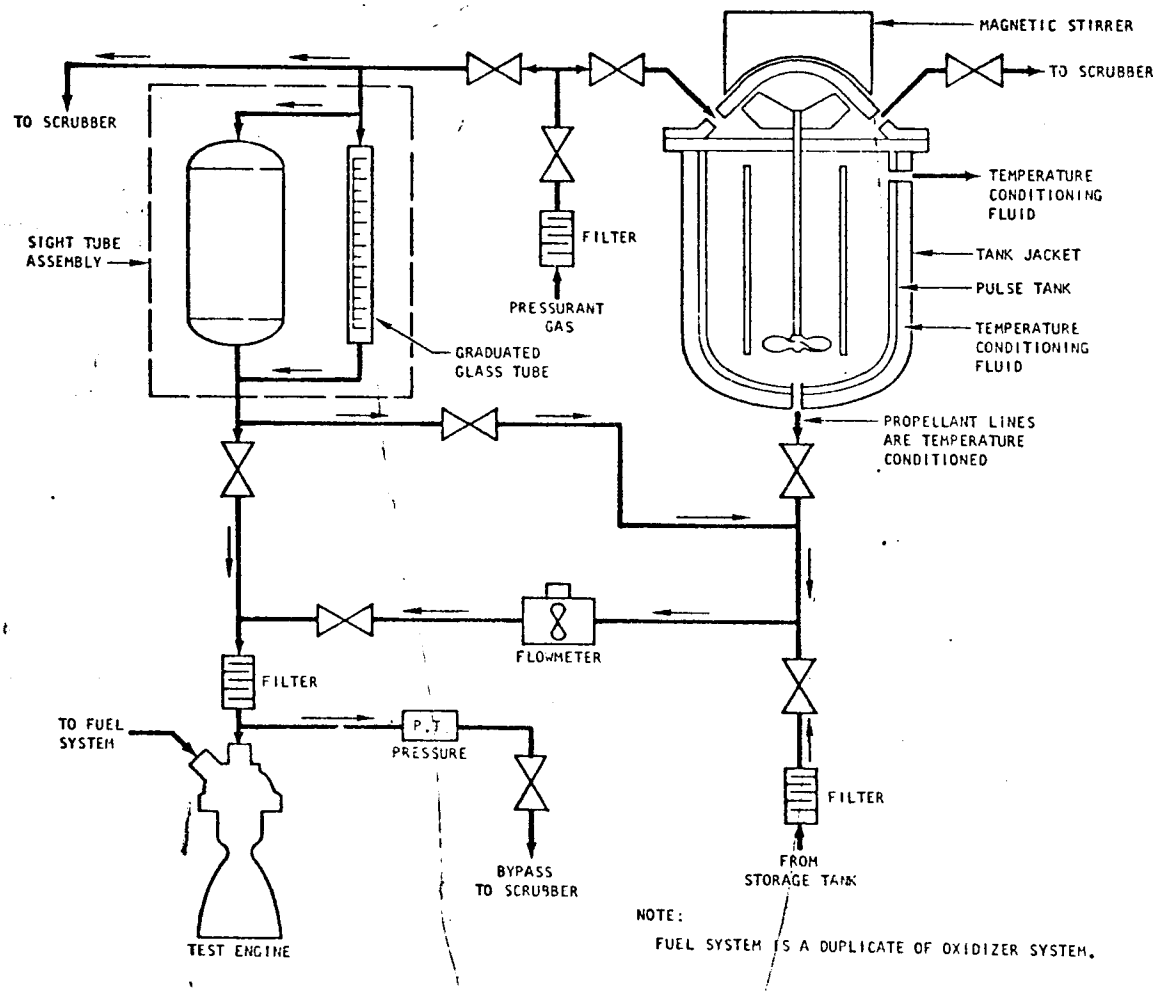

NOTE:
FUEL SYSTEM IS A DUPLICATE OF OXIDIZER SYSTEM.

Figure 7

propellants insuring control of the process. Other methods of saturation, such as bubbling gas through the propellants, can result in super-saturation and/or free gas in the propellants.

In addition to precise temperature, pressure, gas saturation of the propellants, the requirements for (1) priming and purging of the engine, (2) measuring pulse and steady state flow rates, (3) maintaining propellant system cleanliness, (4) sampling the propellant for chemical analysis, (5) making in-cell flowmeter checks, and (6) neutralizing all dumped propellant system effluents makes the propellant system rather complex. The effects of the propellant system on other measured parameters, such as the engine inlet line effects on thrust measurement, must also be considered in the design of the system.

Temperature conditioning of the propellants is accomplished primarily by circulating a temperature conditioned fluid, ethylene glycol, through jacketed run lines and propellant tank jackets. Propellant supply pressures are set by controlling the pressure of the pressurant gas.

The engine is primed by evacuating the supply lines prior to admitting the propellants. Purging of the engine is a process of flowing pressurant gas through the engine and propellant supply lines and then evacuating the lines. The propellant and purge gas dumped from the system pass through a scrubber system prior to release to the atmosphere. A 20% solution of sodium hydroxide is used in the oxidizer scrubber and a 4% solution of sodium hypochlorite in the fuel scrubber.

Extreme care is taken to maintain the cleanliness of the engine. All elements of the propellant system are initially cleaned to rigid standards, MPS 209. The propellants and pressurants used must meet the appropriate Military Specifications, i.e., MIL-P-27401B for nitrogen and MIL-P-27407 for helium. Filters are installed throughout the propellant system to remove any possible contaminant. The propellants and pressurants flow through 5-15 micron filter prior to entering the engine supply lines. In addition, a 15-30 micron filter is installed directly on the engine inlet to further insure contaminant removal.

The engine environmental temperature in Cell 1 can be controlled from -250°F to +250°F. In some particular tests the temperature of the various parts of the engine, valves, head and combustor, were temperature conditioned individually. This environmental conditioning is accomplished by flowing temperature conditioned gaseous nitrogen directly on the engine. Liquid nitrogen and steam condition two sources of gaseous nitrogen. By modulating the quantity of hot or cold nitrogen supplied for engine conditioning, engine temperatures can be accurately controlled.

The engine and facility controls are located on one control panel, see Figure 8. The steam ejector and engine environmental temperature controls are located on the far left of the panel. The propellant system controls are centrally located. The basic propellant system schematic is incorporated directly on the

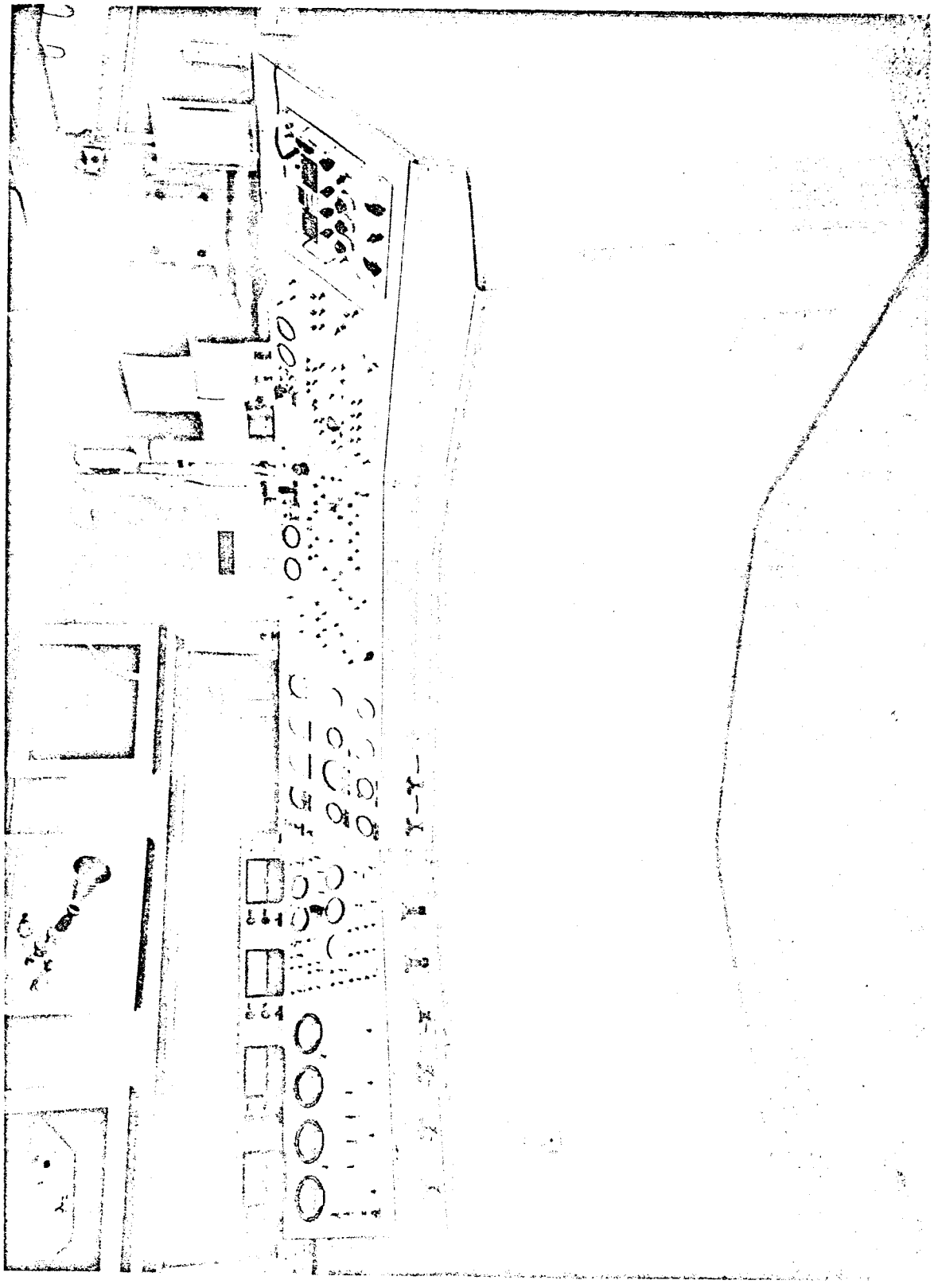

NEG. 8364-8

Cell No. 1

Figure 8

control panels. The engine control pulser is located on the far right of the panel.

The Marquardt designed, Model 14, pulser is a transistorized device which allows the operator to readily preestablish the length of each engine firing, off time between firings and total number of engine firings desired. Power supplied to either the fuel or oxidizer valve can be delayed to obtain a fuel or oxidizer lead. The pulser can also be driven from an external source such as a tape unit. Switches on the pulser allow operation of the direct or automatic engine valve coils and the individual operation of the fuel and oxidizer valves.

The data acquisition system is located in the control room adjacent to the engine and facility control console, see Figure 9. A 36-channel oscillograph and some 20 strip chart recorders are available for recording data. Signal conditioning equipment is available for 12 pressure channels, 24 temperature channels and 5 flow channels.

There are also several specialized instrumentation calibration and signal conditioning systems located within the cell. The thrust system is a typical example and is covered in detail in the thrust measurement section of this report.

Multi-Altitude Space-Ignition Facility

The absolute simulation of space pressure with a rocket engine firing during earth ground testing is virtually impossible. One pound of engine exhaust gases, approximately a 3-second firing on the R-4D engine, would occupy a space of some 13,000,000 cubic feet at a 10 microns pressure. It is evident, therefore, that a tremendous pumping system capable of producing the extremely low pressures would be required to fire even the 100 pound thrust engine at steady-state conditions. The purpose of the extremely low pressure, space, facility is actually to determine the engine ignition characteristics. Performance characteristics, such as Isp and impulse bit, can be obtained at a cell pressure sufficient to fill the engine nozzle, 40:1 on the R-4D engine. To determine the ignition characteristic of the engine, the cell pressure must approach space conditions prior to ignition and must have sufficient pumping capacity to maintain a choked condition at the throat of the test engine during the engine firing cycle including the residual propellant evaporation time period. The low initial pressure simulates the space conditions at ignition and the rapid cell pressure recovery produces the same effect on propellant residue in the chamber as encountered in space. TMC has a facility, Pad G of the Precision Rocket Laboratory, designed specifically for ignition testing of the R-4D engine at simulated space conditions.

The Pad G facility is capable of firing an R-4D engine at a simulated space pressure of 10 microns, approximately 50 miles altitude, and recovering to the simulated space pressure in less than 100 milliseconds. The actual recovery time is somewhat dependent upon the propellants or rather the propellant residue remaining in the combustion chamber following an engine firing. The cell pressure recovery time is also dependent upon the test section volume and the pumping capacity. During the design phase of this facility the chamber volume and the pumping

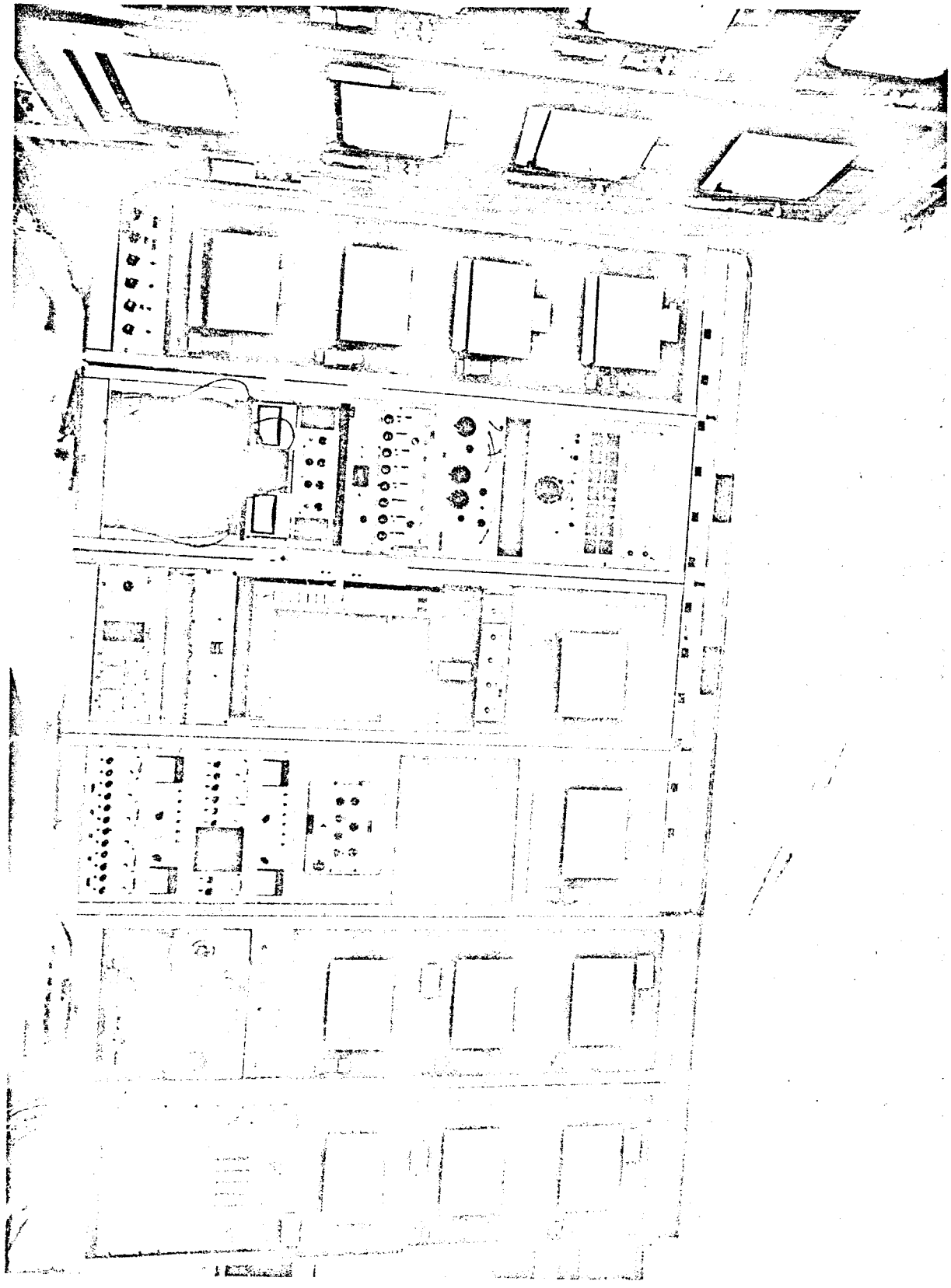

NEG. 8364-9

Cell No. 1

capacity were carefully evaluated to insure the 100 millisecond recovery time.

The engine can be fired in any attitude; engine exhaust plume up, down or horizontal. The space temperature is simulated by shrouding the engine combustor and bell with an LN_2 cold wall. The internal portions of the engine, combustor and engine throat, can be viewed during the engine firing by closed circuit TV or movie camera. The test engine is installed within a chamber which is directly attached to the rotatable test section. The engine exhaust gases empty into a large LN_2 cold trap which is connected to a 9000 cfm Roots blower backed by three steam ejector stages.

The Pad G exhauster system is shown schematically on Figure 10 and shown pictorally on Figure 11. A typical engine installation in the test chamber is shown in Figure 12. The Pad G cell pressure rise and recovery time with a 100# engine firing is shown on Figure 13.

The Pad G propellant system is very similar to the engine performance test cells. The propellant pressure and temperature are precisely controlled and propellant saturation is available. The engine firing time is limited to two seconds so that the 2-gallon propellant tank is adequate for long test periods.

The products of combustion, as well as raw fuel and raw oxidizer are frozen out in the LN_2 cold trap. Due to the explosive hazard of the frozen engine exhaust products, the amount of material that can be accumulated in the cold trap is limited. This limit for nitrogen tetroxide and hydrazine products is 1.2 pounds of unburned propellant that can be accumulated in the cold trap and is the amount that could detonate without causing serious damage to the cold trap. The cold trap is designed so that it can readily be steam cleaned to remove the accumulated propellant following a series of engine firings.

A large control room is located adjacent to Pad G so that the complete test area can be visually observed. The control room contains provisions for remotely controlling the test facility, the test item, automatically controlling the propellant and test item temperature, and recording the test data.

The normal complement of recording instrumentation includes a 36-channel oscillograph, twenty strip chart recorders, a 100-channel digital data system, a 14-channel analog tape recording system and oscilloscopes as required for the particular test. The 100-channel digital system samples the number of channels to be recorded at a rate of 20 KC. The 14-channel analog system is capable of recording transducer ouptut signal from DC to 600 KC.

In order to record the maximum chamber pressure, a peak meter is used. This instrument is sensitive to pressure changes of 10 microseconds or greater and is normally used in conjunction with a Kistler chamber pressure transducer flush mounted in the engine combustion chamber.

PAD G EXHAUST FLOW SCHEMATIC

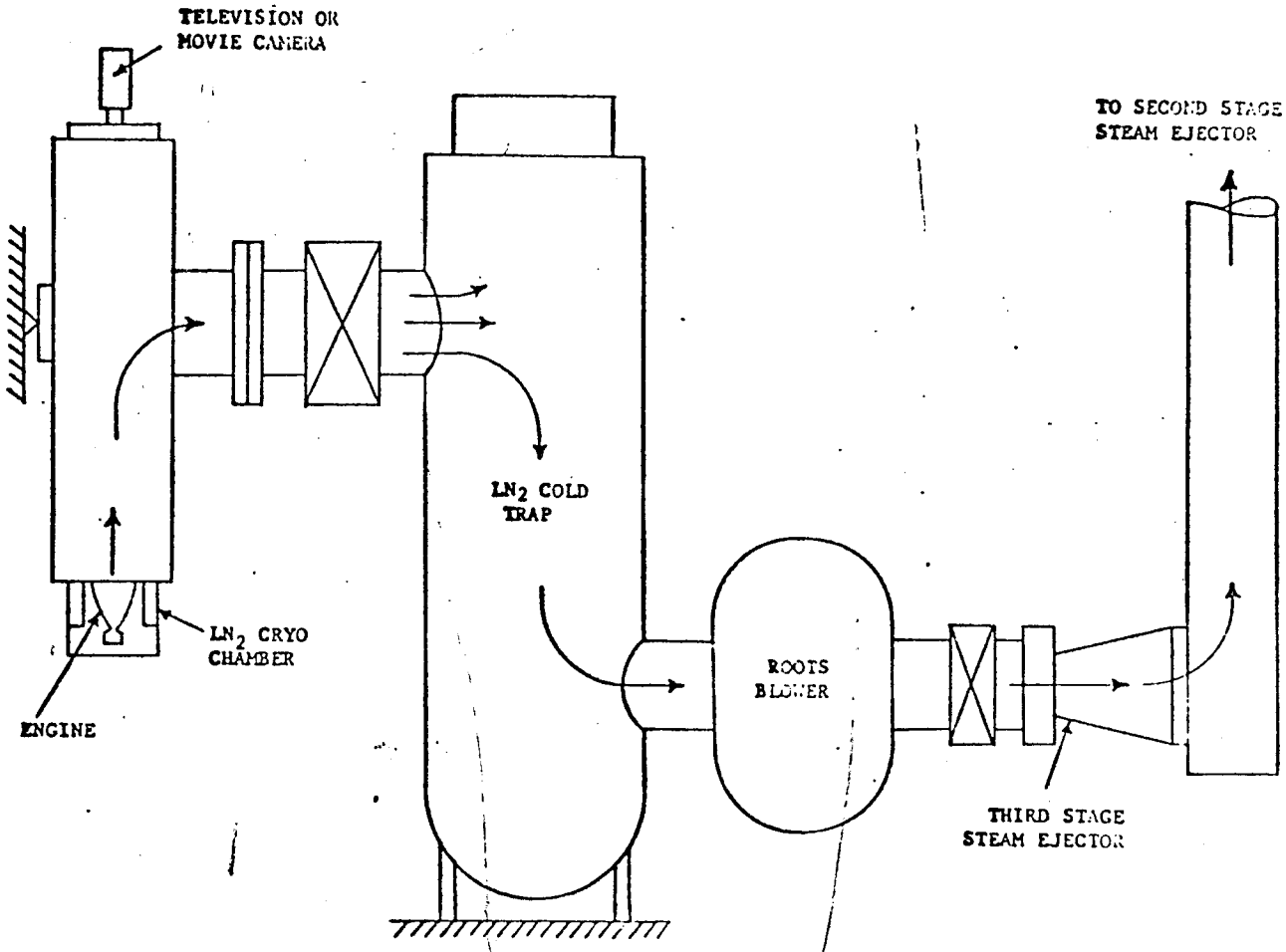

Figure 10

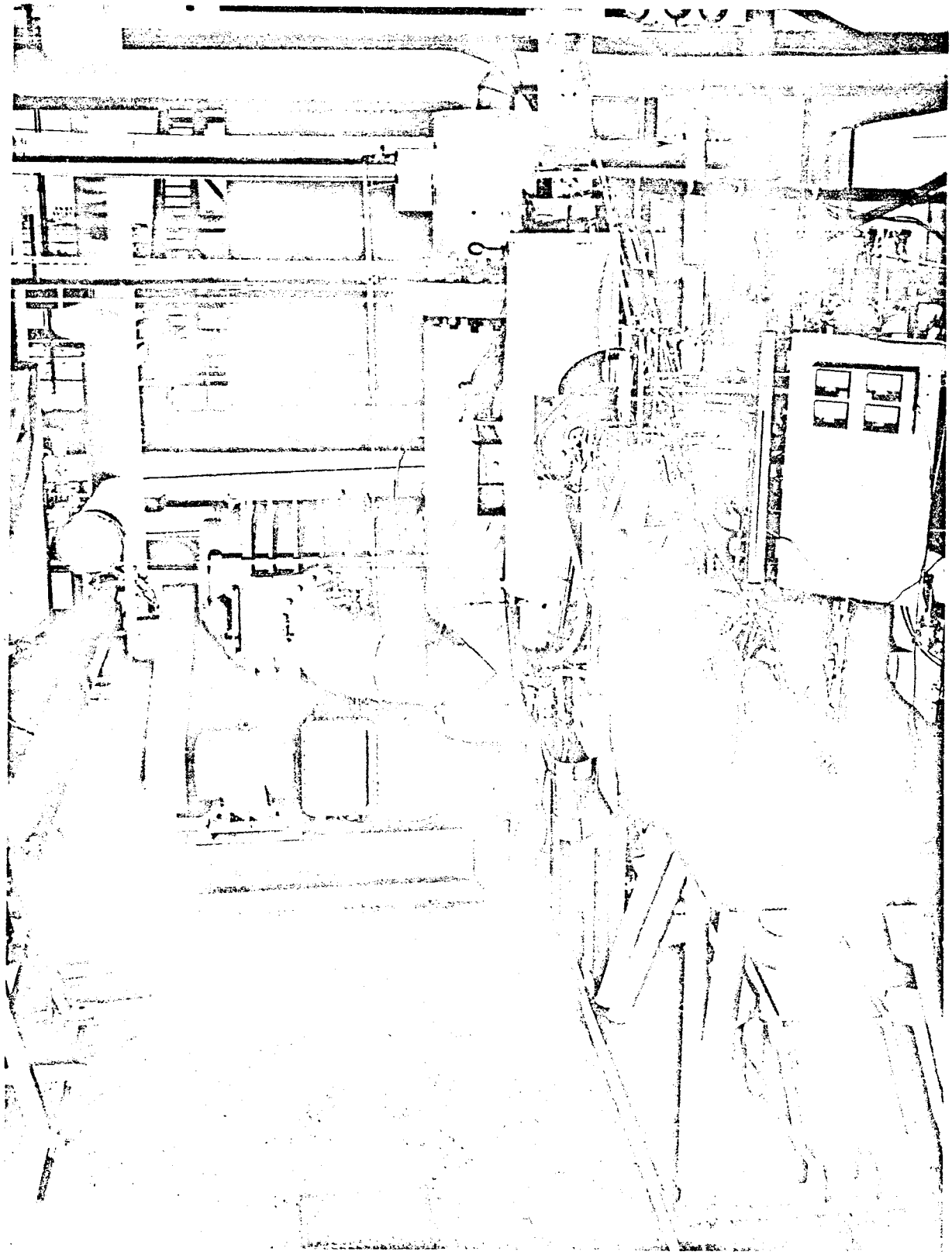

NEG. T3472-2

IMC Multi-Attitude Space Simulation Facility

Figure 11

ENGINE INSTALLATION
TEMPERATURE INSTRUMENTATION
SCHEMATIC - PAD G

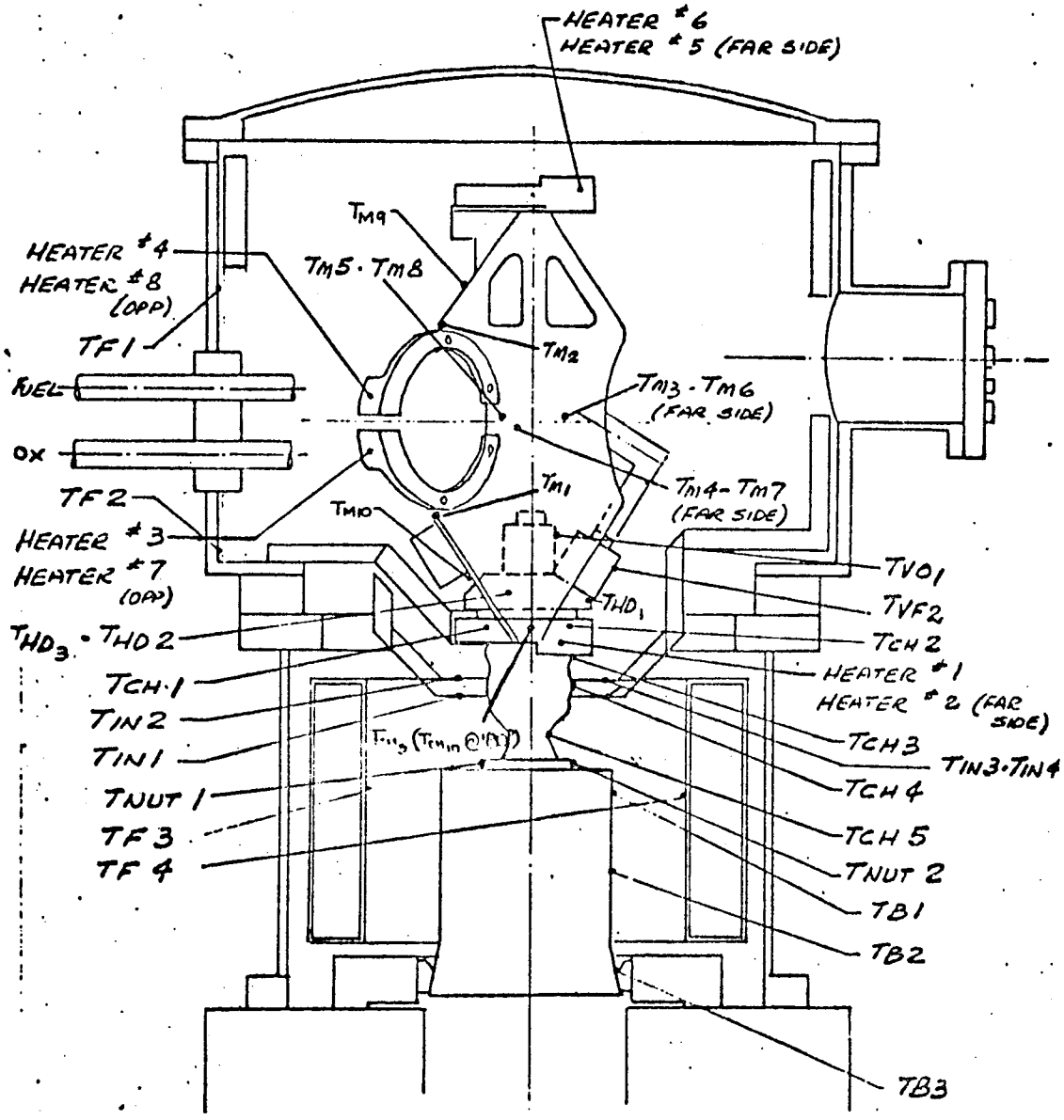

Figure 12

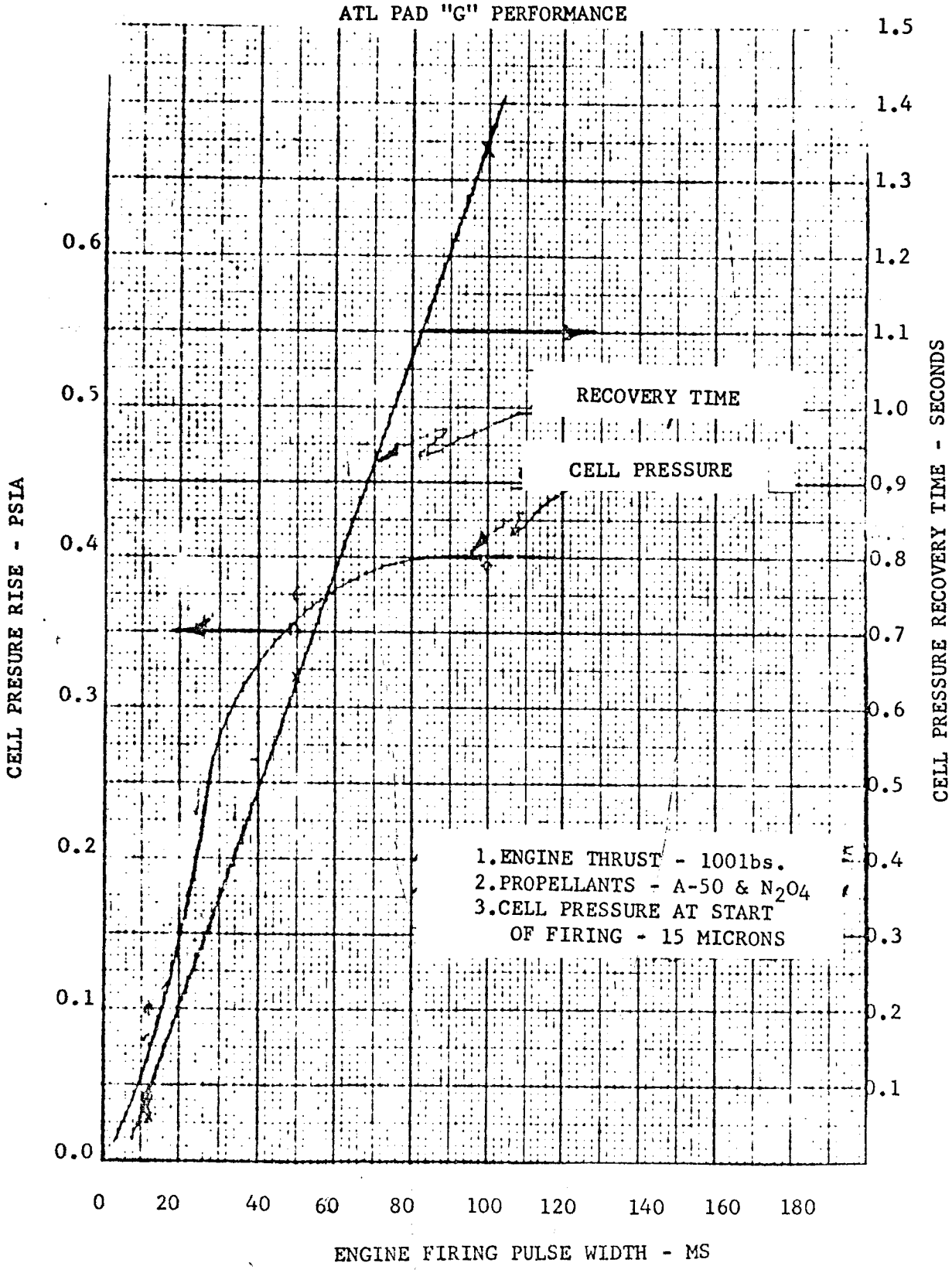
ATL PAD "G" PERFORMANCE
RECOVERY TIME
CELL PRESSURE
1.ENGINE THRUST - 100lbs.
2.PROPELLANTS - A-50 & N_2O_4
3.CELL PRESSURE AT START OF FIRING - 15 MICRONS
CELL PRESURE RISE - PSIA
CELL PRESSURE RECOVERY TIME - SECONDS
ENGINE FIRING PULSE WIDTH - MS
0.0
0.1
0.2
0.3
0.4
0.5
0.6
0.1
0.2
0.3
0.4
0.5
0.6
0.7
0.8
0.9
1.0
1.1
1.2
1.3
1.4
1.5
0
20
40
60
80
100
120
140
160
180

Figure 13

SYSTEMS TEST CELLS

Altitude Test Cell - Cell 9

The complete LM cluster, four each R-4D engines, was tested in the Cell 9 test facility. The engine cluster was mounted in the Cell 9 twenty foot (20') diameter altitude sphere, see Figure 14, which was connected to a three stage steam ejector. This system produced an altitude pressure of 0.02 psia. The remote control room and the instrumentation room contained a normal complement of facility control cluster controls and recording instrumentation.

Cell 9 has been upgraded to closely simulate space environmental conditions, pressure and temperature. Two additional steam ejector stages have been added in series with the existing three stages to produce a cell pressure less than 40 microns, see Figure 15 for the altitude pressure shcematic. The cell pressure will rise slightly when the engine is pulsing. Figure 16 shows the predicted cell pressure rise and cell pressure recovery time after the engine has stopped firing. The complete LM four (4) engine cluster could be installed in a LN_2 cold room within the 20' diameter sphere for actual black space temperature simulation. Propellants saturated with helium gas will be supplied to the cluster at temperatures controlled at any point between 20°F and 120°F. The test will be recorded on the normal oscillograph-strip chart combination and on the new Central Data System. This new Central Data System is capable of recording 108 channels of information from Cell 9 and immediately reducing this recorded information.

Sea Level System Test Cell - M-3, Magic Mountain

The remote Marquardt Rocket Test Laboratory at the top of Magic Mountain was established for rocket testing with highly reactive and/or toxic propellants. This laboratory is some 31 miles from the Van Nuys, California plant and is at an elevation of 4,860 feet. The sea level systems test stand, M-3, is located within this laboratory, see Figures 17 and 18.

Test Stand M-3 is a sea level reaction control system test stand located on a 20 ft. by 32 ft. reinforced concrete test pad. The test stand has been for LM systems testing. During the last two phases of the LM tests, production and design verification, the system was maintained in a Class 100,000 cleanliness environment. High and low temperature ambient and propellants environments were also provided. The test stand is enclosed with a 10 ft. by 20 ft. sheet metal building 10 ft. in height. Four 20 ft. long tie down rails on 42 ft. centers are installed in the test pad. The test exhaust gases are vented directly to atmosphere. Fire protection consists of a deluge system covering the test stand and propellant distribution systems. The Recording Station and Control Consoles for Test Cell M-3 are located in the Control Room of Building 57 at Magic Mountain. The Recording Station shown in Figure 19 consists of signal conditioning and recording equipment for the measurement of flow, pressure, temperature, thrust, and

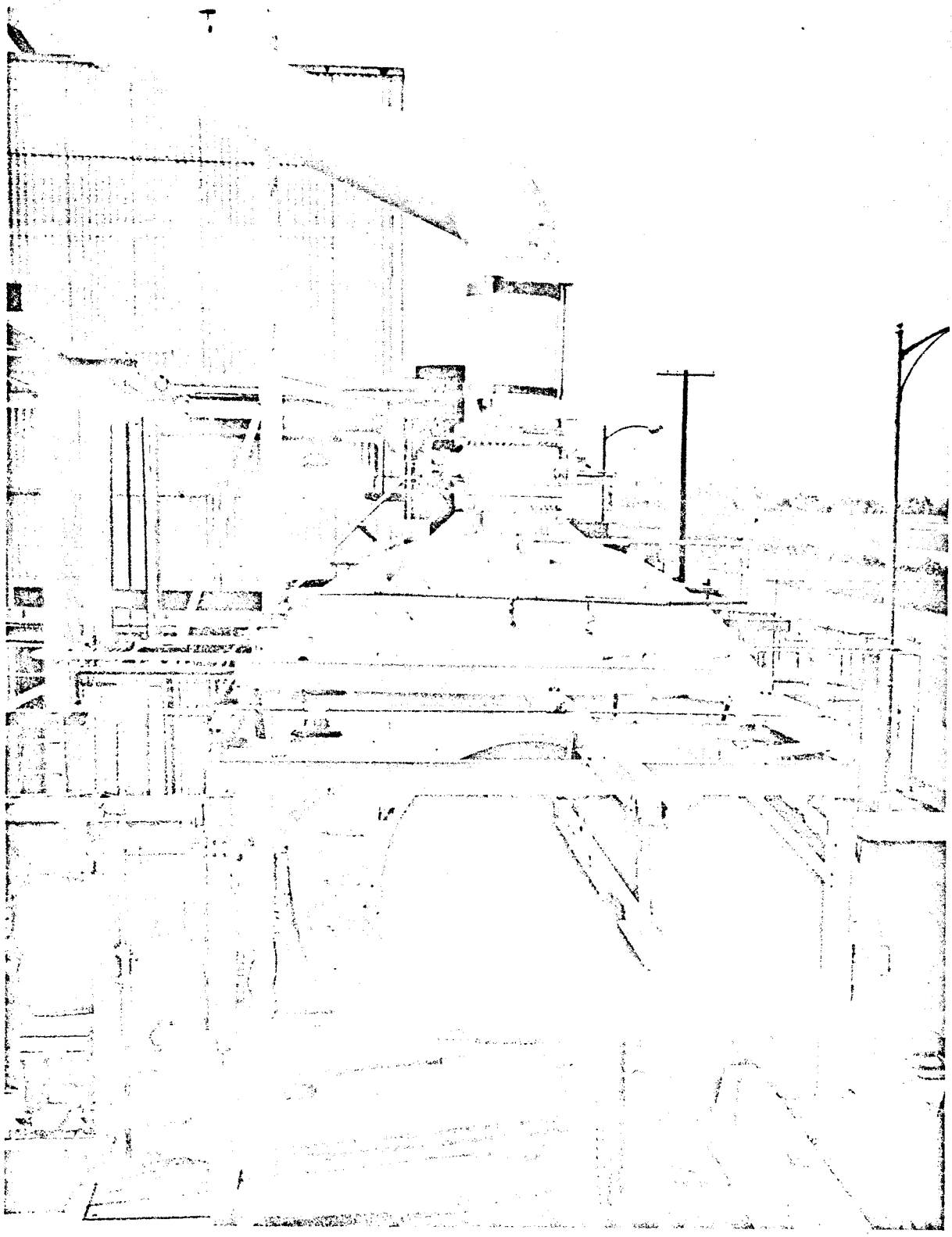

NEG. 4610-46

Test Cell 9

Figure 14

CELL 9 - ALTITUDE PRESSURE

SCHEMATIC

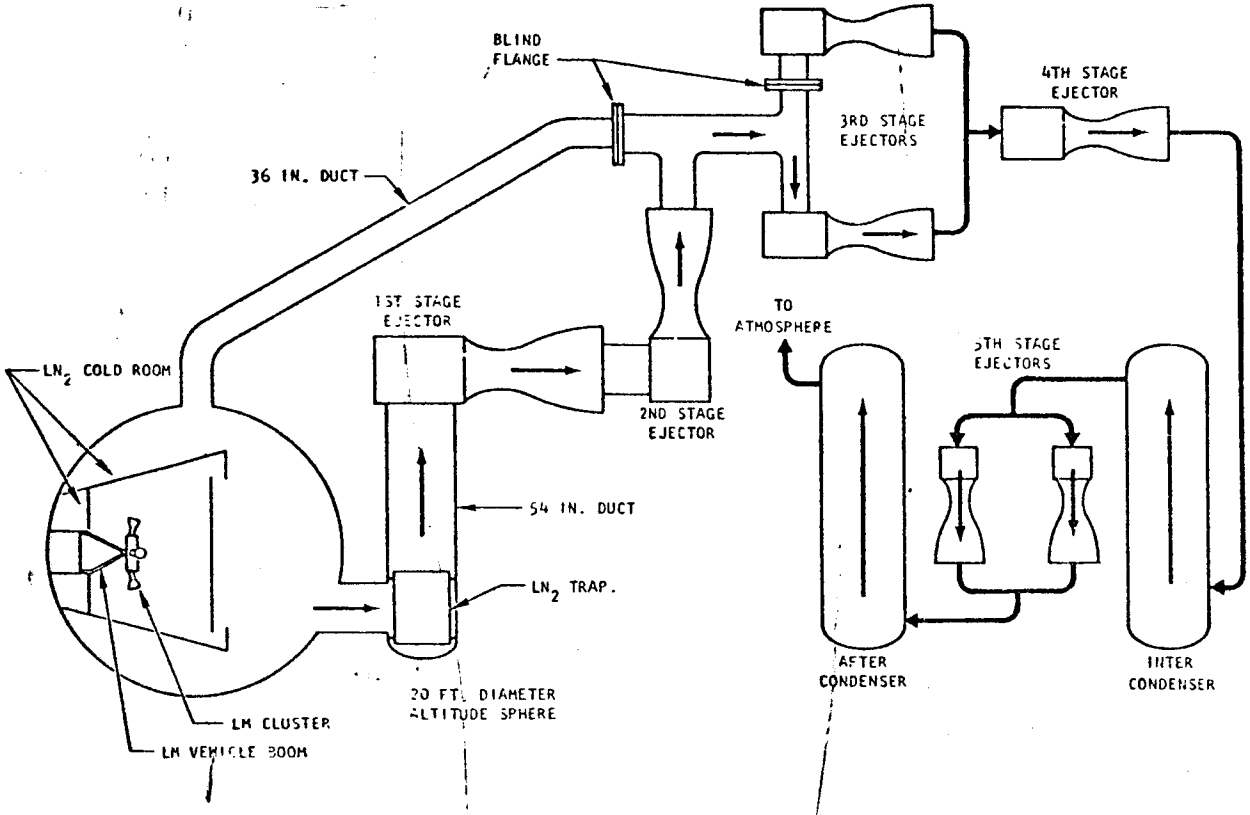

Figure 15

CELL 9 PREDICTED PERFORMANCE

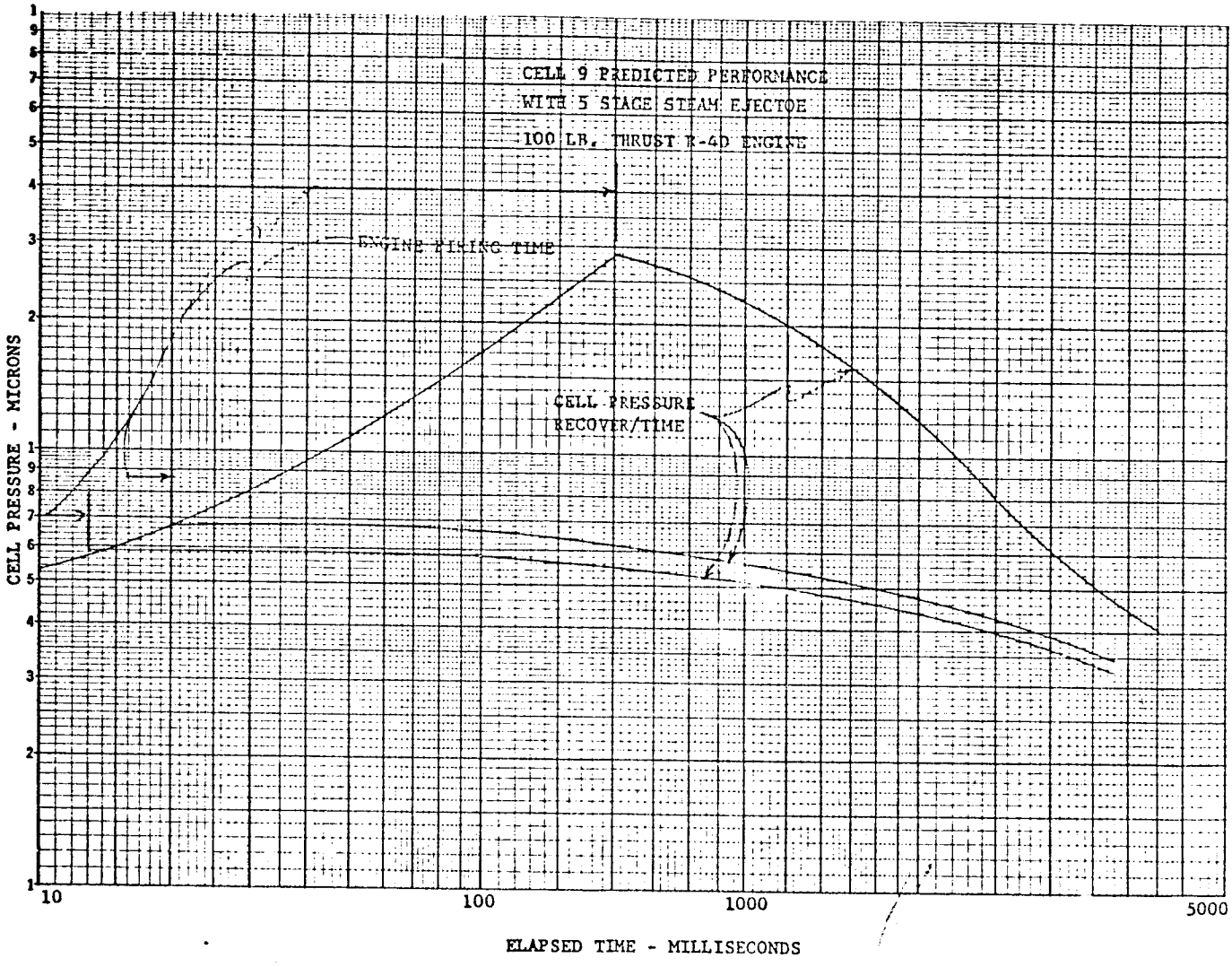

Figure 16

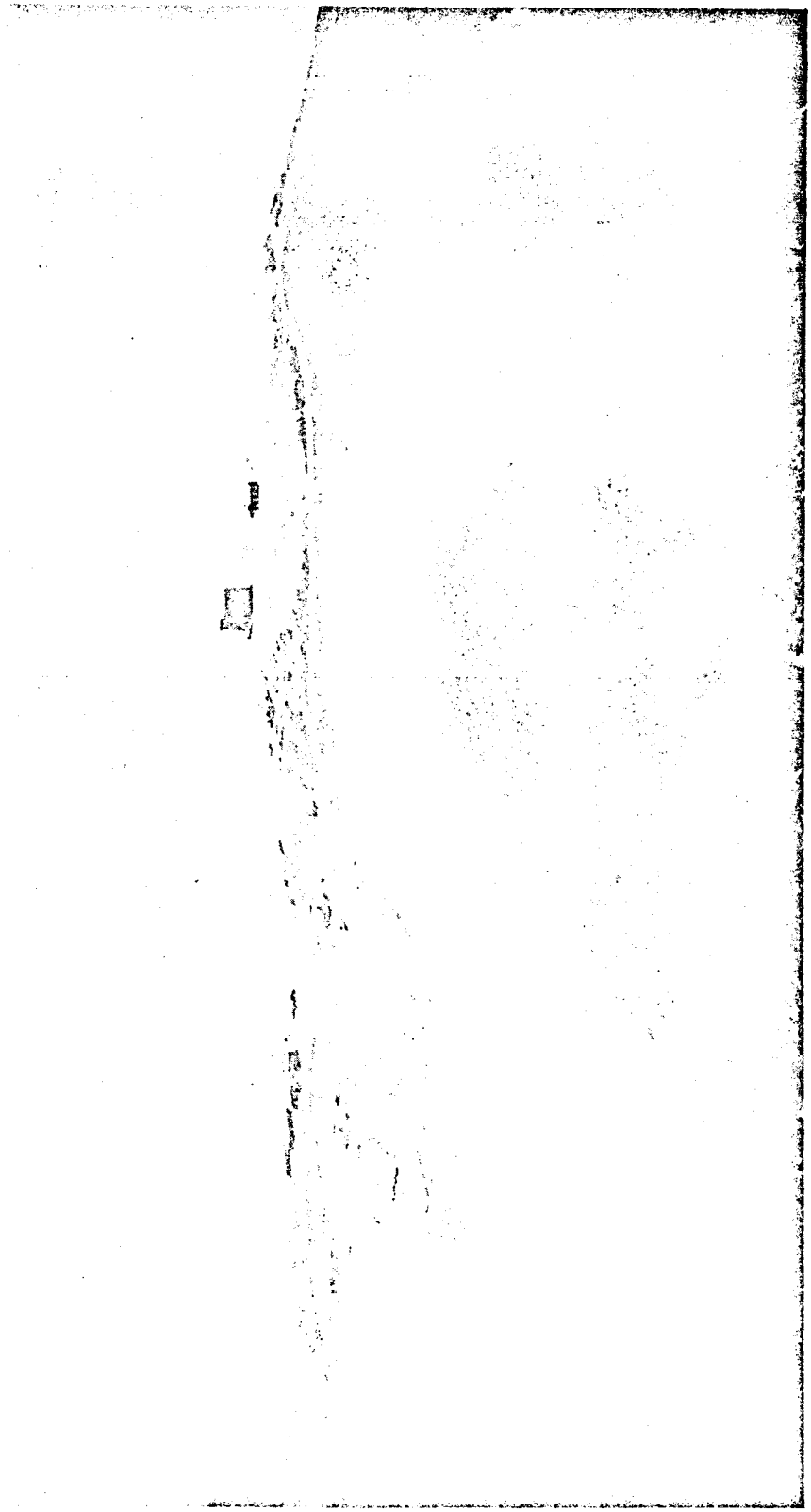

NEG. 6094-11CN

Magic Mountain Laboratory

Figure 17

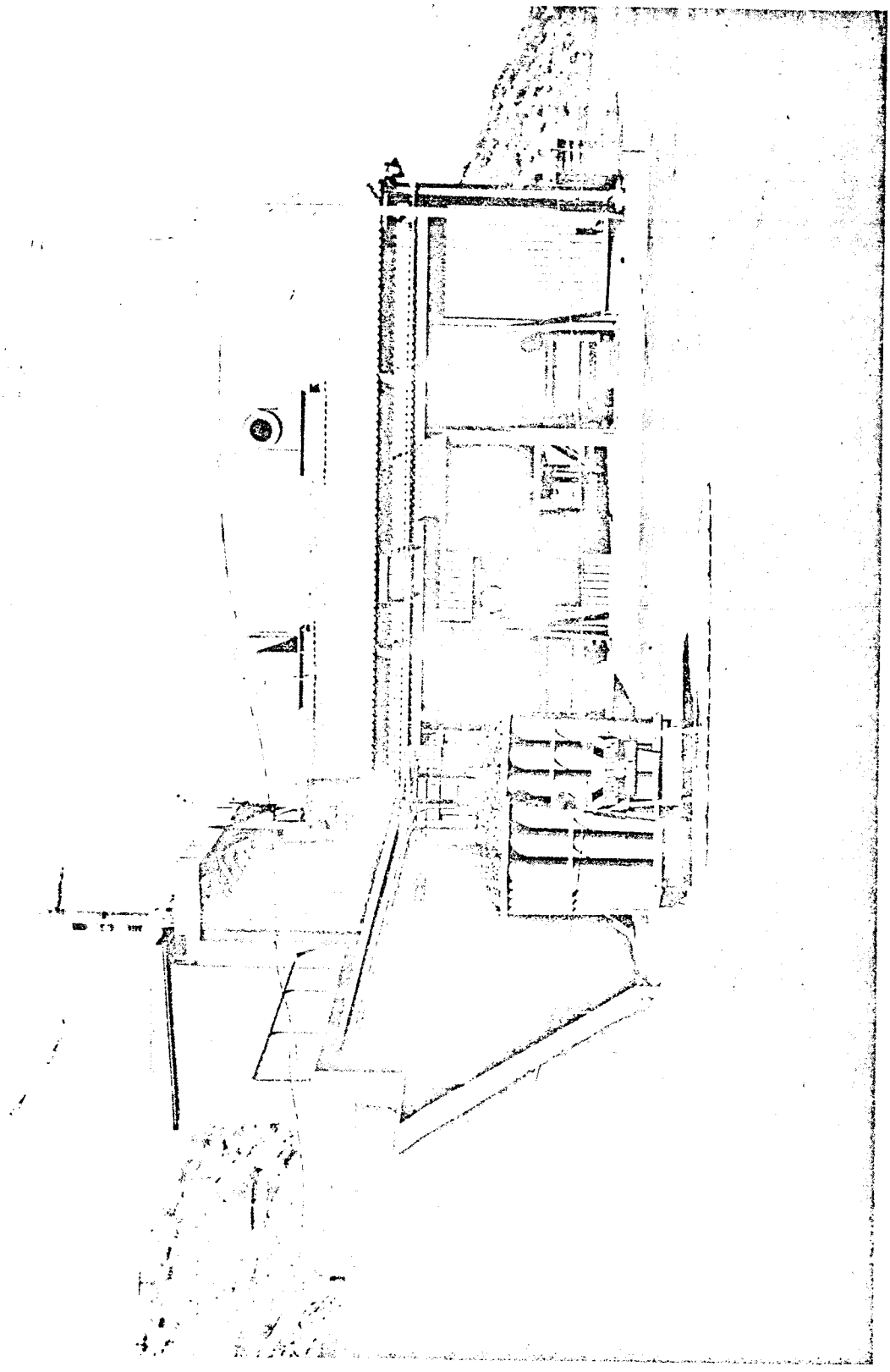

Test Stand M-3

Figure 18

NEG. 6336-32

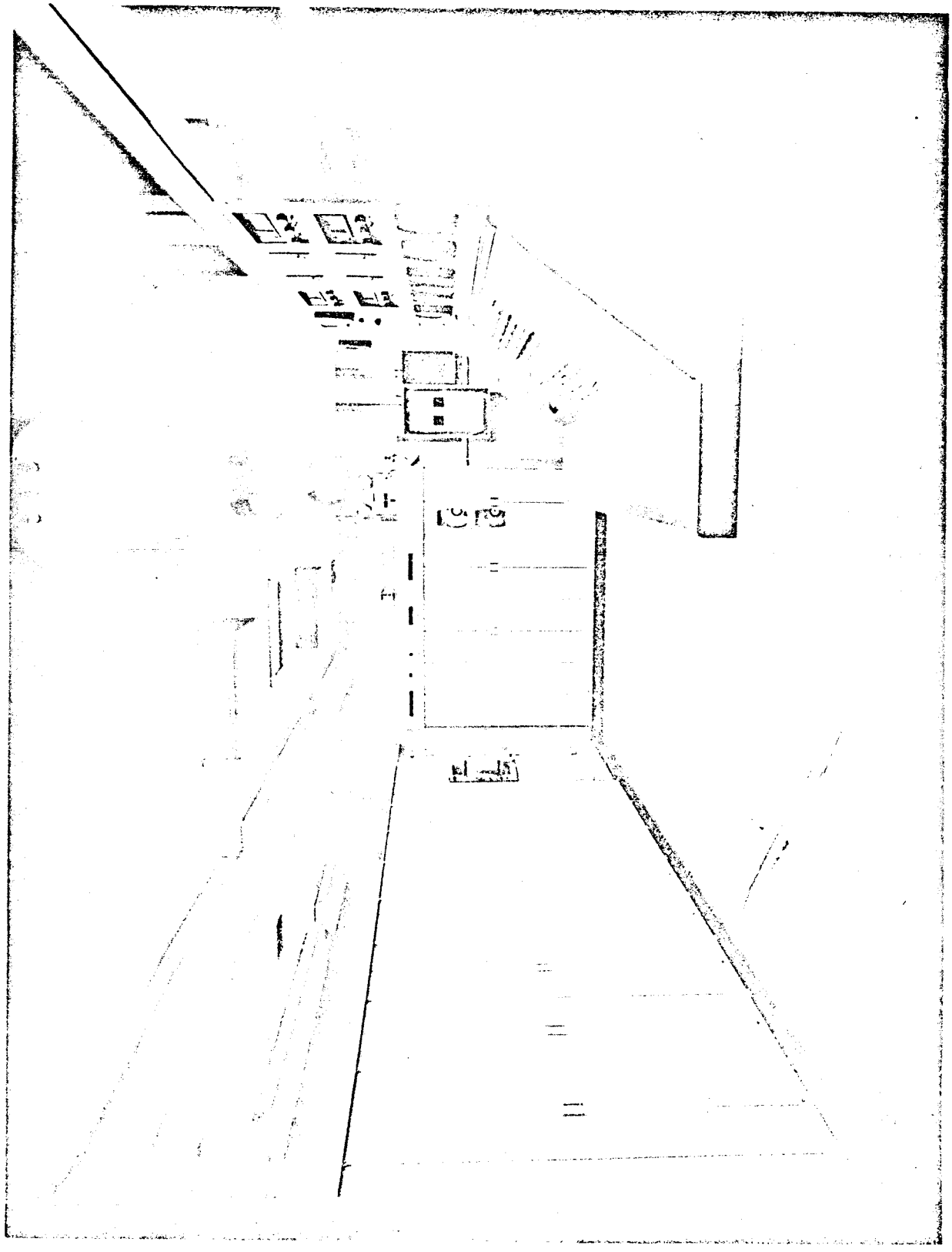

NEG. 6257-1

Signal Conditioning and Recording Equipment

Figure 19

vibration. The recorders include a 36 channel direct write oscillograph, a 100 channel digital tape data recording system and a 14 track analog tape recording system. Operating consoles have independent instrumentation equipment for visual operation and monitoring of flow, pressure, and temperature control parameters.

The instrumentation wiring from the test cell to the recording station is terminated at central "Amp" patch boards for rapid changeover between test cells. The 100 channel digital data recording system is a high speed (20,000 samples/sec.), high accuracy (0.1%) data recording system capable of accepting 100 analog inputs, converting these inputs to their digital equivalent, and recording the accumulated data on computer compatible magnetic tape. The tape is fed into the Marquardt centralized IBM 360 computer complex for data listing and/or data calculations.

The data recording station consists of a fourteen rack console containing the following equipment:

1. Sixty B & F Model 1-220BX Range and Balance Units for signal conditioning of resistance type transducers.

2. Seventeen Anadex Model P1400 Converters for signal conditioning of turbine flowmeters.

3. One Anadex Model CU400 Calibrator for frequency calibration of flow converters.

4. One hundred Preston Model 8300 Wide Bank, Differential Amplifiers.

5. Ninety-two Preston Model 11100 Wide Band Buffer Amplifiers.

6. One Consolidated System Corporation Signal Conditioning Calibration System that provides the following:

   a. A six step resistance calibration to the sixty range and balance units.

   b. A one step frequency calibration to the seventeen flow converters.

   c. A one step millivolt calibration to the one-hundred Preston amplifiers.

   d. A one step voltage calibration to selected buffer amplifiers.

7. One Hyperion Industries Time Code Generator which allows all recorders to have time of day correlation.

8. One thirty-six channel CEC type 5-123 Direct Write Oscillograph for recording dynamic data.

9. One one-hundred channel CSC MicroSadic Digital Tape Data Recording System for steady state data.

10. One ninety-one channel DCS Frequency Modulated Multiplex Tape Data Recording System for recording dynamic data.

11. Five AMP high level Program Patch Boards with patching cables. The patch boards are block identified for ease of setup.

12. Three AMP low level Program Patch Boards with patching cables. The patch boards are block identified for ease of setup.

The facility instrumentation wiring from Test Cell M-3 control room to the recording station and operating consoles is routed in four inch steel conduits. Terminations at the pads are made in J-boxes using KPTO Series connectors. Terminations at the recording station are made through KPTO Series connectors. Terminations at the operating consoles are made at terminal strips. Wiring circuits are available as follows:

1. M-3 Pad J-Box to the Recording Station.

   a. Twenty-four 6 wire and shield circuits for strain gage tranducers.

   b. Twelve 2 wire and shield circuits for turbine flowmeters.

   c. Twelve 2 wire and shield circuits from the Pace 150°F reference junction for iron-constantan, copper-constantan, chromel-constantan, or chromel-alumel thermocouples.

2. M-3 Pad J-Box to the M-3 Operating Console.

   a. Eight 6 wire and shield circuits for monitoring or pressures.

   b. Six 2 wire and shield circuits for auxiliary parameters.

   c. One special 6 wire and shield for the Revere Model CS17 thrust calibration system.

The following monitors are provided at the control consoles as an aid in the facility operation:

1. Four Taber Model 236R Pressure Indicators

2. Two Dynascan Model 111 Digital Voltmeters

3. Two Anadex Model CF 201R electronic Counters

4. One Esterline-Angus Model AW 20 Pen Event Recorder

5. One Revere Model CS17 Three Channel Thrust Calibration System (shared with M-2 Pad).

6. One Packard-Bell 17 inch TV Monitor (shared with M-2 Pad).

One Model HM7-03-A6-02, Seven Contact Eagle Timer is available for automatic sequencing of facility control valves.

IV. COMPONENT AND ENGINEERING FUNCTIONAL TEST AREAS

In addition to the rocket engine and systems test facilities previously described, basically all of the other test facilities within Van Nuys complex have been used on the rocket engine programs. These facilities include the vibration, acceleration, shock, structural, instrumentation, standards, flow calibration and Materials and Process Laboratories. The other test facilities that are used almost exclusively on the rocket programs are discussed in some detail in the following paragraphs.

Controlled Area No. 1 (CA-1)

The CA-1 contains test stands and equipment as required for buildup and removal of engines on thrust stands. Also, performed in this area are certain electrical and pressure checks, and flushing drying operations.

This area is contained within a Class 100,000 controlled area in accordance with FED Standard 209. Humidity, temperature and internal atmosphere contamination are controlled within specification as well as test fluids and supplies. Access to CA-1 is through an air lock system and special clothing is worn by operating personnel.

Major pieces of equipment located in CA-1 are an assembly and disassembly stand, inspection hood, drying oven and miscellaneous tools.

The work stand has distilled water, nitrogen and Freon supplied to it.

Figure 20 is a photo showing installation of an engine in a thrust stand.

Controlled Area No. 2 (CA-2)

Engine components, subassemblies and complete engines are flow and leak tested and trimmed to rigid specification in the manufacture of the R-4D engine. This testing is accomplished in CA-2.

This 1200 square foot test area is contained within a Class 100,000 controlled area in accordance with FED Standard 209. Humidity, temperature, and

NEG. 6990-30

Controlled Area No. 1 - Engine Thrust Stand Buildup

internal atmospheric contamination are through an air lock system and special clothing is worn by operating personnel. Test hardware is accepted for test only when in a cleaned condition. A schematic of Controlled Area #2 is shown in Figure 21.

The test stands located within CA-2 are supplied filtered, temperature-controlled, distilled water from separate supply systems to eliminate interaction between benches. Inert gas supply systems are used for simulated fluid supply tank pressurization, gas dynamic tests, purging and leak checks. The test stands now installed in CA-2 include two Federal Standard 209 Class 100 laminar flow test stands for flow and pressure tests, and flow distribution test stand, one Federal Standard 209 Class 100 work bench and the required peripheral equipment.

Each stand contains a separate facility and test hardware control panel that is installed to match the particular test program requirements. Instrumentation panels and portable systems are also installed to match individual test requirements.

A photo of CA-2 is shown in Figure 22. Two photographs clarifying the test area and associated equipment are presented as Figures 23 and 24.

Space Simulator Environmental Chamber

To obtain the heat transfer characteristic of the R-4D engine under space environmental conditions, extensive testing was conducted in a special test setup known as theSpace Simulator Environmental Chamber. The test engine was placed in a vacuum chamber capable of producing a pressure of 1×10^{-6} mm Hg. The bell and combustor of the engine are allowed to radiate to an LN_2 cooled cold wall while the head of the engine is maintained at a fixed temperature. The power input to maintain the engine head at a fixed temperature is easily obtained as well as the temperature distribution of the engine components, see Figure 25.

The Space Simulator Facility consists of a 3 ft. long by 3 ft. diameter vacuum chamber utilizing a 6-inch oil diffusion pump. Centered in the 3 ft. chamber is a 27-1/2 in. long by 20 in. diameter unsealed space simulator sub-chamber that is cooled with liquid nitrogen to -320°F. Heaters are also incorporated in the Space Simulator for radiation type heating of the test item. Pump down time of the chamber is approximately 4 to 6 hours. The vacuum pumping system and the liquid nitrogen system is capable of operating on a continuous basis.

AF-MDL-Vibration Laboratory

The Vibration Laboratory is contained within a separate building and consists of various vibration heads (exciters) and related amplifiers, controls, data gathering equipment and other equipment as required to successfully conduct vibration tests, refer to Figure 26 for a schematic of the Vibration Laboratory.

FACILITY SCHEMATIC CONTROLLED AREA NO. 2 (CA-2)

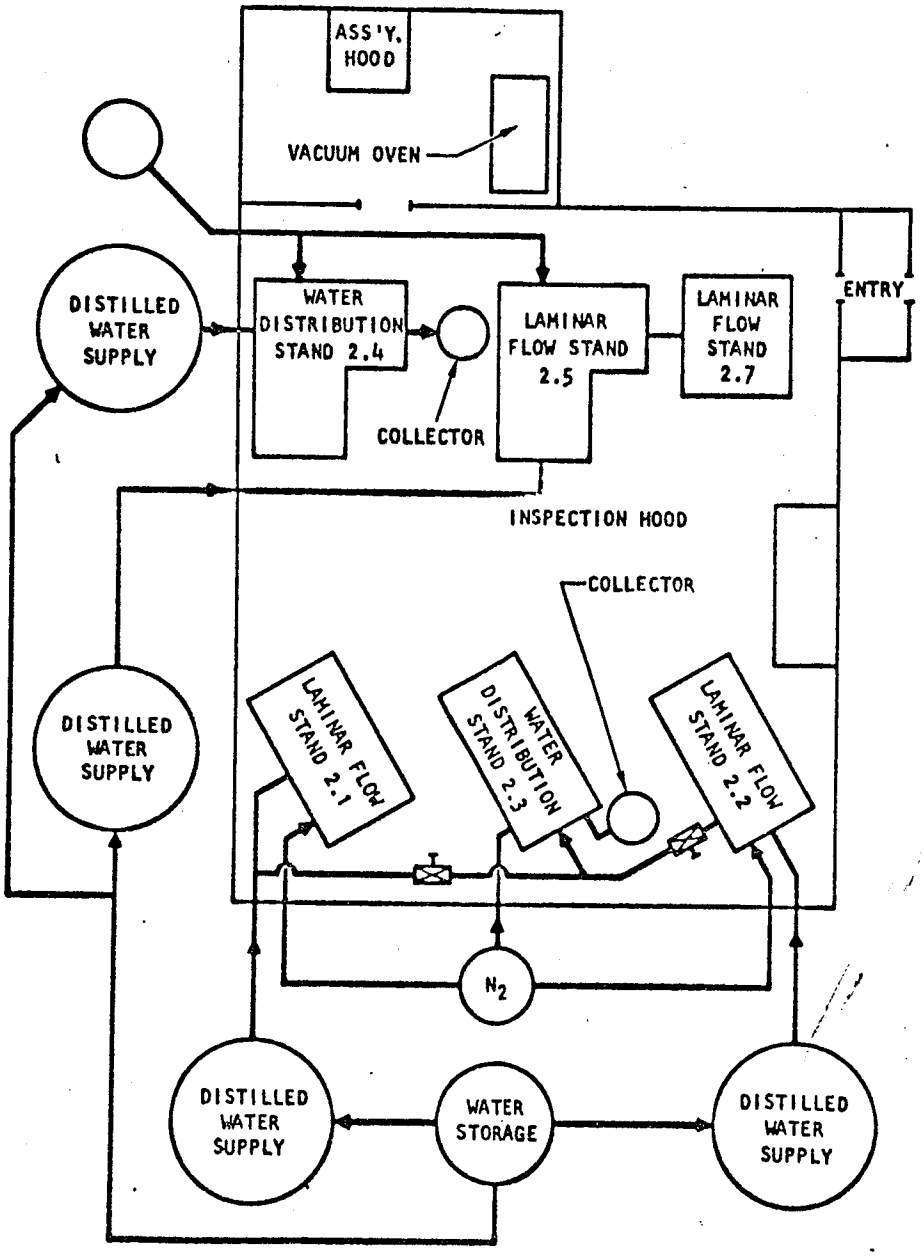

Figure 21

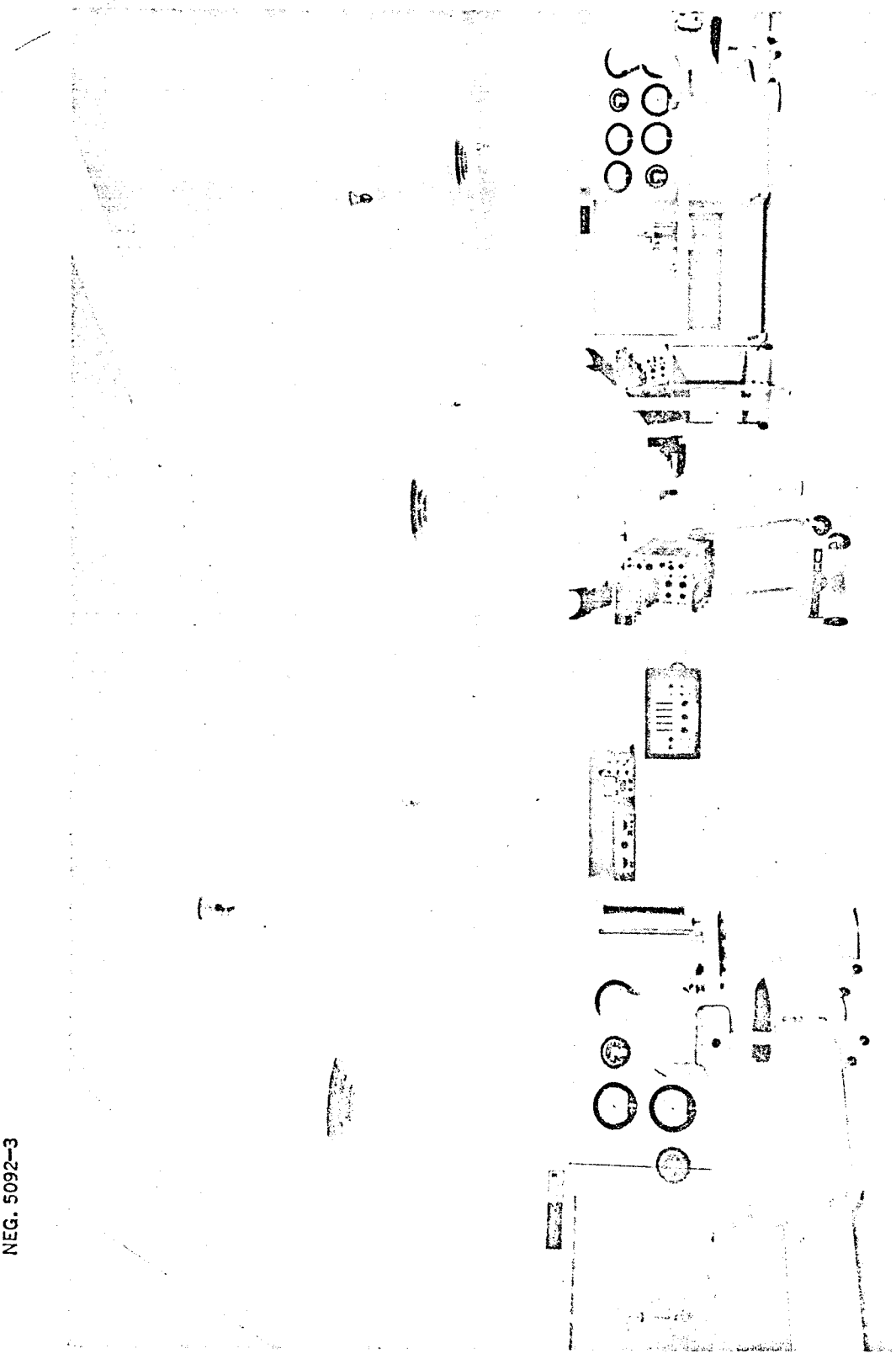

NEG. 5092-3

Controlled Area No. 2

Figure 22

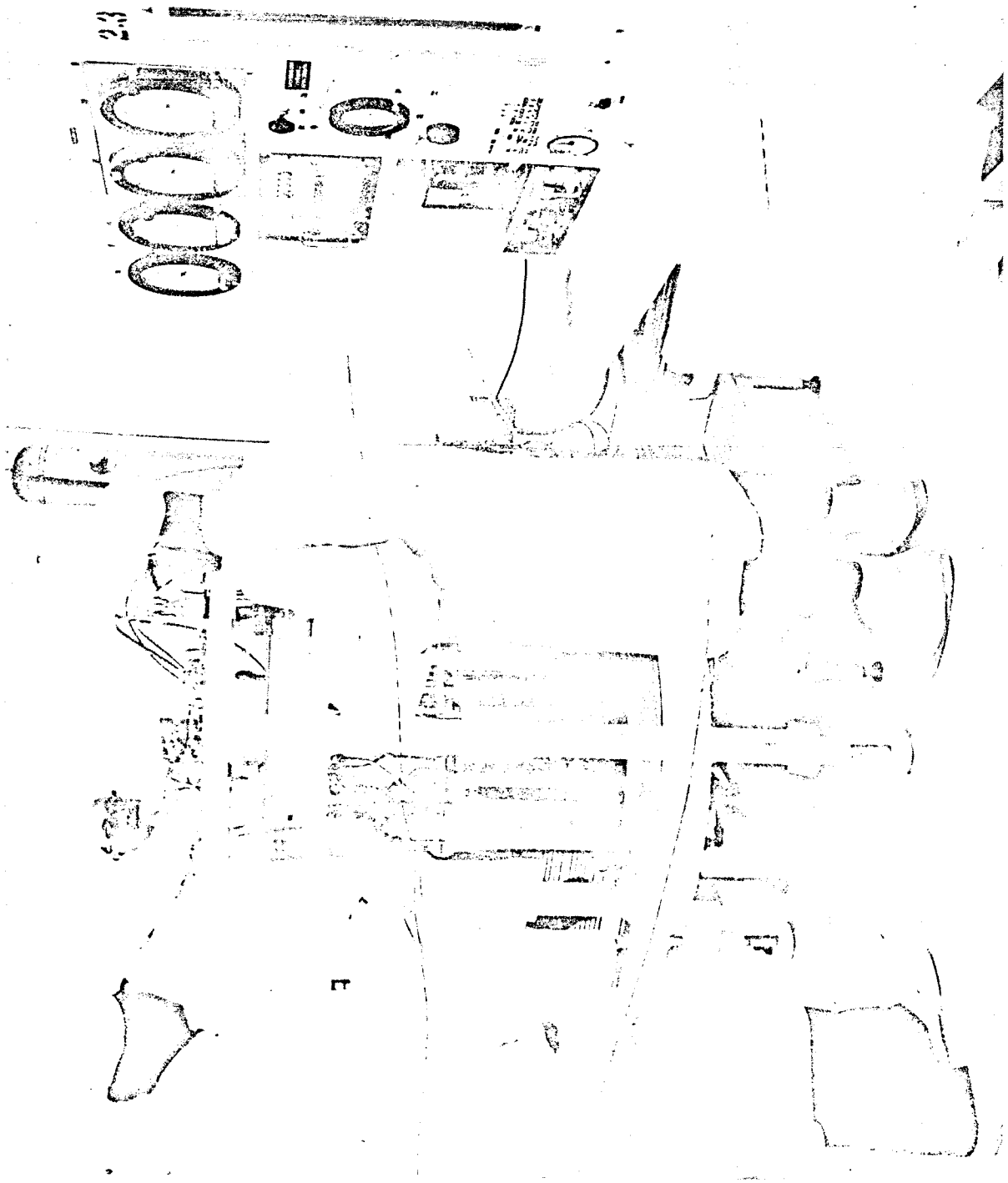

NEG. 6990-15

CA-2 Stand 2.3 Flow Collector

Figure 23

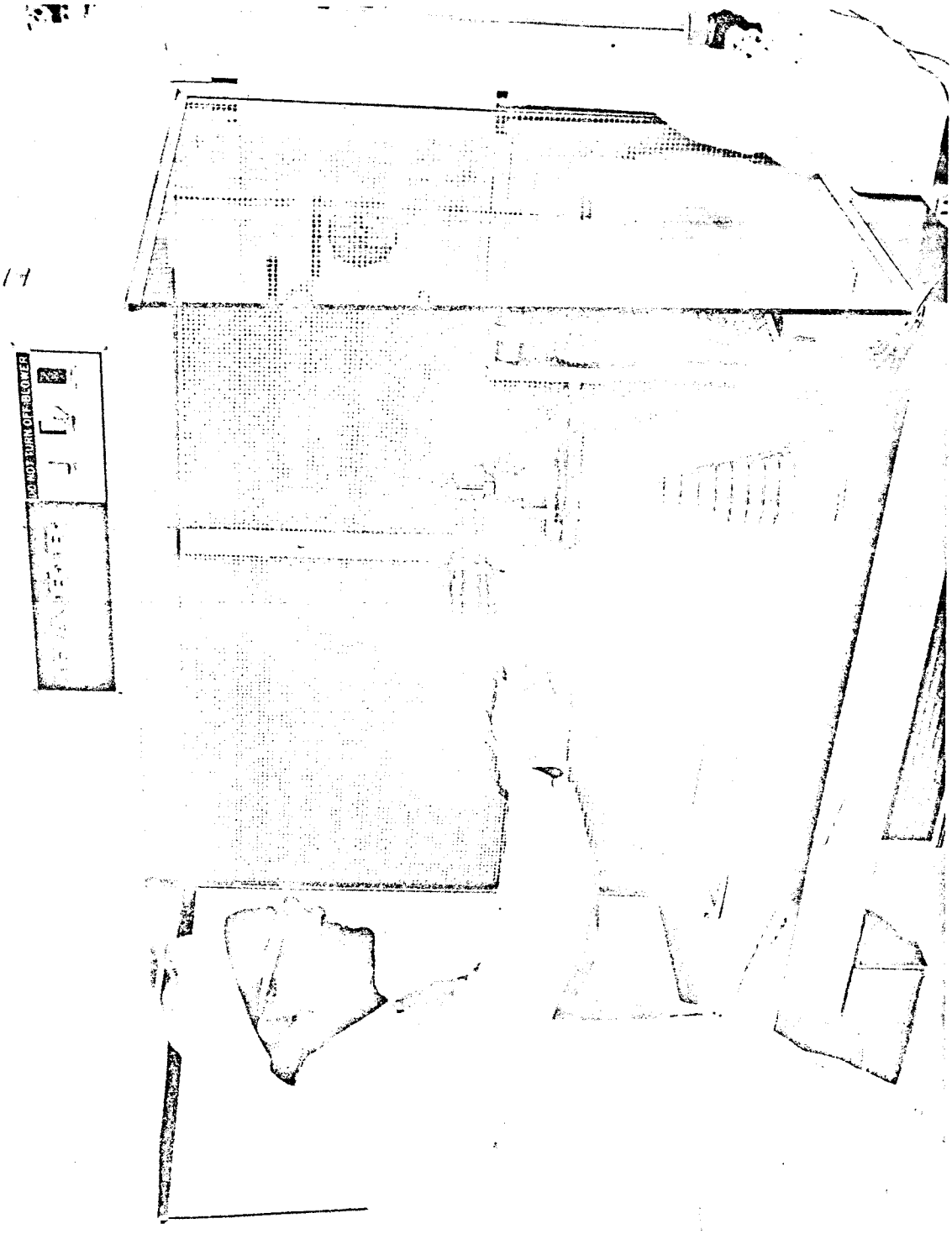

CA-2 Laminar Flow Stand

Figure 24

NEG. 6990-27

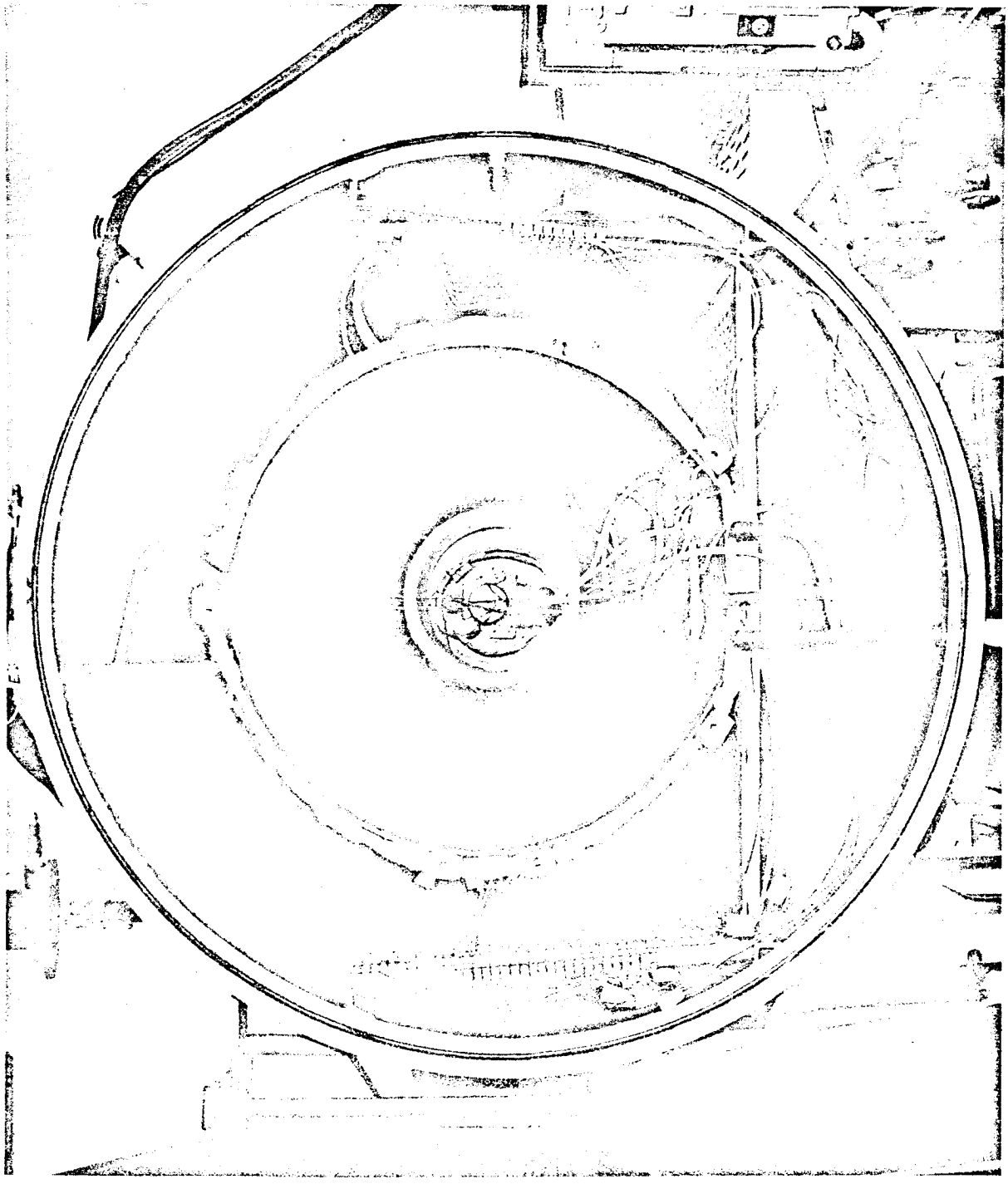

NEG. T3331-4

Lunar Orbiter Qualification Test Cold Soak Test Installation

Figure 25

VIBRATION LABORATORY EQUIPMENT SCHEMATIC

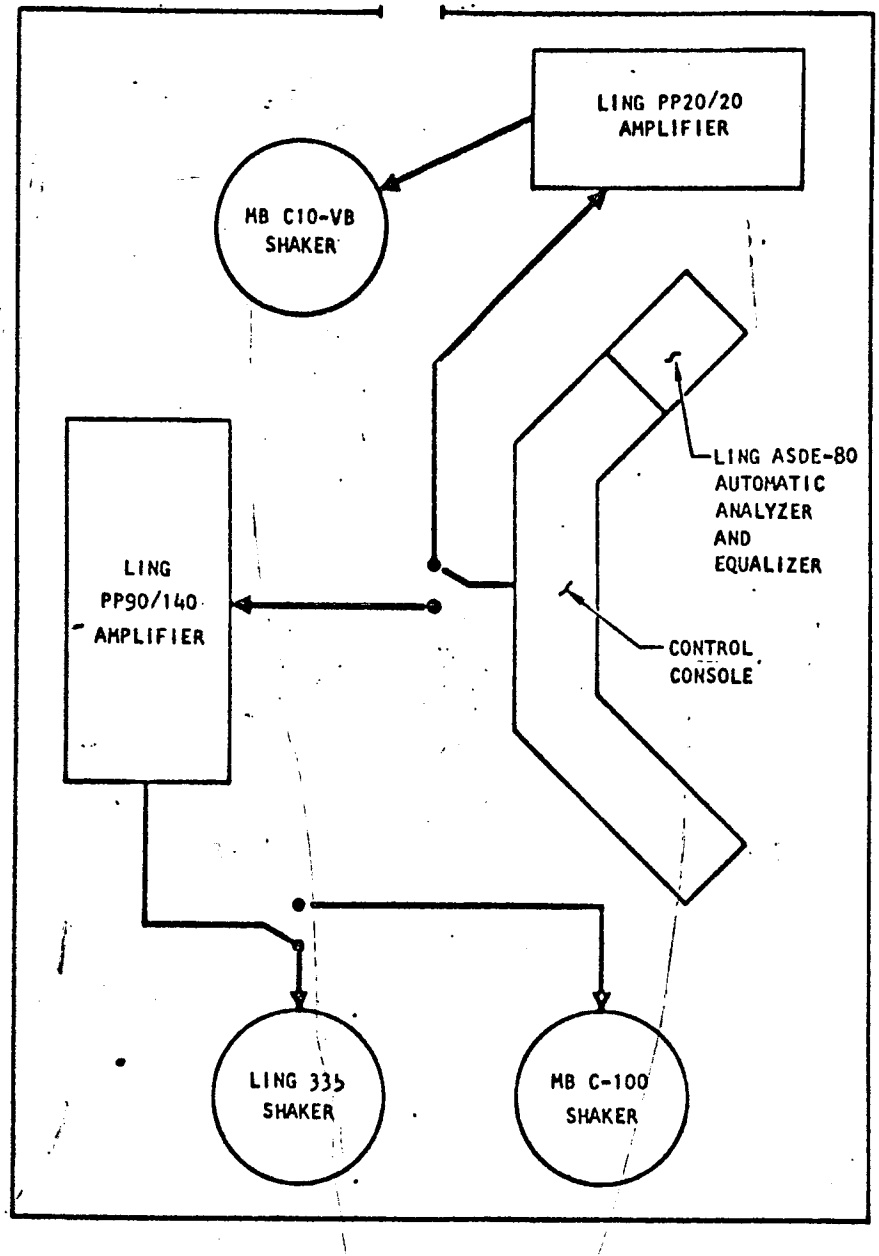

Figure 26

Test items such as components, valves, and complete engine assemblies can be vibrated to sine and random type programs.

Three electromagnetic shakers with the following specifications are available for use.

Manufacturer	Model	Force Rating Force - Lbs.	Displacement Inches Double Amp.
M.B. Mfg. Co.	C10-VB	1,750	1.0
M.B. Mfg. Co.	C-100F	15,000	0.5
Ling Electronics	335	15,000	1.0

Each shaker is driven by a Ling Electronic Power Amplifier which is capable of sine wave, random, or combined sine and random vibration. Random vibration is controlled by a Ling Automatic Analyzer and Equalizer Model ASDE-80. Random vibration data is recorded on an Ampex 14 channel tape recorder and analyzed with a Spectral Dynamic Spectrum Analyzer Model SD101A/SD27 with appropriate filters. Sine wave data is recorded on an X-Y plotter, an oscillograph or on the Ampex Tape recorder. The Vibration Lab data gathering system can accomodate 16 accelerometers.

Figure 27 shows the Ling 335 and M.B. C-100 Shakers. Figure 28 presents the shaker controls and amplifiers.

General Services

Readily available to the test facility are all of the general services required for conducting this specialized testing. These services include a (1) propellant storage area, (2) domestic and industrial water, (3) electrical services, (4) a control nitrogen system, (5) a 1.4 million gallon cooling water reservoir, (6) shop air, (7) propane and natural gas and the related shop and maintenance services required for an efficient testing operation.

The steam system is the heart of the altitude simulation testing.

The two 40,000#/hr. steam boilers are in constant use at the Van Nuys test facility. Boiler No. 1 and the steam distribution system was installed on an Air Force Contract in 1960. Boiler No. 2 and its accessories were installed on a NASA contract in 1964.

Both boilers are Navy "spares" Destroyer Escort packages designed by Combustion Engineering. The marine type boiler was selected to cut down on the time required to get the boilers on and off the line.

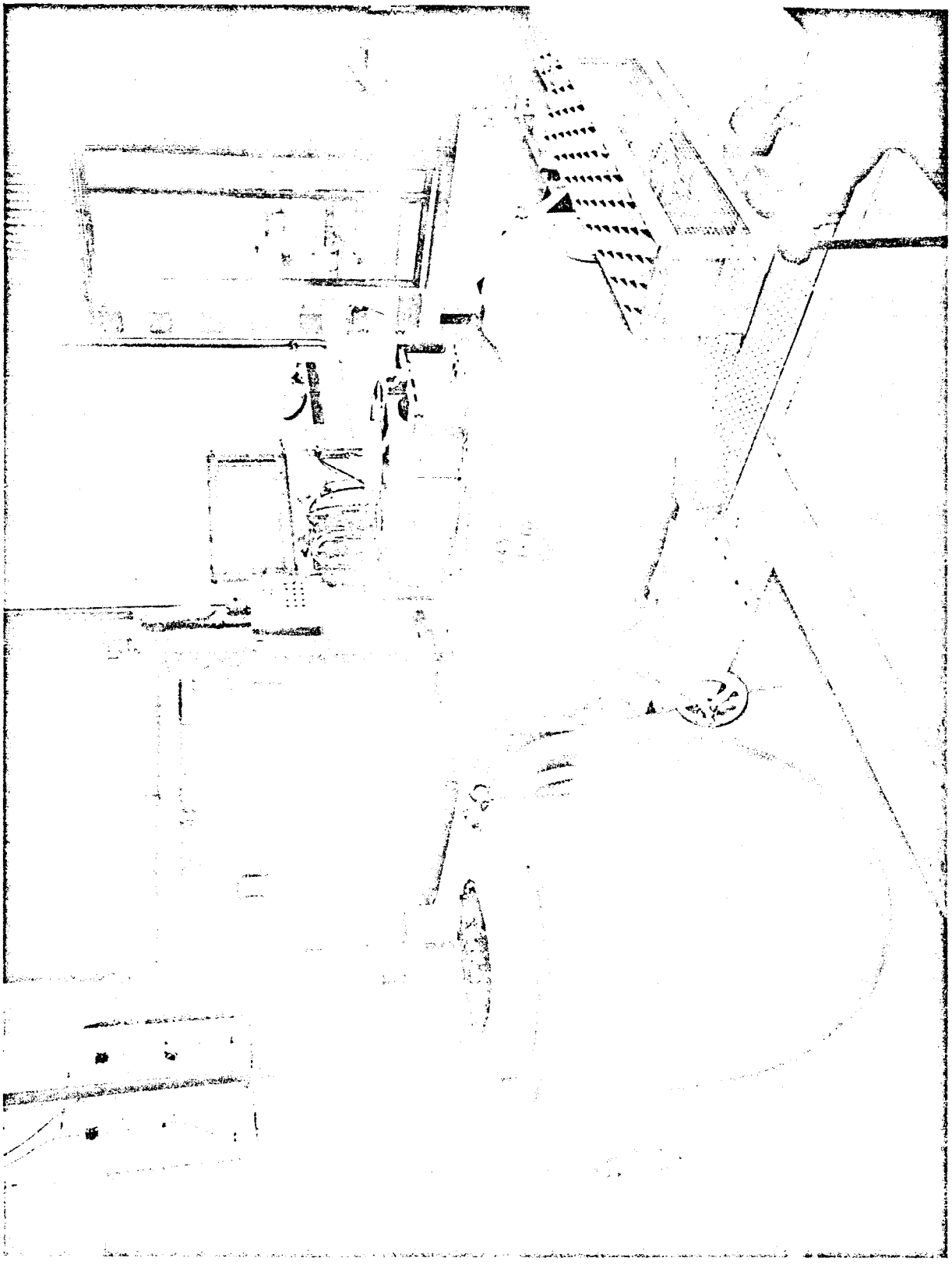

NEG. 8010-3

Vibration Laboratory Ling 335 and M&S-100 Shakers

Figure 27

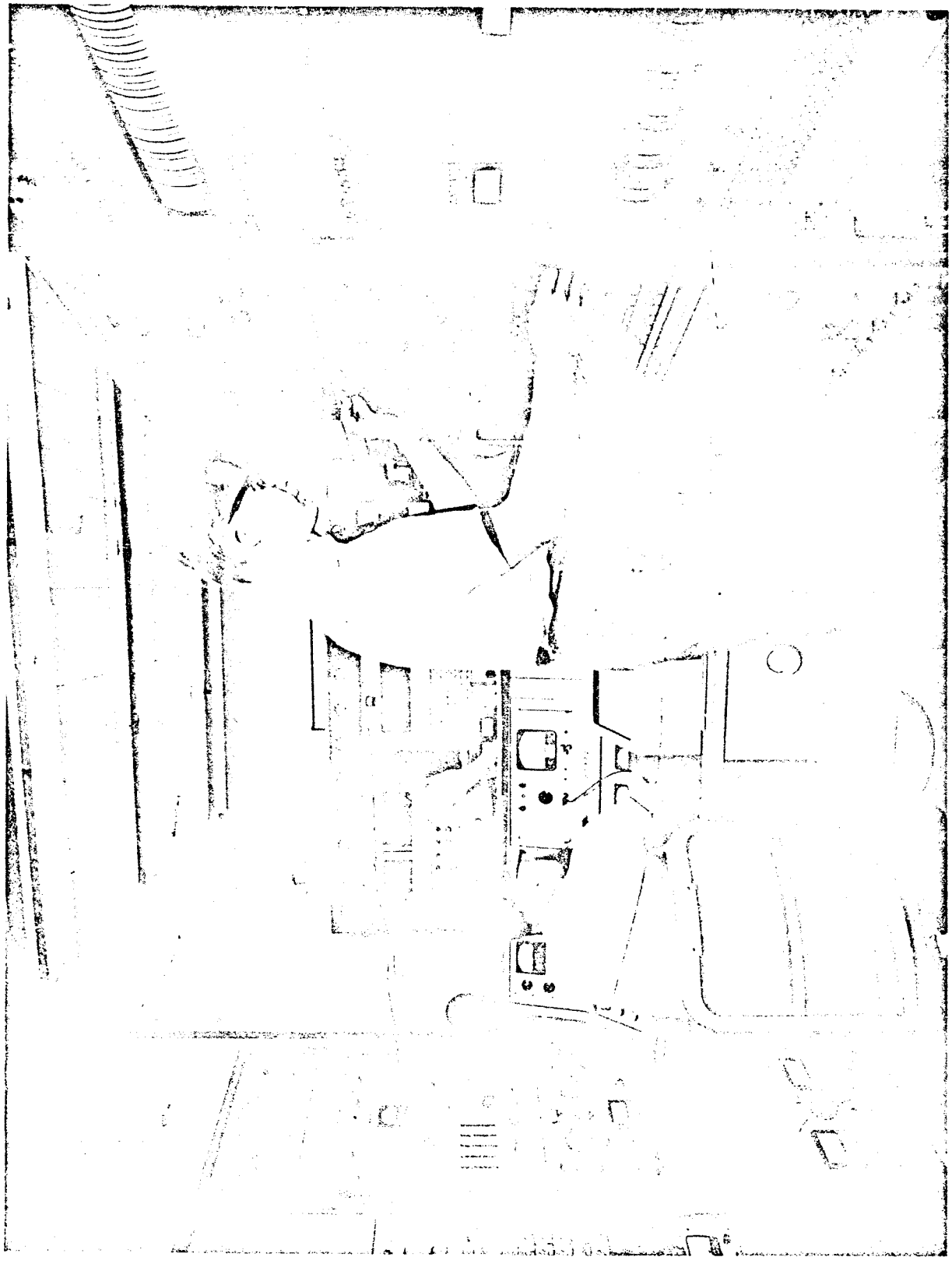

NEG. 7096-42

Vibration Laboratory Sine Wave & Random Control Console

Figure 28

The capacity of each boiler is 43,000#/hr., 450 psig, 750°F superheated steam. The net output capacity of both boilers, however, is 80,000#/hr. due to the steam consumption of the turbine pumps. The plant is set up to use either liquid propane or natural gas. Feed water to the boilers is 100% demineralized water.

The steam distribution system has some 2000 ft. of 6" thermally insulated steam line. The steam is used to drive multi-stage steam ejector and process heat exchangers as required by the particular test cell setup.

V. MEASUREMENTS

The important product of any test program is accurate meaningful data. To obtain this data both precise control of the test conditions and the control of measurement errors are required. The test conditions are controlled by the design and operation of the test facility. Measurement errors are controlled by the use of proven instruments, adherence to written procedures, periodic instrument calibrations traceable to the National Bureau of Standards and the use of electrical calibrations before and after each series of firings. A comprehensive discussion of the measurement, procedures, error sources and data accuracies for the Apollo engine program are described in Marquardt Report A-1043 and L-1030 - "Instrumentation Accuracies and Computed Parameter Error Analysis."

Thrust Measurement

The system used for thrust measurement consists of a large steel seismic mass, a high stiffness semiconductor load cell, a special thrust stand, and the thrust signal processing, compensating and recording equipment. The thrust stand incorporates provisions for calibrating the thrust measuring load cell by using a Secondary Standard load cell and pneumatic cylinder arrangement at the actual pressure and temperature condition of the particular test. Calibrations are periodically performed with propellant pressures applied to the engine when under simulated altitude conditions. The engine installation in the test cell was previously shown in Figure 6.

The engine thrust stand assembly ready for installation in the test cell is shown in Figure 29.

In the pulse thrust measuring system, a special Analog Computer circuit inserts the inverse of the test stand transfer function to arrive at a compensated thrust signal which accurately represents true dynamic thrust up to and somewhat beyond the natural frequency of the thrust stand.

In simplified form, the natural frequency of the thrust stand load cell - engine combination is

(1) $\omega_1 = \sqrt{\frac{K}{M}}$

where: ω_1 = natural frequency in radians/sec.

K = load cell spring constant

M = total mass attached to load cell

The spring constant

$K = \frac{R}{\alpha}$

where: R = load cell range

α = full range deflection of the load cell.

Thus, equation (1) can be written

(2) $\omega_1 = \sqrt{\frac{gR}{\alpha W}}$

where: W = Mg

If "R" is selected equal to the engine rated thrust "F" the maximum possible value for the R/W is just the thrust to weight ratio (F/W), of the rocket motor.

With this condition the stand frequency is:

(3) $\omega_2 = \sqrt{\frac{g}{\alpha} (F/W)}$

where: ω_2 = natural frequency when R = F.

For example, assume a typical case where

F/W = 10

g = 32.2 ft/sec^2 or 386.4 in/sec^2

α = 7×10^{-4} inches

then

$\omega_2 = \sqrt{\frac{386.4}{7 \times 10^{-4}} (10)}$

ω_2 = 2350 radians/sec., or

f = 375 cps.

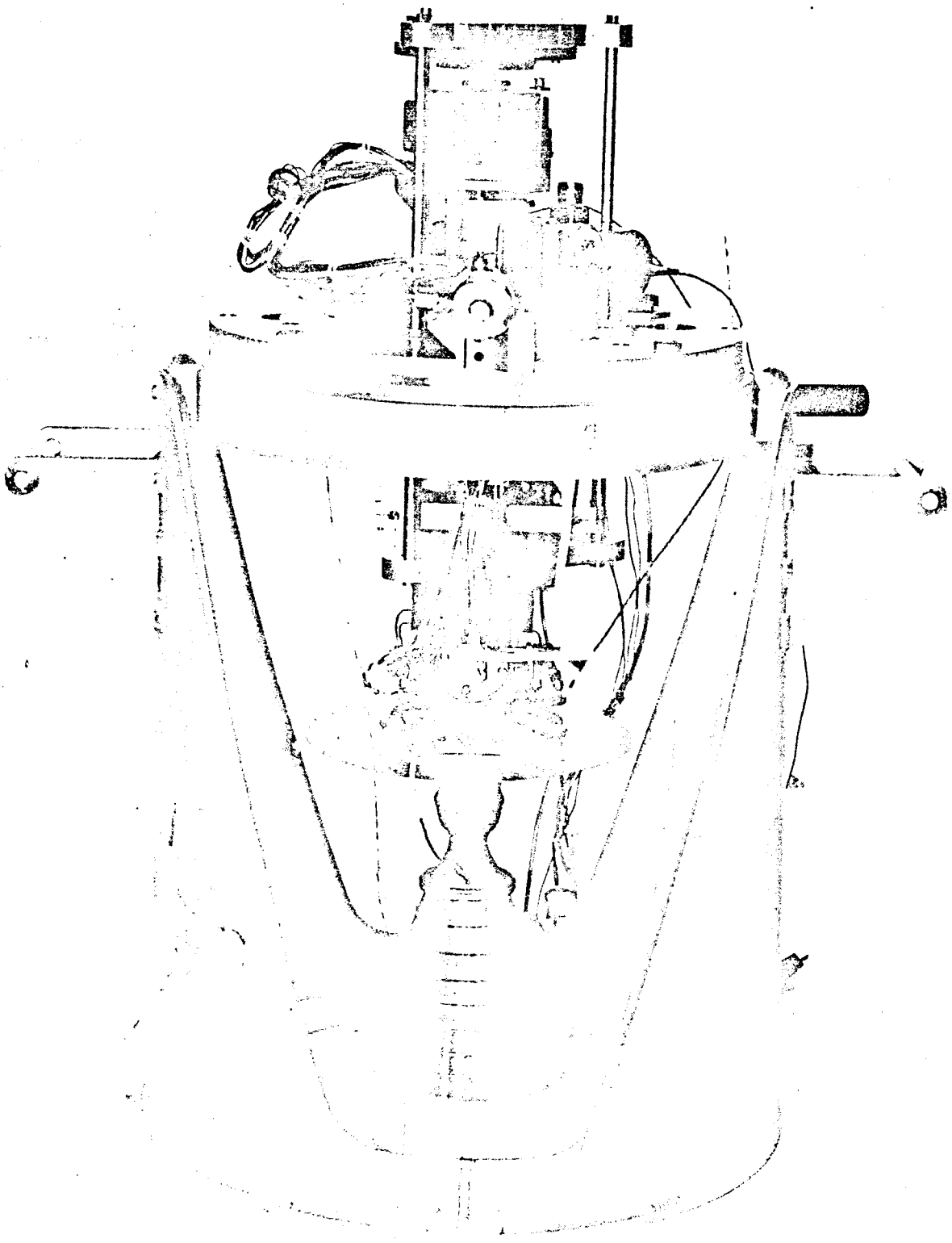

NEG. T3324-42

Qualification Engine Buildup

Figure 29

To increase the stand natural frequency, at the expense of accuracy, the load cell range can be chosen to be "β" times the rated thrust.

(4) $$\omega_3 = \sqrt{\frac{\beta g}{\alpha} \quad (F/W)} = \omega_2\sqrt{\beta}$$

where: ω_3 = natural frequency when $R = \beta F$

It must be noted however, that the error in measuring thrust increases when the load cell is used over only a fraction of its range.

For example, if the load measuring system error is ϵ (%FS) and the allowable error at full thrust is δ (% of value) then

$$\delta F = \epsilon\beta F \text{ or } \beta = \frac{\delta}{\epsilon}$$

and the maximum stand frequency is, using equation (4)

$$\omega_3 = \omega_2 \sqrt{\beta} = \sqrt{\frac{\delta}{\epsilon} \quad \frac{g}{} \quad \frac{(F/W)}{\alpha}}$$

for example, if ϵ is 0.2% FS and δ is 0.5% then using the above example the natural frequency can be extended by a factor $\sqrt{2.5}$

$$\omega_3 = \sqrt{\frac{.5}{.2} \times \frac{386}{7\times10^{-4}} \quad 10} = 3690 \text{ radians/sec.}$$

$$f = \frac{\omega_3}{2\pi} = 587 \text{ cps}$$

The actual value of test stand frequency will not be the same as the theoretical calculated value due to the indeterminate factors of friction and damping.

The ratio of actual to the calculated frequency is a figure of merit of the test stand design and is generally predictable to a factor of approximately 0.7. A general thrust stand design investigation has indicated that a thrust measuring system consisting of a rocket motor, load cell and stand of finite mass and stiffness produces two characteristic frequencies in the presence of thrust, transients. In order to minimize these frequencies, the thrust system must be designed for low values of rocket motor mass to stand mass (Mr/Ms) and Ws/Wl stand frequency to load cell frequency so as to minimize the low frequency oscillation terms in the system output. Experience coupled with analytical studies dictates a ratio of .05 or less (20:1) should be strived for Mr/Ms. The test stands used are not in a ratio of 500:1 minimizing or eliminating the effects of the low frequency component.

In the block diagram of the pulse measuring system, Figure 30, an isolated signal conditioning power supply provides excitation and a balancing network for the transducer. This output is connected directly to a dc amplifier and then to a strip chart recorder for dc or steady-state information. The output of the dc amplifier also inputs to an on-line analog computer circuit, which compensates or modifies the signal to adjust for damping and resonant frequency of the system. This analog computer circuit will be considered in detail below.

The test stand and load cell combination in use at TMC can be simplified into a simple spring and mass system. The differential equation describing the motion of such a system can be written as follows:

(5) $M\ddot{x} + c\dot{x} + kx = F(t)$ = driving function

M = effective mass

c = damping factor

k = spring constant

x = position output

Using the electronic compensation technique, it is desirable that the damping factor be maintained at a low value. In actual fact, it can be stated that the ideal dynamic thrust stand would have a damping factor approaching zero. Utilizing equation (5), it is possible to compute a curve plotting force transmittability vs. the ratio of the driving frequency to the natural resonant frequency (solid line in Figure 31). From this curve, it can be seen that the mechanical amplification of the stand system reaches a sharp peak as it approaches the resonant frequency. Beyond this frequency it falls slowly and approaches zero transmittability. The height of the peak at resonant frequency is a function of the damping of the system. With lower damping, the peak at stand resonance becomes much higher. If it were possible to electronically generate an inverse function (dashed line) to this transmittability curve and superimpose this function with the electrical output of the forced systems, a new curve of effective transmittability could be drawn (see Figure 32). From this curve it can be seen that the effective response of the mechanical plus electrical correction system will yield a transmittability factor of one to some frequency considerably above the natural resonant frequency of the test stand itself.

In actual practice, it has been found that it is difficult to determine the constants used in equation (5). Therefore, the equation must restated in terms of resonant frequency and damping ratio.

PULSE THRUST MEASUREMENT SYSTEM BLOCK DIAGRAM

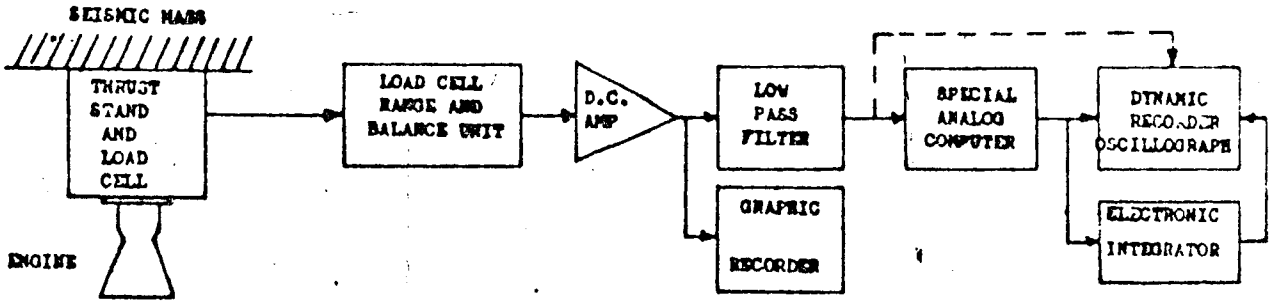

Figure 30

THRUST STAND FREQUENCY RESPONSE-COMPENSATOR
ACTION IN EXTENDING RESPONSE

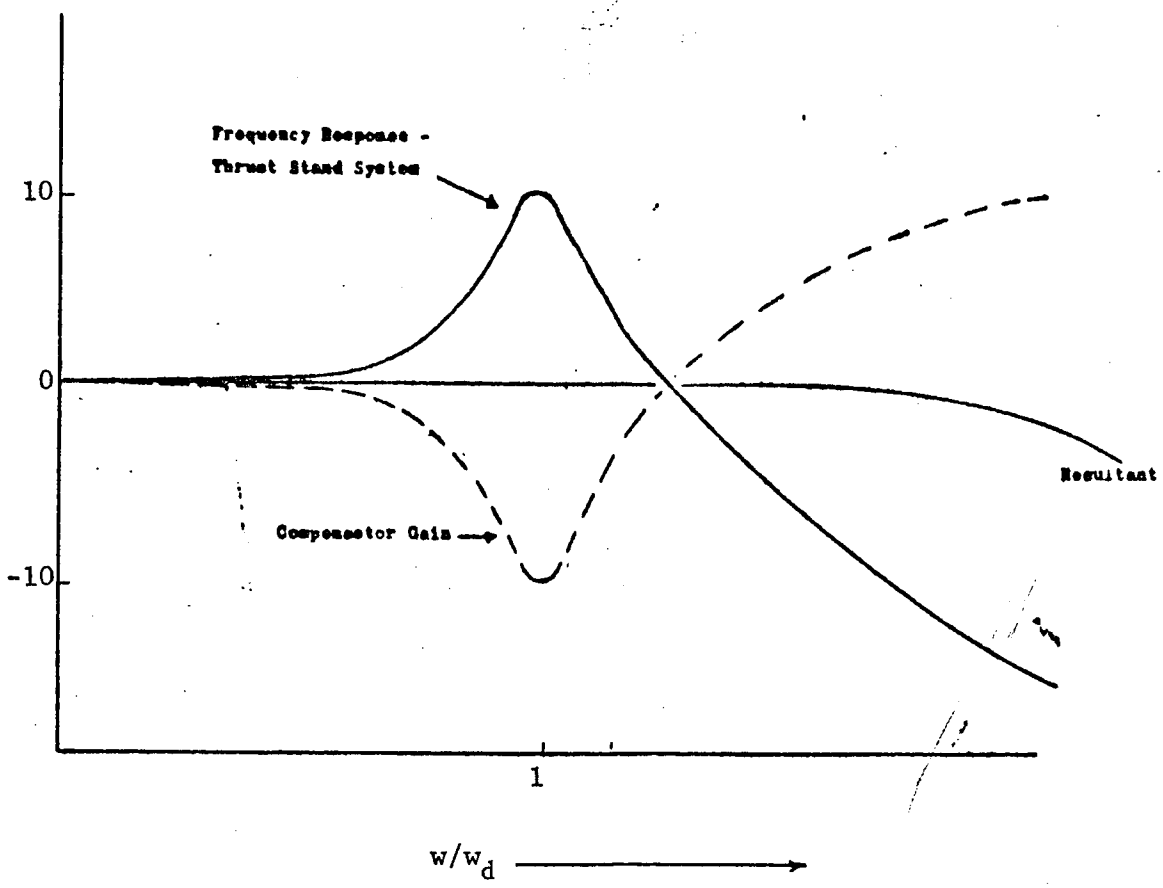

Figure 31

THRUST STAND SYSTEM FREQUENCY RESPONSE
WITH COMPENSATOR

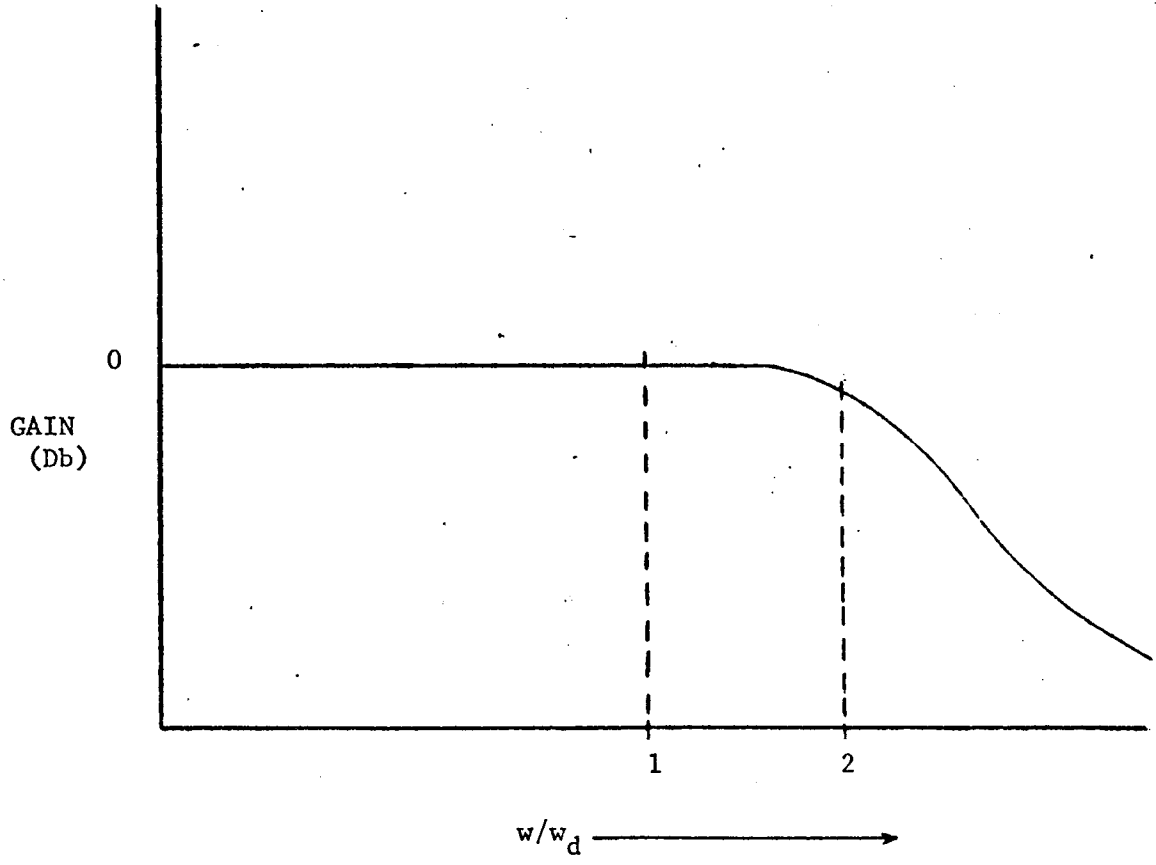

Figure 32

(6) $$\frac{F(t)}{k} = x + \frac{2\zeta}{W_n}\dot{x} + \frac{1}{W_n^2}\ddot{x}$$

where: k = spring constant

ζ = damping ratio

W_n = resonant frequency

The natural resonant frequency of the test stand can easily be determined by introducing a step change on the input system and observing the frequency at which the system rings. This frequency is the stand resonant frequency.

The damping ratio of the system can be determined by measuring the logarithmic decrement of amplitude of the oscillating system. The equation determining the logarithmic decrement is:

(7) $$\frac{x_1}{x_2} = e^d = r \text{ or } d = \ln r$$

where: x_1 = amplitude of one excursion of the resonant ringing

x_2 = the amplitude of the next oscillation

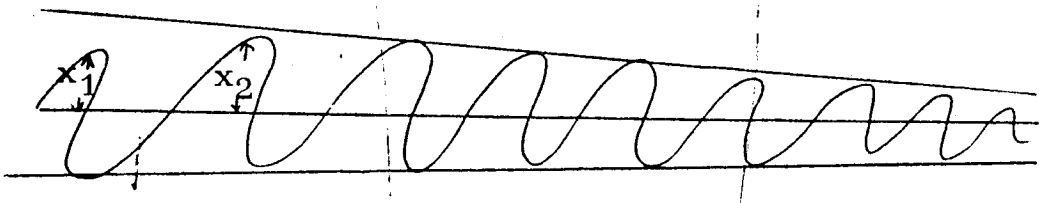

The damping ratio is then.

(8) $$\zeta = \frac{d}{2\pi}$$

Although the actual use the conditions are somewhat more complicated than described here, system operation has proven to be most outstanding. Thus, the output of the analog on-line computer circuit can provide voltages proportional to the force supplied to the measuring system to a frequency several times above the natural resonant frequency of the mechanical system.

The signal is recorded by a light beam galvanometer oscillograph which yields a trace proportional to the values of applied thrust.

This instantaneous value of thrust is also applied to an electronic integrator as shown in Figure 30.

The period of integration is determined by a signal from the electronic device which is pulsing the engine. Thus, the output of the integrator is a dc level proportional to the total impulse delivered to the thrust system during each individual engine pulse. The output of the integrator is reset to zero automatically before the beginning of each new pulse. This output level is recorded by an oscillograph for later data reduction.

The entire thrust system provides three different output recordings, an analog strip chart record representing steady-state thrust levels and analog records on an oscillograph representing instantaneous as well as integrated thrust values for a pulse type firing. The values obtained can then be used for precision performance analysis and research and development information.

Forces on the measuring load cell other than those produced by the engine are minimized by the use of a parallelogram arrangement which removes all load cell side forces and by routing and flexuring the various lines to and from the engine.

The thrust measuring load cell used in the thrust stand is a four active arm, semi-conductor, strain gage bridge type of load cell. The signal output of this load cell is 0.15 millivolts per volt per volt per pound. Total mechanical deflection for 100 pounds force is nominally 0.0007 inches. The calibration load cell is a working secondary standard type instrument. Its readout is digital and its calibration accuracy is 0.05 percent.

Propellant Flow Measurement

Both steady-state flow rate and total flow per pulse are required for determination of specific impulse (Isp) and oxidizer fuel ratio (O/F).

Steady state flow rate is measured with the use of turbine flowmeters. Pulse flow rate is measured by using a sight tube system. The sight tube system consists of a stainless steel cylinder paralleled by a glass tube. The propellant is stored in this sight tube assembly. The sight tube assembly is pressurized to the desired propellant run pressure with inert gas and the propellant is supplied to the engine when the engine valves are opened. The height of the propellant in the glass tube is recorded photographically before and after a series of engine pulses. The weight of the propellant flowing from the sight tube system to the engine is readily determined by knowing the calibration factor of the particular sight tube.

The formula for determining the weight flow of propellants from a sight tube system used is:

$$\omega = SP.GR. \times K_sT \times \Delta cm$$

where: SP.GR. is the specific gravity of the propellant, K_sT is the factor established through calibration of the sight tube using water or other medium-pounds per centimeter displacement of the sight tube. Δcm is the change in height of the sight tube.

The detailed design of the propellant sight tube system to measure engine pulse flow is extremely important as the design can effect engine performance as well as the accuracy of the measurement. Some of the items to be considered in the design are:

1. The sight tube assembly must be sized to obtain sufficient displacement on the sight glass in any particular test firing and also to reduce reading errors of the sight glass to an insignificant amount.

2. The dynamics of the propellant system influences the performance of engine when operating in a pulsing mode. The location of the sight tube assembly and the size and length of the line supplying the propellant to the engine must be carefully evaluated.

3. The temperature of the complete sight tube system must be accurately controlled as temperature variations within the system influences the accuracy of the measurement.

4. The sight tube pressurization system must be sized to maintain a fixed set pressure above the propellant in both the steady-state and pulsing mode of operation.

5. The complete sight tube system must be adequately instrumented to insure compliance with the pressure and temperature requirements specified for the test to be run.

The methods now used have evolved from the evaluation of many flow measuring schemes. Turbine type flowmeter have been used in all phases of the program for measuring steady-state flow rates. The semi-conductor strain gage vane type meter (Ramapo) was initially used to measure pulse flow rates. Since the output of this flowmeter was a square root function of the flow rate, it was necessary to incorporate a linearizer circuit into the electronic portion of the system. An electronic integrator was also used to integrate the total propellant flow per pulse in a series of pulses. Due to the number of components involved and the complexity of operating the many system components the reliability of vane type strain gage flowmeter system was lower than desired and therefore was used only in a small portion of the R-4D development program. Other methods evaluated for measuring pulse flow rate include a positive displacement flowmeter, a specially designed turbine type flowmeter, and special nozzle and orifice meters. Some basic development work was accomplished on a permanent magnet flowmeter which would measure the high response rates of the pulse flows but the sight tube proved adequate and work on the electromagnetic flowmeter was discontinued.

The flowmeters used in the initial phases of the R-4D program were calibrated with water only. It was soon determined that this one calibration was not adequate, particularly in oxidizer use, as major changes in calibration occurred with propellant usage. The North Test Area Facility was immediately set up to calibrate the flowmeters with propellants in addition to the water calibration. The propellant calibration of flowmeters has been maintained throughout the remaining portion of the R-4D program.

The calibration of turbine flowmeters with propellant and the use of the sight tube system for pulse flow measurement eliminated many of the flow measuring problems. It was, however, determined that the time period for recalibration of the turbine flowmeter was initially unpredictable. The solution to this problem was to install a turbine flowmeter calibration system in the test cell which could be used prior to each test run, if required. The sight tube system is now used to check the calibration of the turbine flow meter, with propellant at the particular pressure, temperature and propellant saturation conditions and in the cell. This calibration is readily accomplished in the cell by simple valving of the propellant system.

Temperature Measurement

The temperature of the engine and temperature of the propellants supplied to the engine have an effect on engine performance. Precise temperature measurements must be made to establish engine performance at the various environmental conditions as well as to minimize the temperature effects on other measured parameters. Precise temperature measurements must also be made to accurately establish the engine structural limitations and to control the temperature of the test facility processes. These temperatures range from -320°F to +4000°F.

Standard techniques (thermocouples, resistance bulb, etc.) are normally used to measure the temperatures up to 2000°F. Above this temperature photographic or optical methods of measurement are in use.

The Marquardt Corporation developed photographic temperature measuring technique is an example of TMC "state-of-the-art" techniques accomplished in the measurement field. This novel technique is used for temperatures from 1600°F to well above 4000°F with an accuracy within 1%. The heated image is projected on a radiation sensitive color photographic film, which virtually cannot be overexposed, through a calibrated lens system. By measuring the density of the projected color, an entire temperature profile can be obtained. Both still and motion picture photography are used. The film used is an "extended range film" (XR) manufactured by Edgerton, Germohauser & Grier, Inc., of Boston, Mass. This method of measuring temperatures produces the complete temperature distribution of the item being tested. Figure 33 is an example of the temperature distribution obtained.

COLUMBIUM CHAMBER EVALUATION USING XR FILM

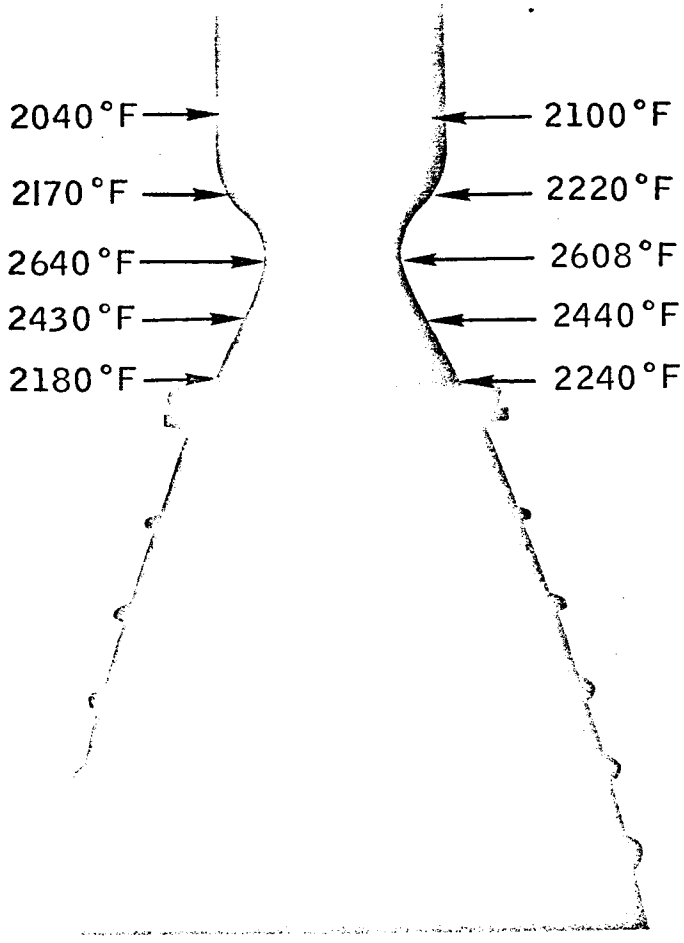

NEG. CT3434-1CN

ENGINE P/N T 12368

COMBUSTOR C129Y

COATING - SYLCOR 512

TEST NO. 3434

CELL NO. ATL PAD (D)

RUN NO. 24

MIXTURE RATIO 1.90

STEADY STATE CONDITION

DATE 7/19/66

Figure 33

An automatic radiation ratio pyrometer (Thermo-O-Scope) is also used to measure the higher temperatures. This type of pyrometer eliminates the errors caused by the geometry of the object, the emittance of the object and radiation attenuating material in the optical path between the radiation source and detector. This is accomplished by measuring the ratio of the radiant powers of two discreet wave-bands. Radiant power from the hot target is allowed to fall on two photo-multiplier detectors, each equipped with a filter. One filter transmitts radiation around 0.65μ and the other in a band around 0.55μ. The amount of radiation falling on the photomultipliers is automatically regulated by a motor driven iris. The iris operates in a servo-loop which works to keep the red tube ($.65\mu$) output signal roughly constant. In addition, an electronic loop adjusts the high voltage applied to both photo-tubes to keep the red output exactly constant. Maintaining the red output constant permits the value of the green tube (0.55μ) output to equal the ratio of the multiplier by a proportionality constant. This enables the ratio of the two signals to be read out directly as temperature by means of a simple differential voltmeter.

The ratio pyrometer was normally focused on the throat of the engine as this was the point of highest heat transfer and the highest temperature for all performance tests of the engine.

The optical temperature measuring systems are calibrated using the same material that will be reviewed in the test. This material is resistance heated and temperature of the system being calibrated compared with the temperatures recorded on a standard pyrometer. The standard pyrometer is periodically calibrated against a GET24 pyrometer calibration lamp periodically certified by the National Bureau of Standards.

Pressure Measurement

The range of pressure measurements on the R-4D program varied from less than 0.0002 psia to several thousand psia. The frequency response of these measurements varied from steady-state to several thousand cycles per second. The type of instrumentation varies therefore from standard gages to high response piezo-electric transducer with oscilloscope camera recording systems.

Combustion chamber, propellant inlet and the cell pressures normally use a strain gage type transducer, the output of which is recorded on an oscillograph or strip chart recorder.

High frequency piezo-electric pressure transducers have been a useful tool in evaluating combustion phenomena. These transducers are flush mounted in the walls of the combustion chamber as well as in the propellant inlet lines. The output of the transducers are recorded on oscilloscope cameras or on an oscillograph. In event only peak pressures are required, the output of transducer is fed to a peak meter and this peak pressure recorded on a strip chart recorder. The peak

meter measures the peak pressure value of a pressure change occurring in 10 microseconds or greater. The oscilloscope-camera recording system has a frequency response above 50,000 cps. The temperature drift of the piezo-electric transducer has been greatly reduced by placing an ablative material, TRV, over the face of the transducer.

Moisture in the system connectors have caused some malfunctions. It is now standard practice to seal these connectors when the system is being installed. A special transducer mount design is in use. In the normal installation of the transducer, propellants would collect around the sides of the transducer which would subsequently burn and fail the transducer by over pressurizing the transducer sides. This cause of failure was eliminated by re-locating the transducer pressure seal.

The cell pressure measuring devices include strain gage transducers thermocouple, Pirani, McLeod and Alphatron gauges. The choice of the particular gauge is dependent upon the particular test requirements.

VI. TEST PROCESS CONTROL AND DOCUMENTATION

In addition to trained personnel, good test facilities, and precise measurements; a successful test program must contain tight control of the test processes and useful documentation of each test. This insures that all of the customer and/or Government requirements are met and that a complete history of each test is available for future review.

Prior to each test program, a Marquardt Test Plan (MTP) or Marquardt Test Specification (MTS) is written which states the type of test of be conducted, the test limits and data requirements. This MTP or MTS is then signed by the customer to verify that the particular test objectives are being met. Test Department Procedures (TDP's) are then written which specify the test setup and a step by step operation to be followed by the test operator for this particular test. Normally in parallel with the writing of the TDP the test facility and/or test setup is designed, fabricated and installed for the particular test. The operating personnel are trained on the particular test and given written tests to verify their knowledge on the facility operation for the test program. To integrate all of these elements; operating personnel, test facilities and/or test setup and written procedures; a referee test item is tested to insure that all elements function together. At this point a certified facility is ready for use on the particular test program.

The general specification; customer, government and other; which must also be followed are further defined by addition of Test Department Procedures, Materials & Process Specification, Quality Assurance Procedures and by Engineering Drawings. A diagram of the controls established for an engine cell firing acceptance test is shown on Figure 34.

TYPICAL CONTROL ESTABLISHED FOR
ENGINE CELL FIRING ACCEPTANCE TEST

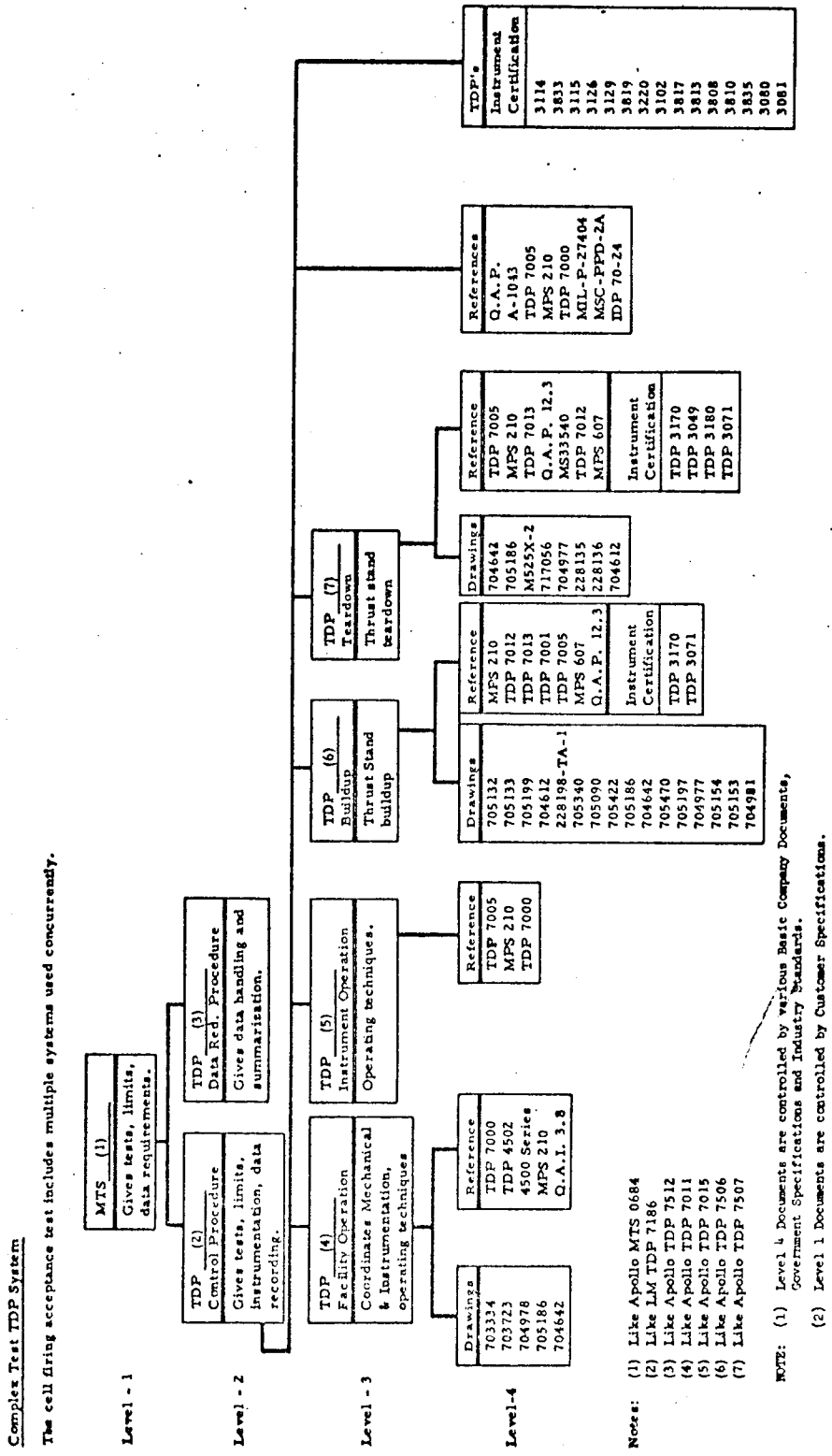

Figure 34

The basic TDP's written for the particular test program also serves as documentation as each major step of the operation is either signed off by the test operator or stamped by the Test Inspector.

CHAPTER 13

TEST DATA ANALYSIS

BY

R. POORMAN

TABLE OF CONTENTS

		Page
I.	SUMMARY	13-1
II.	INTRODUCTION	13-1
III.	CURRENT DATA REDUCTION AND ANALYSIS TECHNIQUES	13-4
	Multiple Correlation Program	13-4
	Engine Hydraulic Characteristics	13-4
	Steady State Performance Reduction	13-5
	Pulse Performance Reduction	13-15
	Temperature Data Reduction	13-19
	Ignition Data Reduction	13-21
IV.	ERROR ANALYSIS	13-23

LIST OF ILLUSTRATIONS

Figure Number	Title	Page
1	Steady State CDAE Burn	13-6
2	Steady State Firing - Test Condition	13-13
3	Steady State Firing - Corrected to Standard Conditions	13-14
4	Oscillograph Pulse Trace	13-16
5	Pulse Firing - 50 millisecond Runs	13-20
6	Temperature vs. Time	13-22

LIST OF TABLES

Table Number	Title	Page
I	Steady State Error Analysis for Calculated Parameters	13-24
II	Steady State Test Data Errors	13-25
III	Pulse Performance Error Analysis	13-26
IV	Pulse Time Error Analysis	13-27

I. SUMMARY

The data reduction and analysis techniques developed during the R-4D program are discussed. This includes the chronological history of significant techniques leading up to and including computer processing of steady state performance, pulse performance, and thermal performance data.

II. INTRODUCTION

Engine testing during the development phase of the R-4D program was varied from test to test to define the operating characteristics of each engine configuration. Data reduction requirements consisted of converting raw data from strip chart, oscillograph and other associated test data records into meaningful engineering unit data. Requirements included the reduction of test data for steady state performance, pulsing performance, thermal characteristics, and ignition characteristics.

R-4D engine tests conducted with end item production hardware require additional data calculations, as well as analysis programs for statistical information and production control. The production engine burn test data are corrected to standard manifold inlet pressure and propellant temperature conditions.

Data reduction and analysis techniques and procedures have evolved from complete hand reduction of data to the present computerized methods, combining higher quality data results with cost savings.

A Clary DE-60 desk-type digital computer was used for approximately two and one-half years for computing steady state and pulse performance data. The Clary computer was also used for limited statistical calculations. Although limited in size and capability, the Clary computer was available for usage at any time and bridged the gap between complete hand reduction and IBM data processing.

The reduction of pulse performance data was significantly changed by the coupling of a Gerber Model GDDRS-3B Digital Data Reduction System to an IBM key punch machine. Data previously reduced by hand from raw data with performance data calculated by hand or Clary Computer, could be read by the Gerber system in digital form and punched directly onto IBM cards for computer processing.

The CalComp Model 750 magnetic tape plotting system, in conjunction with the IBM OS 360 computer, provides the capability of plotting data automatically with complete plot identification. Plot routines included in data reduction programs provide the capability of reading data in raw form, processing the data by computer and automatically plotting the results for final presentation in one job step.

Chronology of Data Reduction and Analysis Techniques

At the start of the Development phase of the R-4D test program in 1962, all test data were reduced by hand. This included the drawing of calibration curves, the reading and hand tabulating of data from strip charts, and the hand calculation of performance parameters on desk-top rotary calculators. The process was very time consuming and required extra time for checking data due to the human error factors involved. The results were tabulated by hand which required additional labor to type the results in a suitable format acceptable for engineering reports, etc.

Data Processing by Clary Computer

In April 1964 a Clary Model DE-60 desk-type digital computer was installed in TMC's Rocket Systems Division on a trial basis. The Clary Model DE-60 computer consists of an 80 instruction program board that can be wired to perform mathematical calculations and print out required results on a modified electric typewriter. During the trial period, a program board was prepared to calculate steady state performance data. Even with the aid of this desk type computer, reduction of recorded parameters from raw test cell data continued to be reduced by hand methods. The time saving involved in performing the data calculations was an order of magnitude (10 to 1) resulting in an overall time reduction of approximately 60%. In addition to the basic computing assets derived from the use of the Clary computer, the typed data output produced by the unit afforded a considerable cost saving due to the engine performance being presented in a format suitable for use in engineering reports without additional work.

The Clary computer was a leased item, leased on an annual basis commencing in May 1964. After acquiring the computer, program boards were wired to compute both engine steady state and pulse performance, the results of which confirmed the anticipated cost savings to the data reduction effort. The Clary computer was used for calculating a printout of steady state and pulse performance data until the IBM computer was installed at The Marquardt Corporation, Van Nuys facilities, after which it was used as an alternate method until the return of the equipment to the supplier in September 1966. Data reduced with the Clary computer included the processing of Development test data, Pre Flight Rating Test (PFRT), and end item burn test data.

Data Processing by IBM Computer

In 1965 work was started to convert existing Clary programs to process data on an IBM 7040 computer system installed at The Marquardt Corporation. The advantages to this method were far greater than the Clary computer method. Due to the large core storage capacity, programs were expanded to accept digital calibration data and digital data readings with all data calculations performed by the computer. The first operational program used on the 7040 computer system was the pulse performance program.

In May 1965 the programming effort was started on the IBM 7040 pulse performance program. In conjunction with the programming effort, a Gerber Model GDDRS-3B Digital Data Reduction System was coupled to an IBM Model 026 keypunch machine to increase the efficiency of the pulse data reduction. Whereas previous to this date pulse performance and time information was reduced by hand, the Gerber method produces digital counts for calibrations and data which are automatically punched on IBM cards to be processed by the computer program. Additional data diagnostics are printed out to ensure the high quality of the data results. In May 1966, the pulse performance program was updated to be compatible with an IBM 360 computer system.

In June 1965 the programming effort commenced on an IBM 7040 steady state performance program. The new program computed all required performance parameters from digital input data, thus increasing the data reduction efficiency and making previous hand reduction techniques obsolete. Additional data diagnostics were printed out to ensure the high quality of the data results.

The original steady state performance reduction program has been modified as required to incorporate new data reduction and analysis techniques. Sight tube flow rate measurement capabilities have been added with the option of propellant calibrating turbine flowmeters from sight tube data runs. Engine hydraulic coefficient (C_DA_E) calculations are performed. In June 1966 the steady state performance program was modified to be compatible with the IBM 360 Computer System.

In December 1965, programming effort commenced on the original IBM 7040-CalComp automatic plotting programs. Many plot routines having been prepared, however, the primary data reduction plot program is used to plot engineering data parameters as a function of run time.

Previous to the computer-CalComp plotter method, all Engineering curves were prepared by hand from the tabulated data. The computer-CalComp plotter method provides the capability of reducing data by computer from digital input data and writing the results out on a magnetic tape for automatic plots which are completely identified with title information and X and Y axis identification.

III. CURRENT DATA REDUCTION & ANALYSIS TECHNIQUES

Multiple Correlation Program (P4009)

The multiple correlation program is used to determine the relationship of one dependent variable as a function or a series of functions of any number of independent variables, where the dependent variable is linearly dependent on the remaining functions. The functional relationship is defined by the user in the form of a subroutine to the main program.

The program performs a regression analysis by method of least squares to determine the linear coefficients of the desired functions. These coefficients can be used to determine an estimate of the dependent variable as a function of the independent variables. The resulting estimate gives the least average error within the given range of the original variables.

In addition to the regression analysis, the program computes an unbiased standard error of estimate. The standard error of estimate is defined as a one sigma deviation to be expected as a result of the given data being a representative sample of an infinite population of data.

The multiple correlation program has been used effectively indetermining many functional relationships with primary importance in determining R-4D "influence coefficients" and burn to water hydraulic coefficient relationships as discussed later on in this report.

Engine Hydraulic Characteristics (C_DA_E)

An effective method of comparing and analyzing the results of engine performance is the hydraulic coefficient (C_DA_E); defined as the pound-per-second flow rate divided by the square root of the product of injector pressure drop and test fluid specific gravity.

$$C_DA_E = \frac{\dot{w}}{\sqrt{(\Delta P)\ (S.G.)}}$$

The relationship of acceptance test burn C_DA_E to the respective preburn water C_DA_E was first compiled for a sample of seventy-four Model R-4D engines in December of 1965. The best estimate of the burn to water relationship was determined by the multiple correlation program. The best estimate of the burn C_DA_E was computed as a linear first order function of the preburn water C_DA_E with the associated error band to be expected with future engine samples.

The C_DA_E burn to water ratio has been used effectively in pinpointing test facility instrumentation problems and in analyzing burn information where engines have had to be reorificed to conform to burn acceptance test limits. A sample of burn test C_DA_E and the C_DA_E burn to water ratio is presented in Figure 1.

Steady State Performance Reduction

Steady state performance of the Model R-4D engine refers to continuous engine firing for a time duration greater than one second. As previously discussed in this section, current data reduction procedures include processing of data by an IBM 360 Computer System. Program options include the capabilities of performing diagnostics of data parameter accuracies, test condition input and calculated performance parameters and the correction of test condition data to standard manifold inlet pressures and propellant temperatures.

The data parameters for burn tests are recorded on Bristol and Esterline-Angus flow pen strip chart recorders including high speed light sensitive oscillograph recorders and polaroid photographs of sight tube propellant levels. Test parameters used as input for steady state performance calculations are normally recorded in the following form.

Parameter	Flow Pen Strip Chart Recorder	Light Sensitive Oscillograph Recorder	Polaroid Photograph
Thrust	×	×	
Chamber Pressure	×	×	
Oxidizer Manifold Inlet Pressure	×	×	
Fuel Manifold Inlet Pressure	×	×	
Cell Pressure	×	×	
Turbine Meter Oxid.Propellant Flow Measurement	x D.C.	× A.C.Scalers	
Turbine Meter Fuel Propellant Flow Measurement	x D.C.	× A.C.Scalers	
Sight Tube Oxid. Propellant Flow Measurement			×
Sight Tube Fuel Propellant Flow Measurement			×
Oxidizer Propellant Temperature	×	x	
Fuel Propellant Temperature	×	x	

× - Primary recording mode.
x - Backup recording mode.

Additional test information, including the instrument calibrations, are recorded in Test Department Procedures (TDP's) and Test Cell Log Sheets which provide for complete documentation of the test procedures as required and specified for each engine test.

STEADY STATE C_DA_E BURN

SIGHT TUBE RUN AVERAGE OF 7 RUNS

P/N S/N TEST DATE

RUN NUMBER	OX CDAE X 1000	OX CDAE (BURN/H20)	OX TEMP	FUEL CDAE X 1000	FUEL CDAE (BURN/H20)	FUEL TEMP
5938	19.336	1.028	72.0	14.649	1.001	72.3
5939	19.197	1.020	72.9	14.593	0.998	72.9
5940	19.254	1.023	72.2	14.587	0.997	72.6
5945	18.990	1.009	24.2	14.580	0.997	77.0
5946	18.920	1.006	23.2	14.582	0.997	76.2
5948	18.997	1.010	24.3	14.505	0.992	71.4
5949	19.021	1.011	25.2	14.503	0.991	73.3
AVERAGE	19.102		44.9	14.571		73.7

Figure 1

All computer inputs for processing steady state performance data is punched on IBM input cards. Pressure transducer pound per square inch calibration values are coded and punched onto IBM cards with their respective recorder deflection unit levels from a zero reference punched to the nearest one hundredth of an inch. The deflection unit levels for engine run data are key punched by the same method as that used for the placing of calibration values on the cards.

Single point thrust load cell mechanical calibrations are taken at various times during a test, usually at a time prior to each run. Calibration and run data points are coded and punched onto IBM cards by the same method as pressure data parameters described above.

Engine flow rates are normally recorded by turbine flowmeters or by the sight tube system of measurement which consists of a stainless steel tube of one-half inch nominal I.D. and a glass tube of five millimeters nominal I.D. connected in parallel. The stainless steel tube provides the necessary augmentation for flow through the sight tube. The computer program has the option of accepting input data for either method.

The turbine meter output in the form of A.C. scaler cycles is recorded on the oscillograph recorder. Flowmeter cycles are counted for a 0.5 second period at the time point reduced, the result is multiplied by two to provide cycles per second experienced by the meter, this data is then punched onto IBM cards. The flowmeter calibration data in the form of cycles per second and corresponding lb H_2O referenced to 4°C are punched on IBM cards with a sufficient number of calibration points to cover the range of cycle per second test data. An alternate strip chart recorded DC trace of flowmeter output may also be punched onto IBM cards by the same method as pressure data parameters. Calibration data is input the same for either reduction method.

Sight tube propellant flow measurement data inputs are in the form of prerun and post run propellant levels in the sight tubes punched on IBM cards to the nearest one hundredth of a centimeter. The augmented sight tubes are calibrated on an annual basis in the TMC Standards Laboratory, the results of these calibrations are input into the program in the form of pounds of H_2O per centimeter.

Various additional program inputs are required for data identification, some of which are the engine part number, engine serial number, test date, injector head and valve assembly part number and serial number, test run numbers and the actual run times of the run being reduced are required and necessary for the correct identification of the printed output data.

Calculations are performed to convert the measured strip chart deflection units to engineering units, the results are then used to calculate additional required engine performance and related parameters. The results of such calculations are printed out in a standard type format from which direct copies are made for use in the final test reports.

The engineering unit - strip chart deflection unit calibrations are evaluated by a sub-routine called LINFIT. LINFIT computes the best fit least squares linear relationship between the engineering unit calibration values and their corresponding strip chart deflection unit values. The sub-routine returns the slope (engineering units per one unit deflection change), the intercept (engineering units), one standard error of estimate about the correlation (engineering units) and a coefficient of correlation to the main program. The slope (m) and intercept (b) are used to calculate engineering unit run data (y) from run data deflection units (x) where $Y = mx + b$. The standard error of estimate and coefficient of correlation indicates the accuracy of the calibrations.

Propellant temperature calibrations are in millivolts vs. deflection units and the resulting run data are in millivolts. A sub-routine called TEMP converts the millivolt data into degrees fahrenheit based on the thermocouple type and returns the converted data to the main program. The correlation of millivolts to degrees fahrenheit is based on NBS Circular 561.

Fuel and oxidizer propellant flow rates may be measured by two different methods - turbine flowmeters or sight tubes. Turbine meter flow rates are determined by computing the pound H_2O per cycle calibration factor ("K") and multiplying the "K" factor by the run point cycles per second and the run specific gravity.

The sight tube flow rates are determined by computing the difference in sight tube centimeter level from prerun to post run multiplied by the sight tube H_2O pound per centimeter calibration factor and the run specific gravity divided by the run time.

The following test condition input parameters are calculated by the program.

1. Thrust - pounds
2. Chamber pressure - psia
3. Oxidizer manifold pressure - psia
   (a) Set (non-flowing)
   (b) Inlet (flowing)
4. Fuel Manifold Pressure - psia
   (a) Set (non-flowing)
   (b) Inlet (flowing)
5. Cell pressure - psia
6. Oxidizer propellant temperature - °F
7. Fuel propellant temperature - °F
8. Oxidizer specific gravity
9. Fuel specific gravity
10. Oxidizer flow rate - pps
11. Fuel flow rate - pps

Additional performance calculations are made as follows:

1. Vacuum thrust - lbs. = test thrust + (exit area × cell pressure).
2. Propellant flow rate - pps = oxidizer flow rate + fuel flow rate.
3. Mixture ratio = oxidizer flow rate/fuel flow rate.
4. Specific impulse - sec. = vacuum thrust/propellant flow rate.
5. Characteristic velocity - ft/sec. = (chamber pressure × g × throat area)/propellant flow rate.
6. Thrust coefficient = vacuum thrust/(throat area × chamber pressure).
7. Oxidizer side injector pressure drop - psi = oxidizer manifold pressure - chamber pressure.
8. Fuel side injector pressure drop - psi = fuel manifold pressure-chamber pressure.

The program provides an option to correct test condition data to standard manifold inlet pressures and propellant temperatures for presenting all data results at nominal conditions. The TMC procedure for correcting test data to standard conditions is presented in TMC Report A-1050A, MTS 0684, Appendix IV.

Abreviations and symbols used for performance parameters herein are as follows:

C^*	Characteristic velocity - feet per second
C_f	Thrust Coefficient
F_{VAC}	Vacuum Thrust - lbs.
I_{sp}	Specific Impulse - seconds
O/F	Mixture Ratio
P_{ch}	Chamber Pressure - psia
S_{g_o}	Oxidizer Specific Gravity
S_{g_f}	Fuel Specific Gravity
T_P	Average of oxidizer and fuel propellant
P_{m_o}	Oxidizer Manifold Inlet Pressure (flowing)- psia temperature
P_{m_f}	Fuel Manifold Inlet Pressure (flowing) - psia
$\dot{w}_o$	Oxidizer flow rate - pps
$\dot{w}_f$	Fuel flow rate - pps
$\dot{w}_p$	Sum of the fuel and oxidizer propellant flow rates - pps
ΔP_o	Oxidizer side injector pressure drop - psi
ΔP_f	Fuel side injector pressure drop - psi
g	Gravitational constant - 32.2 feet per second.

Additional subscripts used:

t test condition data

s standard condition data.

Standard condition performance parameters are calculated as follows:

$$(O/F)_s = (O/F)_t \sqrt{\left(\frac{S_{g_o}}{S_{g_f}}\right)_s \times \left(\frac{S_{g_f}}{S_{g_o}}\right)_t \times \left(\frac{\Delta P_f}{\Delta P_o}\right)_t}$$

$$Rc^* = 1 + \left[\left(\frac{\Delta C^*}{\Delta O/F}\right)\left[(O/F)_s - (O/F)_t\right] + \left(\frac{\Delta C^*}{\Delta T_p}\right)_t \times \left(T_{P_s} - T_{P_t}\right)\right]\left(\frac{1}{C^*}\right)_t$$

$$(\dot{w}_f)_s = \frac{-b + \sqrt{b^2 + 4ac}}{2a}$$

where: $a = 1$

and $b = \left[\frac{1 + (O/F)_s}{1 + (O/F)_t}\right]\left[\frac{(\dot{w}_f)_t\ (Pch)_t}{(\Delta P_f)_t}\right]\left[\frac{(S_{g_f})_s}{(S_{g_f})_t}\right]\left(Rc^*\right)$

and $c = (\dot{w}_f)_t^2 \left[\frac{(S_{g_f})_s}{(S_{g_f})_t}\right]\left[\frac{(Pmf)_s}{(\Delta P_f)_t}\right]$

$$(\dot{w}_o)_s = (\dot{w}_f)_s\ (O/F)_s$$

$$(\dot{w}_p)_s = (\dot{w}_f)_s + (\dot{w}_o)_s$$

$$(I_{sp})_s = (I_{sp})_t + \left[\left(\frac{\Delta I_{sp}}{\Delta O/F}\right)\left[(O/F)_s - (O/F)_t\right] + \left(\frac{\Delta I_{sp}}{\Delta T_p}\right)\left[(T_p)_s - (T_p)_t\right]\right]$$

$$(F_{VAC})_s = (I_{sp})_s\ (\dot{w}_p)_s$$

$$(C^*)_s = (C^*)_t \, (Rc^*)$$

$$(Pch)_s = \left[(Pch)_t \, (\dot{w}_p)_s \, (Rc^*)\right] \div (\dot{w}_p)_t$$

$$(C_f)_s = \left[(I_{sp})_s \, (\varepsilon)\right] \div (C^*)_s$$

All data terms required for the standard condition equations defined above come from test condition parameters except the values of $\left(\frac{\Delta C^*}{\Delta O/F}\right)$, $\left(\frac{\Delta C^*}{\Delta T_P}\right)$, $\left(\frac{\Delta I_{sp}}{\Delta O/F}\right)$ and $\left(\frac{\Delta I_{sp}}{\Delta T_P}\right)$ defined as "influence coefficients." These four "influence coefficients" were defined for the R-4D engine by correlating 5 second burn data for Engine P/N T-11042, S/N 0001-8 tested with nitrogen tetroxide and aerozine-50. The multiple correlation program was used to compute the regression coefficients defining specific impulse and characteristic velocity as a function of propellant temperature and mixture ratio. The matrix of test data analyzed included propellant temperatures in the range of 30°F to 120°F and mixture ratio data from 1.7 to 2.2.

The engine firing data were fitted to an equation of the form

$$I_{sp} = A_1 + A_2(T_P) + A_3 \, (T_P)^2 + A_4(O/F) + A_5(O/F)^2 + A_6(O/F) \, (T_P)$$

A similar equation was used for the C* correlation.

A simplification of the use of these coefficients for data correction was effected by evaluating the first partial derivatives of I_{sp} and C*; namely

$$\left(\frac{\partial I_{sp}}{\partial O/F}\right)_{T_p} \left(\frac{\partial I_{sp}}{\partial T_P}\right)_{O/F} \quad \left(\frac{\partial C^*}{\partial O/F}\right)_{T_p} \quad \text{and} \left(\frac{\partial C^*}{\partial T_P}\right)_{O/F} \quad \text{at } O/F = 2.0$$

and $T_P = 75°F$. The final "influence coefficients" used in the correction to standard equations are:

$$\left(\frac{\Delta I_{sp}}{\Delta O/F}\right) = -45$$

$$\left(\frac{\Delta I_{sp}}{\Delta T_P}\right) = +0.135$$

$$\left(\frac{\Delta C^*}{\Delta O/F}\right) = -769$$

$$\left(\frac{\Delta C^*}{\Delta T_P}\right) = +2.397$$

These "influence coefficients" are valid for R-4D engines tested with nitrogen tetroxide and aerozine-50 at manifold inlet pressures designed to produce a nominal mixture ratio of 2.0 with propellant at ambient temperature. In October, 1967 the "influence coefficient" equations were rewritten using Taylor's Theorem for a function of two variables. This allows for test condition data between the limits of 30°F and 120°F propellant temperature, and mixture ratios of 1.7 to 2.2 to be corrected to standard conditions.

Computer output is in the form of printed pages of tabulated performance data suitable for presentation as final output and in the form of punched cards.

The printed output includes test condition data identified by run number and run time and optional standard condition data. Examples of test condition and standard condition printed output data are presented in Figures 2 and 3, respectively. The standard error of estimate and coefficient of correlation values are printed out for all calibrations processed by the subroutine LINFIT, and provide a method of checking the accuracies involved in determining the calibration slopes. If three standard error of estimates (3σ) for chamber pressure, oxidizer or fuel manifold pressure or cell pressure are greater than the expected errors based on a previous calibration analysis, an error message is printed out indicating the need for checking the input data.

C_DA_E results for the preburn waterflow test are printed out if the option is specified. Oxidizer and fuel C_DA_E data are printed out for all burn test runs and the ratio of burn to water C_DA_E results are printed if the water data is specified.

When the correction to standard option is specified, an analysis matrix consisting of the mean, minimum value, maximum value, difference between the minimum and maximum values and 1 sigma deviation is printed out for all performance parameters.

IBM punched cards are part of the program output and contain the performance parameters punched in the same format as the printed output. Card files are maintained for production burn tests and are invaluable for data correlations and further analyses.

1846-36C

PREPARED BY	CHECKED BY	DATA REDUCTION DATE
Edwin M. Fuller	Al Foster	

TEST DATE	TEST NO.	APPROVED BY & DATE
		MA 61

TMC P/N ____ S/N ____ SCD NO. ____

THE MARQUARDT CORPORATION

DATA SUMMARY SHEET

ENGINE ASSEMBLY FIRING TEST (Con't.)

STEADY STATE FIRING – TEST CONDITIONS

	RUN NO.	DATA STATION	cps_o	T_{fm_o} -°F	cps_f	T_{fm_f} -°F	F_{test} -lbs.	P_{cell} -psia	$P_{ch_{test}}$ - psia	P_{m_o} - psia set	P_{m_o} - psia inlet	P_{m_f} - psia set	P_{m_f} - psia inlet
5 SEC. RUN	11144	5	1280.	75.5	986.	76.0	97.8	.0502	94.5	183.0	169.8	177.0	170.5
	SG_o	SG_f	$\dot{w}_{o_{test}}$ -pps	$\dot{w}_{f_{test}}$ -pps	$\dot{w}_{P_{test}}$ - pps	O/F_{test}	$F_{vac_{test}}$ - lbs.	$I_{sp_{vac_{test}}}$ - sec.	$C_{f_{vac_{test}}}$	C^*_{test} -ft/sec.	ΔP_o -psi	ΔP_f -psi	
	1.4371	.8964	.2408	.1171	.3579	2.056	99.0	276.5	1.770	5027.	75.3	76.0	
50 SEC. RUN	11145	5	1277.	76.1	986.	76.0	98.1	.0512	94.4	183.1	170.2	177.2	170.7
	SG_o	SG_f	$\dot{w}_{o_{test}}$ -pps	$\dot{w}_{f_{test}}$ -pps	$\dot{w}_{P_{test}}$ - pps	O/F_{test}	$F_{vac_{test}}$ - lbs.	$I_{sp_{vac_{test}}}$ - sec.	$C_{f_{vac_{test}}}$	C^*_{test} -ft/sec.	ΔP_o -psi	ΔP_f -psi	
	1.4363	.8964	.2401	.1171	.3572	2.050	99.3	278.1	1.778	5031.	75.8	76.3	
5 SEC. RUN	11146	5	1280.	74.0	987.	74.5	98.0	.0525	94.5	183.1	170.1	177.5	170.9
	SG_o	SG_f	$\dot{w}_{o_{test}}$ -pps	$\dot{w}_{f_{test}}$ -pps	$\dot{w}_{P_{test}}$ - pps	O/F_{test}	$F_{vac_{test}}$ - lbs.	$I_{sp_{vac_{test}}}$ - sec.	$C_{f_{vac_{test}}}$	C^*_{test} -ft/sec.	ΔP_o -psi	ΔP_f -psi	
	1.4391	.8971	.2411	.1173	.3584	2.055	99.2	276.9	1.775	5019.	75.6	76.4	
5 SEC. RUN	11147	5	1277.	74.7	986.	75.1	97.9	.0521	94.5	183.1	170.1	177.1	170.6
	SG_o	SG_f	$\dot{w}_{o_{test}}$ -pps	$\dot{w}_{f_{test}}$ -pps	$\dot{w}_{P_{test}}$ - pps	O/F_{test}	$F_{vac_{test}}$ - lbs.	$I_{sp_{vac_{test}}}$ - sec.	$C_{f_{vac_{test}}}$	C^*_{test} -ft/sec.	ΔP_o -psi	ΔP_f -psi	
	1.4382	.8968	.2404	.1171	.3575	2.052	99.1	277.2	1.772	5032.	75.6	76.1	

A-1080

THE MARQUARDT CORPORATION

TMC P/N ____ S/N ____ SCD NO. ____

DATA SUMMARY SHEET

ENGINE ASSEMBLY FIRING TEST (Con't.)

A-1080

PREPARED BY	CHECKED BY	DATA REDUCTION DATE
Edwin M. Fuller	Al Foster	

TEST DATE	TEST NO.	APPROVED BY & DATE
		MA 51

STEADY STATE FIRING – CORRECTED TO STANDARD CONDITIONS

	RUN NO. SG_o	DATA STATION SG_f	$P_{ch_{test}}$ -psia	$\dot{w}_{f_{test}}$ -pps	$\dot{w}_{p_{test}}$ -pps	O/F_{test}	$I_{sp_{vac_{test}}}$ -sec.	C^*_{test} -ft/sec.	ΔP_o -psi	ΔP_f -psi
TEST DATA	11144	5								
	1.4371	.8964	94.5	.1171	.3579	2.056	276.5	5027.	75.3	76.0
	O/F_s	$I_{sp_{vac_s}}$ -sec.	$\dot{w}_{f_s}$ -pps	$\dot{w}_{o_s}$ -pps	$\dot{w}_{p_s}$ -pps	F_{vac_s} -lbs.	C^*_s -ft/sec.	P_{ch_s} -psia	$C_{f_{vac_s}}$	
CORRECTED TO STD. COND.	2.065	276.0	.1168	.2413	.3581	98.8	5018.	94.4	1.770	
	RUN NO. SG_o	DATA STATION SG_f	$P_{ch_{test}}$ -psia	$\dot{w}_{f_{test}}$ -pps	$\dot{w}_{p_{test}}$ -pps	O/F_{test}	$I_{sp_{vac_{test}}}$ -sec.	C^*_{test} -ft/sec.	ΔP_o -psi	ΔP_f -psi
TEST DATA	11145	5								
	1.4363	.8964	94.4	.1171	.3572	2.050	278.1	5031.	75.8	76.3
	O/F_s	$I_{sp_{vac_s}}$ -sec.	$\dot{w}_{f_s}$ -pps	$\dot{w}_{o_s}$ -pps	$\dot{w}_{p_s}$ -pps	F_{vac_s} -lbs.	C^*_s -ft/sec.	P_{ch_s} -psia	$C_{f_{vac_s}}$	
CORRECTED TO STD. COND.	2.057	277.6	.1168	.2401	.3569	99.1	5024.	94.2	1.778	
	RUN NO. SG_o	DATA STATION SG_f	$P_{ch_{test}}$ -psia	$\dot{w}_{f_{test}}$ -pps	$\dot{w}_{p_{test}}$ -pps	O/F_{test}	$I_{sp_{vac_{test}}}$ -sec.	C^*_{test} -ft/sec.	ΔP_o -psi	ΔP_f -psi
TEST DATA	11146	5								
	1.4391	.8971	94.5	.1173	.3584	2.055	276.9	5019.	75.6	76.4
	O/F_s	$I_{sp_{vac_s}}$ -sec.	$\dot{w}_{f_s}$ -pps	$\dot{w}_{o_s}$ -pps	$\dot{w}_{p_s}$ -pps	F_{vac_s} -lbs.	C^*_s -ft/sec.	P_{ch_s} -psia	$C_{f_{vac_s}}$	
CORRECTED TO STD. COND.	2.065	276.5	.1168	.2411	.3579	99.0	5014.	94.3	1.775	
	RUN NO. SG_o	DATA STATION SG_f	$P_{ch_{test}}$ -psia	$\dot{w}_{f_{test}}$ -pps	$\dot{w}_{p_{test}}$ -pps	O/F_{test}	$I_{sp_{vac_{test}}}$ -sec.	C^*_{test} -ft/sec.	ΔP_o -psi	ΔP_f -psi
TEST DATA	11147	5								
	1.4382	.8968	94.5	.1171	.3575	2.052	277.2	5032.	75.6	76.1
	O/F_s	$I_{sp_{vac_s}}$ -sec.	$\dot{w}_{f_s}$ -pps	$\dot{w}_{o_s}$ -pps	$\dot{w}_{p_s}$ -pps	F_{vac_s} -lbs.	C^*_s -ft/sec.	P_{ch_s} -psia	$C_{f_{vac_s}}$	
CORRECTED TO STD. COND.	2.057	277.0	.1168	.2404	.3572	98.9	5028.	94.4	1.772	

MEAN O/F_s	$\Delta O/F_s$	MEAN F_{vac_s} - lbs.	ΔF_{vac_s} - lbs.	MEAN $I_{sp_{vac_s}}$	$\Delta I_{sp_{vac_s}}$	
* 2.061	* 0.008	* 99.0	* 0.3	* 276.8	* 1.6	* LIMITS ARE AS INDICATED ON PAGE 7.

Pulse Performance Reduction

Pulse performance of the R-4D engine refers to an engine firing for a time duration less than one second in length. Pulse performance data is reduced by a Gerber Model GDDRS-3B Digital Data Reduction System coupled to an IBM Model 026 or 029 key punch machine. The reduced data are processed by an IBM 360 Computer System. Computer output is in the form of tabulated performance data and printed diagnostics of data parameter accuracies.

The major performance parameters for pulse performance burn test data are recorded on light sensitive oscillograph recorders due to the high speed data recording capabilities required to document engine and valve response characteristics. An example of a typical oscillograph recorded pulse trace is presented in Figure 4. (Normal recorder speeds are forty or eighty inches per second.) Oxidizer and fuel flow data are recorded on polaroid photographs of the sight tube levels before and after each pulse run. Propellant temperatures are recorded on Bristol flow pen strip chart recorders. Additional test information, including the instrument calibrations are recorded in Test Department Procedures (TDP's) and test cell log sheets completed as required for each engine test.

All inputs for processing pulse performance data are in the form of IBM punched cards. All oscillograph recorded data are reduced by the Gerber digital reader. The Gerber reader has X-axis and Y-axis adjustable hairlines with a sensitivity of 300 counts per one inch movement of the hairline along the X or Y axis. When the Gerber Reader is coupled to an IBM keypunch machine, the four position digital readout is automatically punched on an IBM card with a plus or minus sign.

Gerber deflection unit - engineering unit calibrations are punched for each oscillograph recorded parameter to be reduced. The program accepts inputs for the following oscillograph recorded data:

DATA PARAMETER	Usage
Electronic Integration of Thrust - lb/sec (single pulse)	Optional
Electronic Integration of Thrust - lb/sec for total run (variable number of pulses)	Optional
Electronic Integration of chamber pressure - psi-sec (single pulse)	Optional
Electronic Integration of chamber pressure for total run- psi-sec (variable number of pulses)	Optional
Cell Pressure - psia	Optional
Time of valve electrical on signal	
Time of oxidizer valve full open	
Time of fuel valve full open	

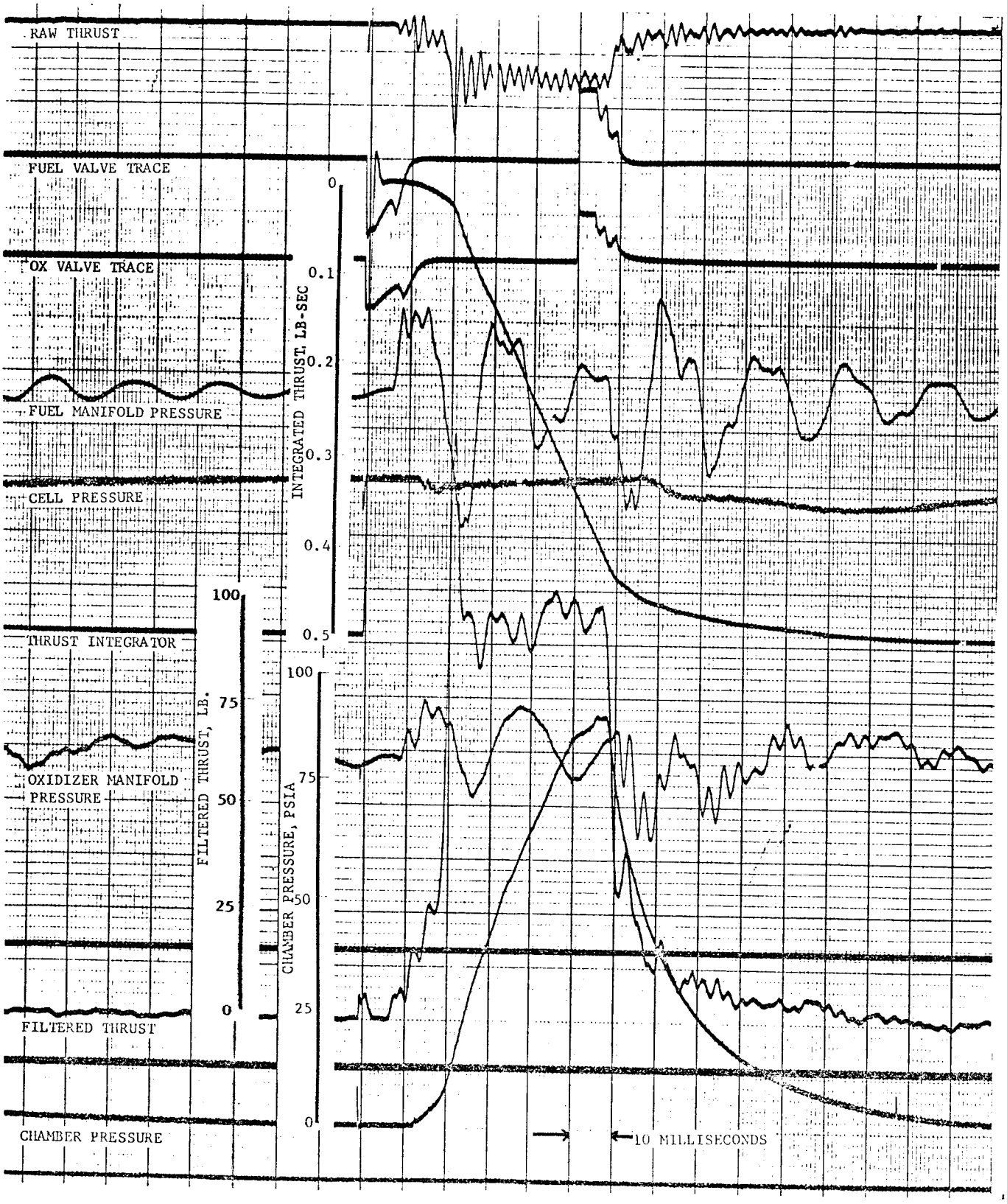

Typical Oscillograph Pulse Trace

Figure 4

DATA PARAMETER (Continued) Usage

Time of valve electrical off signal
Time of fuel valve full closed
Time of oxidizer valve full closed
Time of thrust start to rise
Time point where an extension of the thrust decay trace intersects zero thrust
Thrust readings defining the response characteristics (rise and decay) Optional

All data referencing events occurring at specific points in time during a pulse are punched on IBM cards by positioning of the Gerber X-axis hairline. A four point calibration is punched at an arbitrary increment of time, such that the total time span of the calibration covers the pulse being reduced.

Inputs for integrated thrust or chamber pressure are in the form of a deflection unit level for the electronic integrator at an initial point prior to the start of thrust or chamber pressure rise and at a point where thrust or chamber pressure has returned to the prerun zero level. Electronic integrator calibrations are recorded prior to each run at a constant input signal to the integrator. A four-point deflection unit calibration is input to the Program at a constant time interval to define the calibration slope.

Sight tube propellant flow measurement data inputs are in the form of prerun and postrun propellant levels in the sight tubes recorded to the nearest one hundredth of a centimeter. Current sight tube calibrations are input to the program in pounds of H_2O per centimeter.

Prerun and post run propellant temperatures are input in degrees fahrenheit.

The program performs calculations to convert input data into meaningful performance data to be printed out in a standard format.

The sub-routine LINFIT converts the four-point deflection unit time calibration for each pulse inot a millisecond per deflection unit slope by the best fit least squares linear relationship. Based on the time calibration and the data point readings, the following pulse time information data are calculated for each pulse reduced:

Electrical pulse width (the difference in time from electrical on to electrical off)
Effective pulse width (the difference in time from the point thrust starts to rise to the point where an extension of the thrust decay trace intersects zero thrust)
Oxidizer valve full open time (the difference in time from oxidizer valve full open to oxidizer valve full closed)

Electrical on to fuel valve full open
Electrical on to oxidizer valve full open
Electrical off to fuel valve full close
Electrical off to oxidizer valve full close
*Thrust Rise time (electrical on to the point where the thrust rise trace crosses X percent of full engine rated thrust)
*Thrust Decay time (electrical off to the point where the thrust decay trace crosses & percent of full rated thrust)

The electronic integrator calibrations for thrust and chamber pressure are converted to lb/sec or psi/second per deflection unit slopes by sub-routine LINFIT. The integrated thrust and chamber pressure data for a pulse run can be calculated for each pulse reduced if the off time between pulses is long enough for the thrust and chamber pressure traces to return to zero between pulses. Otherwise, the integrated thrust and chamber pressure data are calculated for the entire run and divided by the number of pulses to produce a pulse average. Vacuum impulse (integrated thrust) is computed as follows:

1. Individual Pulse reduction

vacuum impulse-lb/sec. = test impulse-lb/sec. + [(effective pulse width-sec.) × (exhaust nozzle exit area-in^2) × (cell pressure-psia)]

2. Total Pulse reduction

$$\text{Average vacuum impulse-lb/sec.} = \left[\text{total test impulse-lb/sec.} + \left[\left(\frac{\sum_{i=1}^{N} \text{effective pulse width-sec.}}{N}\right)(\text{exhaust nozzle exit area-in}^2)\left(\frac{\sum_{i=1}^{N} \text{cell pressure-psia.}}{N}\right)(M)\right]\right]/M$$

3. where N = number of pulses reduced
M = number of pulses in run.

Specific gravities of the fuel and oxidizer propellants are based on an average of the start and end of run propellant temperatures. Oxidizer and fuel propellant flows are determined by computing the difference in pre to post run sight tube centimeter levels multiplied by the sight tube H_2O pound per centimeter calibration factor and the run specific gravity. Additional performance data are calculated as follows:

*X and Y values are input variables.

Total propellant weight flow-lbs. = oxidizer propellant weight flow + fuel propellant weight flow

Mixture ratio = oxidizer propellant weight flow ÷ fuel propellant weight flow

$$\text{Average Pulse specific impulse-seconds} = \frac{(\text{average vacuum impulse})(M)}{\text{Total propellant weight flow}}$$

Computer output is in the form of printed pages of tabulated performance data suitable for presentation as final output. The reduced time and performance data are summarized with a single line of output for each pulse reduced. One line of average performance data for the entire pulse run is printed at the bottom of the last page of output for each run. The line of average output contains the following data:

Average fuel propellant temperature - °F
Average oxidizer propellant temperature - °F
Fuel propellant weight flow - lbs.
Oxidizer propellant weight flow - lbs.
Total propellant weight flow - lbs.
Mixture Ratio
Average Impulse - lb/sec. (arithmetic average of pulses reduced)
Average Specific Impulse - seconds
Average Oxidizer valve full open time - milliseconds (Arithmetic average of pulses reduced)
Average Effective pulse width - milliseconds (Arithmetic average of pulses reduced)
Average Electrical pulse width - milliseconds (Arithmetic average of pulses reduced)
Average Integrated Chamber pressure - psi/seconds (Arithmetic average of pulses reduced)

An example of pulse performance output is presented in Figure 5.

The standard error of estimate and coefficient of correlation produced by sub-routine LINFIT are part of the printed output for the integrated thrust, integrated chamber pressure and cell pressure calibrations for each run and the time calibration for each pulse reduced. These values provide a method of checking for input errors.

Temperature Data Reduction

Raw temperature data are processed by an IBM 360 Computer System. Two computer programs are currently being used to process data. Both programs produce tabulated output data and one program has an option to produce machine plots of temperature in degrees fahrenheit versus run time.

THE MARQUARDT CORPORATION

ENGINE ASSEMBLY FIRING TEST (Con't.)

DATA SUMMARY SHEET

A-1080

TMC P/N _____ S/N _____ SCD NO. _____

PREPARED BY	CHECKED BY	DATA REDUCTION DATE
Edwin M. Fuller	Al Foster	

TEST DATE	TEST NO.	RUN NO.	APPROVED BY & DATE
			MA 61

PULSE FIRING – 50 millisecond RUNS

PULSE NO.	t_p - ms	t_{e_p} - ms	t_{on} to VFO_f - ms	t_{on} to VFO_o - ms	t_{on} to .70 F - ms	t_{off} to VFC_f - ms	t_{off} to VFC_o - ms	t_{off} to .25 F - ms	$I_{t_{test}}$ - lb-sec.	P_{cell} - psia	$I_{t_{vac}}$ - lb-sec.
1	52.0	50.5	7.0	9.0	21.5	5.5	7.5	13.0	4.45	.058	4.52
5	54.0	50.5	7.0	9.5	21.5	6.0	7.0	13.0	4.40	.107	4.54
10	53.5	50.5	7.0	9.0	21.0	5.5	7.5	11.0	4.37	.119	4.52
15	56.0	50.5	7.0	9.0	20.5	6.0	7.5	13.0	4.42	.121	4.58
20	55.5	50.5	7.0	9.0	21.0	5.5	7.0	13.0	4.45	.128	4.61
25	56.0	51.0	7.5	9.5	21.5	5.5	7.0	12.5	4.44	.122	4.60
30	55.5	50.5	7.0	9.0	21.0	5.5	7.0	12.5	4.45	.121	4.61

T_{st_f} - °F (avg)	W_f - lbs.	T_{st_o} - °F (avg)	W_o - lbs.	W_p - lbs.	O/F	* $\frac{I_{t_{vac}}}{\text{pulse}}$ - lb-sec. (avg)	$\frac{I_{sp_{vac}}}{\text{pulse}}$ - sec. (avg)	t_p - ms (avg)	t_{e_p} - ms (avg)	
51.	0.2044	51.	0.3891	0.5935	1.903	4.568	238.6	54.6	50.6	* @ 4 CPS ☒ YES ☐ NO

LIMITS: $I_{sp} \geq 215$ sec.; t_{on} to .70F $\leq$ 26ms; t_{off} to .25F $\leq$ 15ms

General Temperature Reduction Program

The General Temperature Reduction Program provides for the reduction and printout of data from one to ten parameters where the test data can be reduced at the same data taking stations for all parameters. The results are printed out in a matrix with parameter headings and three additional columns allowed for identification such as run number, pulse number, run time, etc.

The program accepts data for iron constantan, chromel constantan and chromel alumel type thermocouples. The millivolt calibrations with their corresponding deflection unit levels are coded as to thermocouple type and punched onto IBM cards.* Deflection unit levels for data points are punched onto IBM cards by the same method as calibrations.

The calibration slope and intercept points are evaluated by sub-routine LINFIT. The test data are then computed and the results converted to degrees fahrenheit.

Temperature Reduction and Plot Program

The Temperature Reduction and Plot Program provides for the reduction, printout and automatic plotting of temperature data versus run time. The process for converting raw data into degrees fahrenheit is the same as discussed above, however, each parameter is handled separately. Therefore, the number of data points required to define the temperature trace as a function of run time may vary for each parameter.

The final plotted data results are controlled by the program user. One to twelve different temperature parameters can be plotted on a single graph. The Y-axis graph dimension is fixed at eleven inches with a maximum of nine inches available for plotting. The time (X axis length) and the X and Y axis scale factors are chosen by the program user. Each plotted parameter has a different symbol and the symbols can be connected by straight lines from point to point if desired. Each plot is identified by a main title and three subtitles of descriptive information and a table of the symbols used and their parameter identification. An example of a temperature time history plot is presented in Figure 6.

Ignition Data Reduction

Ignition tests on the R-4D engine are conducted to define the engine response characteristics and their effects on ignition pressures. Current data reduction procedures include the processing of data by IBM OS360 Computer.

*Although the program was designed primarily for temperature data reduction, a special code exists for reduction of parameters where calibrations can be input in engineering units and their corresponding deflection unit levels.

TEMPERATURE VS. TIME .

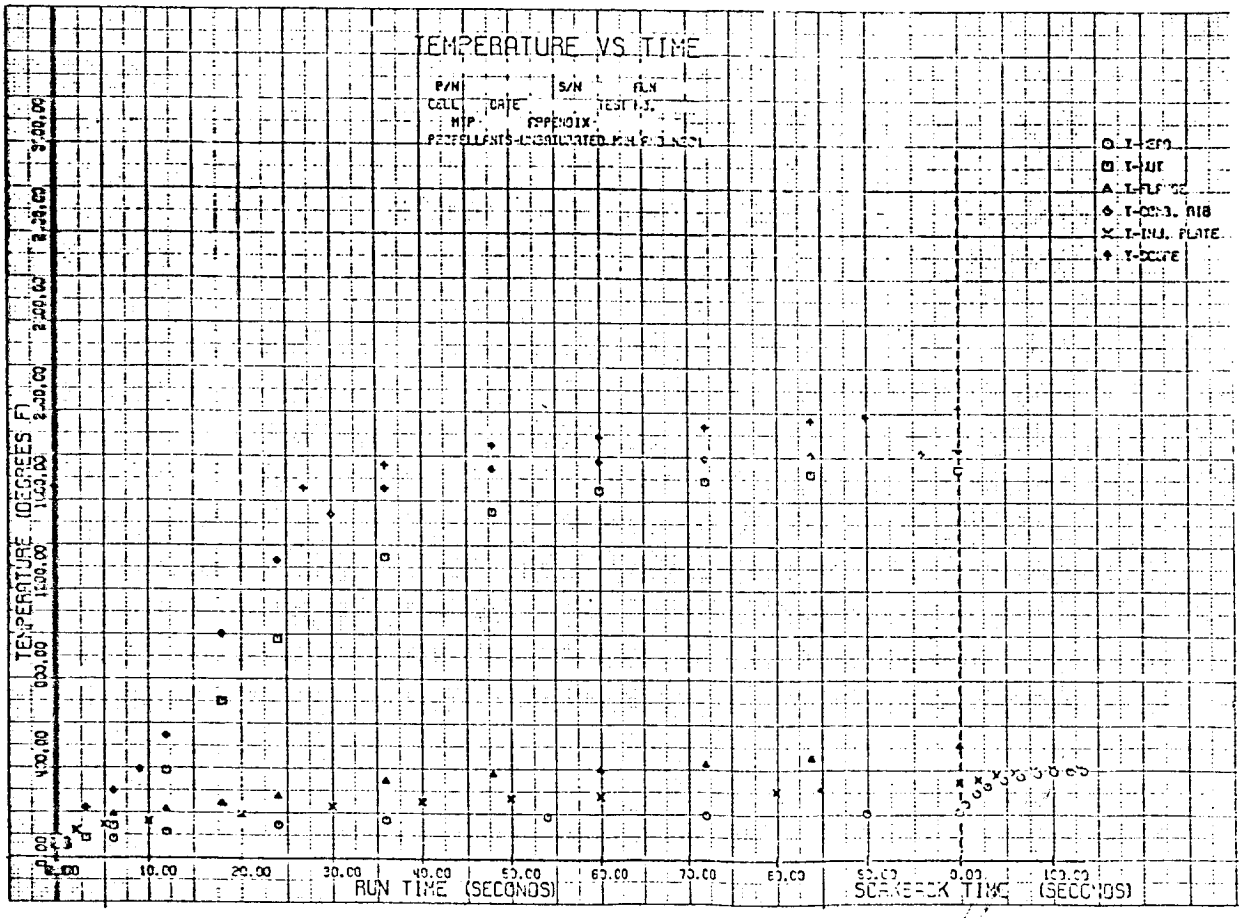

Figure 6

The data parameters for ignition tests are recorded on high speed light sensitive oscillograph recorders.

All inputs for processing ignition test data are in the form of IBM punched cards. Calibrations for dynamic ignition pressure measurement are punched on cards in deflection unit levels with the corresponding pressure values, The deflection unit levels for test data are key punched by the same method as calibrations.

The computer program performs calculations to convert input data into engineering data in the form of engine response characteristics and ignition pressure data. The following calculations are performed:

1. Valve opening response times
2. Mechanical valve mismatch times
3. Hydraulic valve mismatch times
4. Ignition delay times
5. Ignition pressure data.

Computer output is in the form of the tabulated data described above. Punched output cards are prepared that contain the calculated data. The output cards can be used as input data for automatic data plotting.

IV. ERROR ANALYSIS

This section contains a brief summary of the instrumentation accuracies and error analyses for computed parameters expected for steady state and dynamic pulse performance data for the R-4D engine based on the instrumentation system used for tests conducted in Cells 1 and 6 at The Marquardt Jet Laboratory, Van Nuys, California. The completed error analyses are presented in detail in TMC Report A-1043.

Standard statistical techniques using partial differentiation were used to determine individual effects of measurement errors and the root-sum-square technique was used to determine the total error in calculated parameters. The total errors in calculated parameters are expressed as a three sigma (3σ) percentage about the operating point.

Tables I to IV present the results of the error analysis for reduced steady-state and pulse data.

TABLE I

STEADY STATE ERROR ANALYSIS FOR CALCULATED PARAMETERS

Calculated Parameter	Nominal Value	Error* % Deviation	Nominal Value Error Band
VACUUM THRUST			
Strip Chart (Unfiltered)	100 lbs.	± 0.65%	± 0.65 lbs.
Oscillograph (Filtered)	100 lbs.	± 1.73%	± 1.73 lbs.
VACUUM SPECIFIC IMPULSE			
Strip Chart (Unfiltered)	280 sec.	± 1.02%	± 2.86 sec.
Oscillograph (Filtered)	280 sec.	± 1.85%	± 5.18 sec.
FUEL FLOW RATE			
Strip Chart	0.1191 pps	± 1.03%	± 0.001227 pps
Oscillograph (Scaler)	0.1191 pps	± 0.83%	± 0.000988 pps
OXIDIZER FLOW RATE			
Strip Chart	0.2382 pps	± 1.05%	± 0.002501 pps
Oscillograph (Scaler)	0.2382 pps	± 0.86%	± 0.002408 pps
MIXTURE RATIO			
Strip Chart	2.0	± 1.47%	± 0.0294
Oscillograph (Scaler)	2.0	± 1.20%	± 0.0240
CHARACTERISTIC VELOCITY (C*)			
Strip Chart	5100 ft/sec.	± 1.33%	± 67.8 ft/sec.
Oscillograph	5100 ft/sec.	± 2.02%	± 103.1 ft/sec.
THRUST COEFFICIENT (C_f)			
Strip Chart	1.75	± 1.26%	± 0.0221
Oscillograph	1.75	± 2.58%	± 0.0452

*The Error Percentage are 3 Sigma Values.

TABLE II

STEADY STATE TEST DATA ERRORS

Parameter	Nominal Value	Error % Deviation	Nominal Value Error Band
THRUST			
Strip Chart (Unfiltered)	100 lbs.	± 0.65%	± 0.65 lbs.
Oscillograph (Filtered)	100 lbs.	± 1.73%	± 1.73 lbs.
CHAMBER PRESSURE			
Strip Chart	95 psia.	± 0.86%	± 0.83 psia.
Oscillograph	95 psia.	± 1.80%	± 1.74 psia.
CELL PRESSURE			
Strip Chart	0.065 psia.	± 1.70%	± 0.0011 psia.
Oscillograph	0.065 psia.	± 3.4%	± 0.0022 psia.
FUEL MANIFOLD PRESSURE			
Strip Chart	170 psia.	± 0.93%	± 1.58 psia.
Oscillograph	170 psia.	± 2.08%	± 3.54 psia.
FUEL PROPELLANT TEMPERATURE			
Strip Chart	70°F	± 2.98%	± 2.1°F
OXIDIZER MANIFOLD PRESSURE			
Strip Chart	170 psia.	± 0.93%	± 1.58 psia.
Oscillograph	170 psia.	± 2.08%	± 3.54 psia.
OXIDIZER PROPELLANT TEMPERATURE			
Strip Chart	70°F	± 2.98%	± 2.1°F

TABLE III

PULSE PERFORMANCE ERROR ANALYSIS

Off Time Between Pulses ≥ 90 Milliseconds where thrust is integrated on a single pulse basis.

Pulse Width Milliseconds	No. of Pulses	Vacuum Impulse	Error Average Vacuum Impulse per Pulse	% Deviation Fuel Flow	% Deviation Oxidizer Flow	Mixture Ratio	Total Propellant Flow
10	300	5.91	1.87	0.68	0.74	1.00	0.52
15	200	4.66	1.48	0.77	0.81	1.12	0.58
20	150	3.74	1.18	0.80	0.80	1.13	0.59
30	100	2.55	0.81	0.85	0.82	1.18	0.61
40	75	2.55	0.81	0.86	0.83	1.19	0.61
60	50	2.56	0.81	0.88	0.83	1.22	0.62
100	30	2.56	0.81	0.88	0.82	1.20	0.62
200	15	2.56	0.81	0.91	0.84	1.24	0.64
500	10	2.56	0.81	0.70	0.68	0.97	0.51

Off Time Between Pulses < 90 Milliseconds where thrust is integrated on a total run basis.

Pulse Width Milliseconds	No. of Pulses	*Error Average Vacuum Impulse per Pulse	% Deviation Fuel Flow	% Deviation Oxidizer Flow	Mixture Ratio	Total Propellant Flow	Average Specific Impulse
20	150	0.31	0.92	0.82	1.04	0.63	0.70
40	75	0.29	0.92	0.84	1.24	0.64	0.70

TABLE IV

PULSE TIME ERROR ANALYSIS

3 SIGMA ABSOLUTE ERRORS - MILLISECONDS

Time Parameter	10 to 60 MS Pulse Width	100 MS Pulse Width	200 MS Pulse Width	500 MS Pulse Width
Electrical Pulse Width	0.141	0.142	0.143	0.152
Effective Pulse Time	0.141	0.142	0.143	0.152
Electrical on to Fuel Valve Full Open	0.141	0.141	0.141	0.141
Electrical on to Oxidizer Valve Full Open	0.141	0.141	0.141	0.141
Oxidizer Valve Full Open Time	0.244	0.245	0.245	0.251
Rise Time to 70% of Full Thrust	0.141	0.141	0.141	0.141
Electrical Off to Fuel Valve Full Close	0.141	0.141	0.141	0.141
Electrical Off to Oxidizer Valve Full Close	0.141	0.141	0.141	0.141
Decay Time to 25% of Full Thrust	0.141	0.141	0.141	0.141
Average Oxidizer Valve Full Open Time	0.077	0.078	0.078	0.079
Average Electrical Pulse Width	0.045	0.045	0.045	0.048
Average Effective Pulse Time	0.045	0.045	0.045	0.048

CHAPTER 14

FLIGHT SUMMARY

by J. B. Gibbs

TABLE OF CONTENTS

		PAGE
I.	SUMMARY	14-1
II.	LUNAR ORBITER FLIGHTS	14-1
	A. Propulsion Subsystem	14-1
	B. General Flight Description	14-5
	C. Flight Results	14-5
III.	APOLLO SERVICE MODULE AND LUNAR MODULE FLIGHTS	
	A. RCS Description	
	B. Apollo Flight Results	

LIST OF FIGURES

FIGURE NO.		PAGE
1	Model R-4D Space Firing Summary	14-2
2	Model R-4D Liquid Rocket Engine	14-3
3	Lunar Orbiter Velocity and Reaction Control System	14-4
4	Lunar Orbiter Velocity Control Subsystem	14-6
5	Lunar Orbiter Typical Trajectory	14-8
6	Storage Effects	14-10
7	Lunar Orbiter III Propulsion System Temperatures vs. Mission Time	14-12
8	Typical Thrust Vector Control	14-15
9	Model R-4D Recket Engine Comparison of Flight and Acceptance Test Performance	14-17
10	Service Module Reaction Control Subsystem, Mission As-201	14-20
11	Schematic of Typical SM RCS Quad Mission AS-201	14-21
12	Lunar Module RCS Installation	14-22
13	Lunar Module Reaction Control Subsystem Schematic	14-23
14	Apollo Flights	14-26

LIST OF TABLES

TABLE NO.		PAGE
I	Lunar Orbiter Velocity Control System Components	14-7
II	Lunar Orbiter Engine Flight Log	14-9
III	Trajectory Change Summary Lunar Orbiter 1	14-14
IV	Comparison of Flight and Acceptance Test Performance	14-18
V	Summary of Starts and Burn Time of SC 009	14-28
VI	Summary of Starts and Burn Time of AFRM 11	14-29
VII	Summary of Starts and Burn Time for Apollo 4 Flight	14-30

FLIGHT EXPERIENCE

I. SUMMARY

Through July 1969, 213 Model R-4 rocket engines have been flown with complete success on three types of space vehicles; Apollo's Service Module and Lunar Module, and Lunar Orbiter. Engine operation on the 15 separate flights is summarized in Figure 1. Sixteen of the engines were the 95-lb. thrust Model R-4C PFRT type engine on the first Apollo A S-201 flight. The remaining 197 were the qualified Model R-4D engines with 100-lbs. thrust. The 213 engines have accumulated 373,418 in-space ignitions, 5.86 hours of burn time, and 3 years in the space environment while remaining in an operating condition. During these flights, space engine records for bipropellant rockets were established as follows:

1.	Longest single burn duration	10.2 minutes
2.	Longest total burn time on one engine	12.53 minues
3.	Longest space exposure time between burns, one engine	127 days
4.	Longest total space exposure time, one engine	338 days

Details of engine operation on the 15 flights is discussed in the following paragraphs. In the discussion, emphasis has been placed on the engines on the five Lunar Orbiter flights because sufficient flight instrumentation was available to determine accurate space performance on those engines. However, on the ten Apollo flights, all maneuvers commanded of the RCS engines were successfully completed including long periods of holding attitude control and translation of the LM to avoid the initial rocky landing site on Apollo 11.

II. LUNAR ORBITER FLIGHTS

Engine data on Lunar Orbiter flights were obtained from Reference 1 through 4 and numerous personal contacts with Boeing and NASA Langley operations personnel during the conduct of the flights.

Propulsion Subsystem

For Lunar Orbiter, one Model R-4D engine was used as the velocity control (or main spacecraft) rocket and was fitted with an electrical heater and inner gimbal ring which was mounted on the injector head as shown in Figure 2. Because of these additions, the engine part number (228390-501) was different from the Apollo engines. The Lunar Orbiter engine was mounted on the spacecraft as shown in Figure 3 which placed it in the shadow of the vehicle except for short periods during maneuvers. During engine firings, vehicle attitude control was maintained

MODEL R-4D SPACE FIRING SUMMARY

JULY 24, 1969

LUNAR ORBITER PROGRAM (FIVE FLIGHTS)

SPACECRAFT IDENTIFICATION	TOTAL ENGINE STARTS	TOTAL BURN TIME	SPACECRAFT TIME IN SPACE	ENGINE TIME IN SPACE (ENGINE DAYS)	NO. OF ENGINES
L. O. I	5	12.2 MIN.	80 DAYS	80 DAYS	1
L. O. II	7	12.5 MIN.	338 DAYS	338 DAYS	1
L. O. III	7	12.5 MIN.	243 DAYS	243 DAYS	1
L. O. IV	4	11.9 MIN.	176 DAYS	176 DAYS	1
L. O. V	6	12.5 MIN.	180 DAYS	180 DAYS	1
TOTAL TIME HISTORY FOR LUNAR ORBITERS	29	1.03 HOURS	2.79 YEARS	2.79 YEARS	5

APOLLO SPACECRAFT PROGRAM (TEN FLIGHTS)

MISSION IDENTIFICATION	SPACECRAFT IDENTIFICATION	TOTAL ENGINE STARTS	TOTAL BURN TIME	SPACECRAFT TIME IN SPACE	ENGINE TIME IN SPACE (ENGINE DAYS)	NO. OF ENGINES
APOLLO (AS 201)	SC 009	1,818	4.1 MIN.	0.5 HRS.	0.3 DAYS	16
APOLLO (AS 202)	SC 011	7,040	8.0 MIN.	1.5 HRS.	1.0 DAYS	16
APOLLO 4	SC 017	15,749	9.3 MIN.	8.5 HRS.	5.7 DAYS	16
APOLLO 5	LM 1	8,540	36.5 MIN.	8.0 HRS.	5.3 DAYS	16
APOLLO 6	SC 020	19,472	17.5 MIN.	9.6 HRS.	6.4 DAYS	16
APOLLO 7	SC 101	61,000	41.5 MIN.	10.8 DAYS	172.8 DAYS	16
APOLLO 8	SC 103	46,240	27.3 MIN.	6.0 DAYS	96.0 DAYS	16
APOLLO 9	SC 104	41,100	25.8 MIN.	10.0 DAYS	160.0 DAYS	16
	LM 3	25,230	17.4 MIN.	4.2 DAYS *	67.2 DAYS	16
APOLLO 10	SC 106	44,700	28.1 MIN.	8.0 DAYS	128.0 DAYS	16
	LM 4	34,650	23.9 MIN.	4.5 DAYS *	72.0 DAYS	16
APOLLO 11	SC 107	50,900	27.8 MIN.	8.0 DAYS	128.0 DAYS	16
	LM 5	16,950	12.1 MIN.	5.5 DAYS	88.0 DAYS	16
TOTAL TIME HISTORY FOR APOLLO R.C.S. ENGINES		373,389	4.65 HOURS	58.2 DAYS	2.55 YEARS	208

TOTAL SPACE FIRING TIME HISTORY FOR R-4D ENGINES USED ON APOLLO AND LUNAR ORBITER SPACECRAFT

ENGINE STARTS	TOTAL BURN TIME	SPACECRAFT TIME IN SPACE	ENGINE TIME IN SPACE	NO. OF ENGINES
373,418	5.68 HOURS	2.94 YEARS	5.34 YEARS	213

* TIME PERIOD FROM EARTH LAUNCH TO FINAL JETTISON OF LM ASCENT STAGE FROM COMMAND SERVICE MODULE.

Figure 1

THE MODEL R-4D LIQUID ROCKET ENGINE

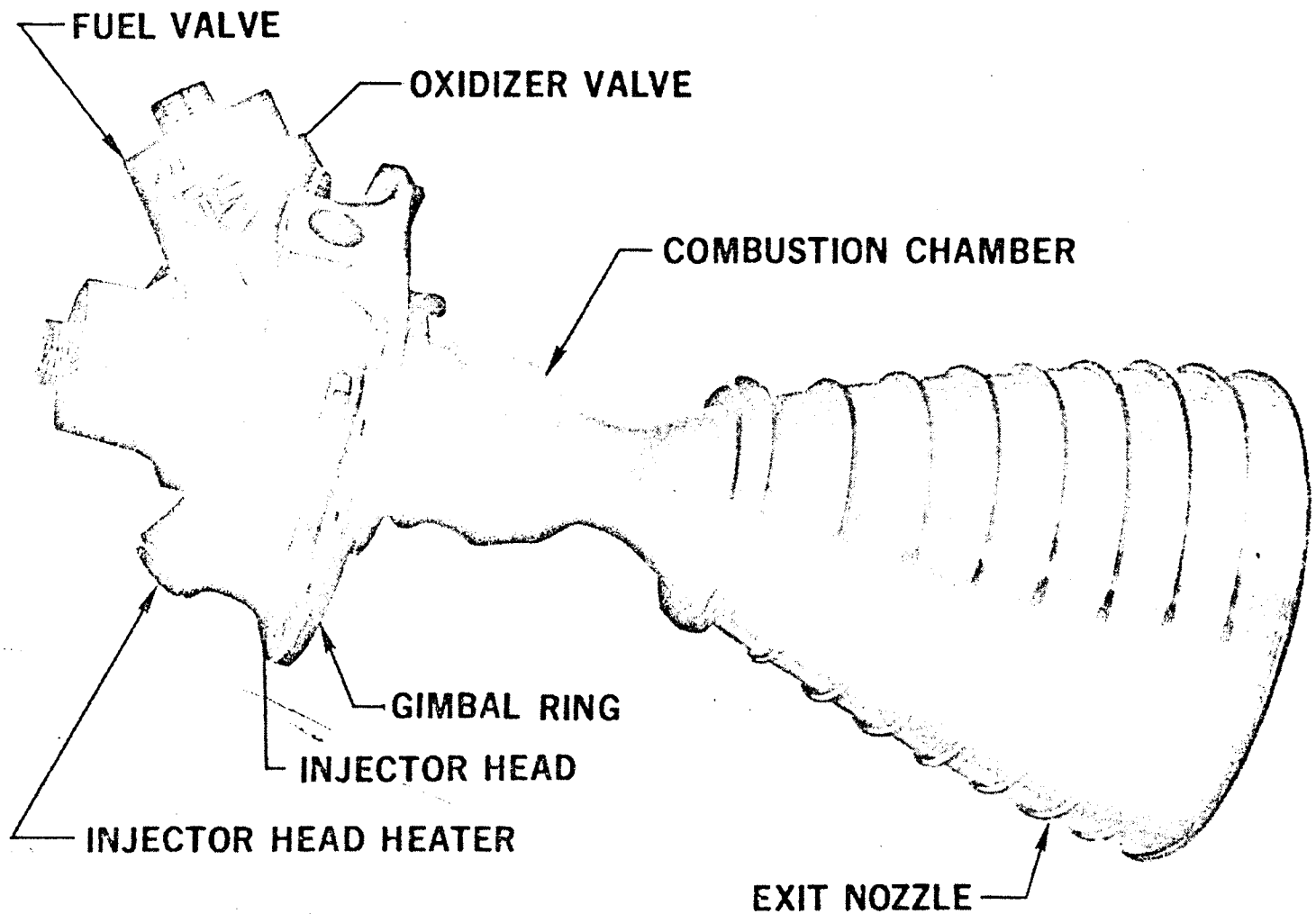

NEG. C8420-3

THE MARQUARDT CORPORATION

V5050-12

A-1080

FIGURE 2

LUNAR ORBITER VELOCITY AND REACTION CONTROL SUBSYSTEM

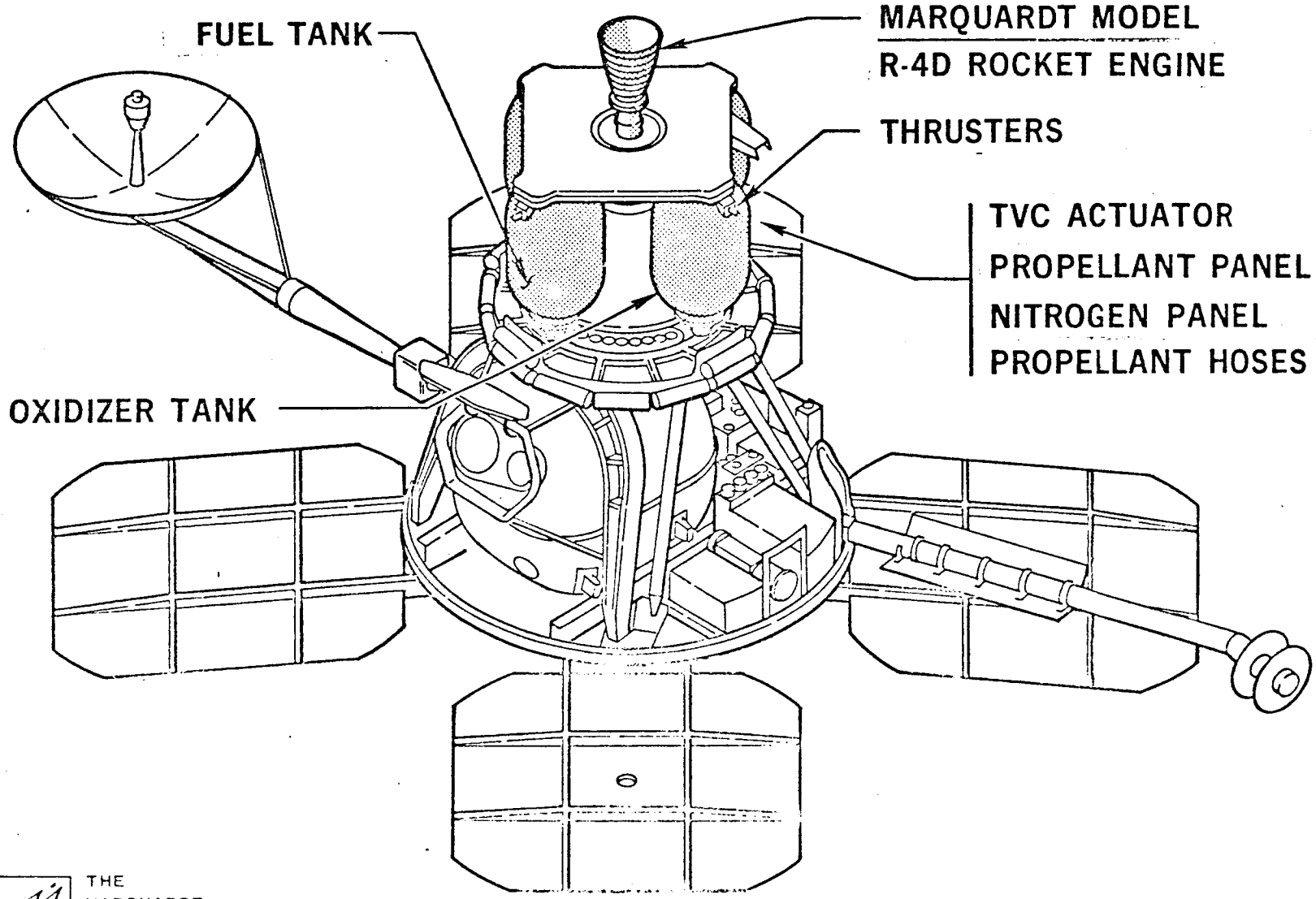

THE MARQUARDT CORPORATION

V5050-6

A-1080

FIGURE 3

by the gimballed Model R-4D engine. At other times, attitude control was provided by 0.05# thrust GN_2 thrustors mounted on the corners of the vehicles aft structural plate surrounding the engine (Figure 3).

The velocity control subsystem shown schematically in Figure 4 utilized common usage components developed mainly for the Apollo program as shown in Table I. Teflon aluminum foil laminate propellant bladders were used to reduce saturation of the propellants by the pressurizing nitrogen over the long mission durations.

B. General Flight Description

The objectives of the five flight Lunar Orbiters were achieved with spectacular success. Over 1,500 detailed photographs covering nearly all of the moon's surface were returned in addition to data on the magnitudes of micrometeoroid and radiation fluxes near the moon. Also, more accurate determination of the lunar gravitational field has been obtained.

The velocity control subsystem was required to provide precise lunar orbit injection and orbit trim maneuvers. Engine firing durations were from 3 seconds to over 10 minutes. A typical flight with the engine firings listed is depicted in Figure 5. Although design allowances were made for two such maneuvers, only one midcourse correction firing (from 4 to 53 seconds duration about one day from launch) was required for each of the five flights. About two days after the midcourse maneuver, a long (10 minute) retrofire was made to place the vehicles in their initial lunar orbit. About seven days later, the engines were fired to reduce the perilune to altitudes as low as 24 miles for high resolution photography. On each mission, these three engine firings completed the velocity control subsystems primary objectives. Other engine firings were made on the various orbiters to rephase the orbit for lunar eclipses, extent orbit life, intentionally crash the vehicle, etc.

C. Flight Results; Velocity Control Subsystem

The required precise vehicle maneuvers were made without any engine anomaly of any kind during 29 engine firings on the five Lunar Orbiters as summarized in Table II. The total burn time of all 5 engines was 61.6 minutes and the engines accumulated 1,018 days of space exposure time while remaining in an operable condition. Several notable records for bipropellant rockets were accomplished as listed at the bottom of Table II.

Engine Non-operating

During engine-off and storage times, the Lunar Orbiter engines successfully withstood the ground storage and handling and space environments for the time periods shown in Figure 6. From delivery of the engine (which occurred shortly after completion of the acceptance test) to termination of the flight,

LUNAR ORBITER VELOCITY CONTROL SUBSYSTEM

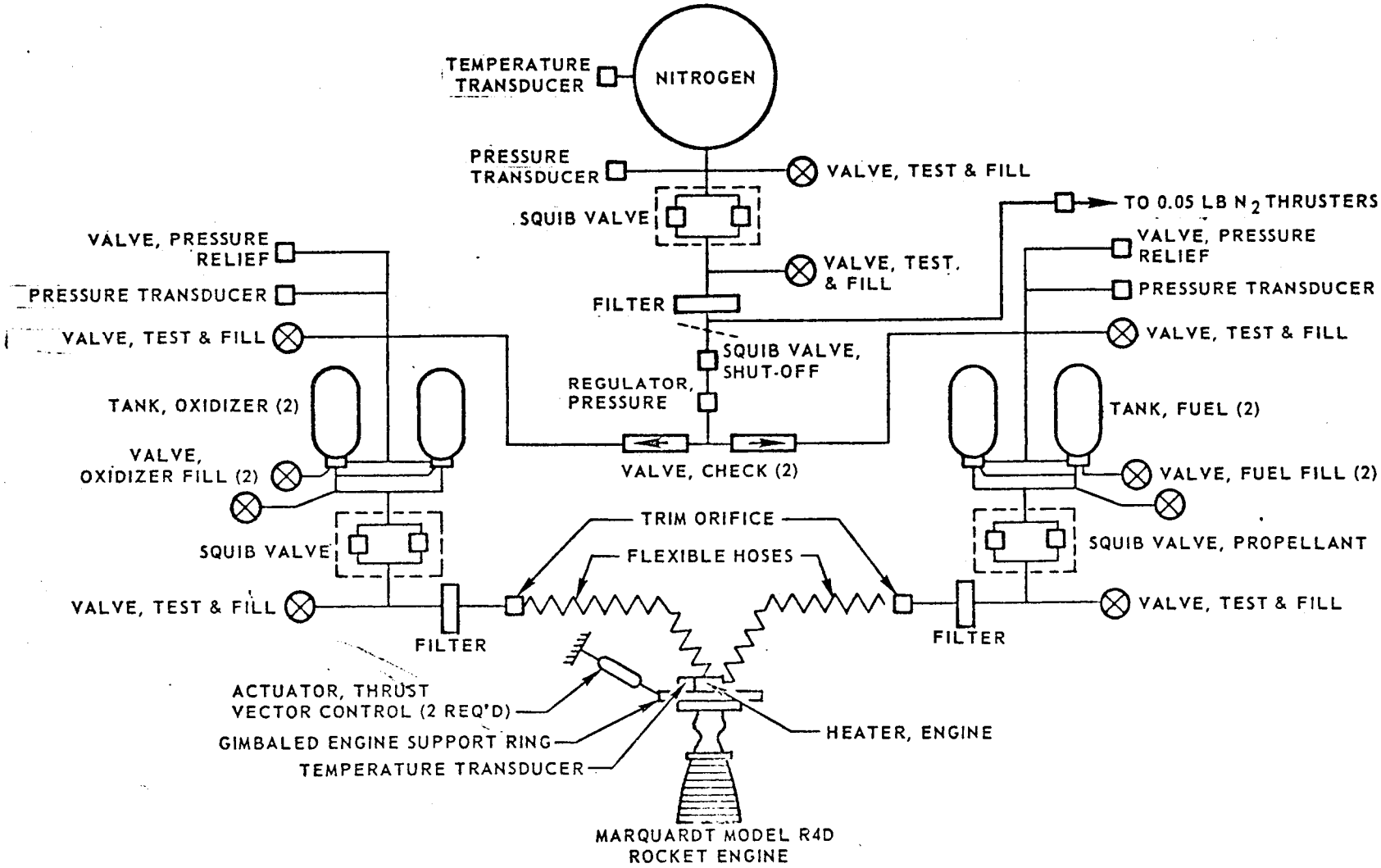

THE MARQUARDT CORPORATION

V5050-10

A-1080

FIGURE 4

TABLE I

LUNAR ORBITER VELOCITY CONTROL SYSTEM COMPONENTS

COMPONENT	COMMON USAGE (MODIFIED DESIGN)	SUPPLIER	APPROX. WEIGHT LB	NUMBER USED
Oxidizer Tank	Apollo	Bell Aerosystems	10.8	2
Fuel Tank	Apollo	Bell Aerosystems	7.1	2
Pressure Regulator (190 psi)	Gemini	National Water Lift Co.	1.54	1
Nitrogen Check Valve	Apollo	Accessory Products Co.	0.4	2
Pressure Regulator (20 psi)	Ranger	Sterer Engrg. & Mfg. Co.	0.93	1
Propellant Filter		Vacco Valve Co.	0.9	2
Nitrogen Filter	Apollo	Vacco Valve Co.	0.38	1
Propellant Squib Valve		Ordnance Engrg. Assoc.	0.72	2
Shutoff Squib Valve		Ordnance Engrg. Assoc.	0.26	1
Pressure Relief Valve	Apollo	Calmac Mfg. Co.	0.8	2
Nitrogen Squib Valve		Ordnance Engrg. Assoc.	0.8	1
Propellant Fill and Vent Valves	Apollo	J. C. Carter Co.	0.35	4
Propellant Hose		Resistoflex Corp.	0.62	2
Reaction Control Thruster, (Yaw)	Ranger	Sterer Engrg. & Mfg. Co.	0.23	2
Reaction Control Thrusters (2 Roll and Pitch	Ranger	Sterer Engrg. & Mfg. Co.	0.67	2
Rocket Engine	Apollo	The Marquardt Corp.	5.1	1
Test and Fill Valve		The Firewel Co., Inc.	0.21	6
TVC Actuators		Kearfott Div. of General Precision	3.7	2
		Subtotal	63.6	
		Propellants	276.0	
		TOTAL	339.6	

LUNAR ORBITER
TYPICAL TRAJECTORY

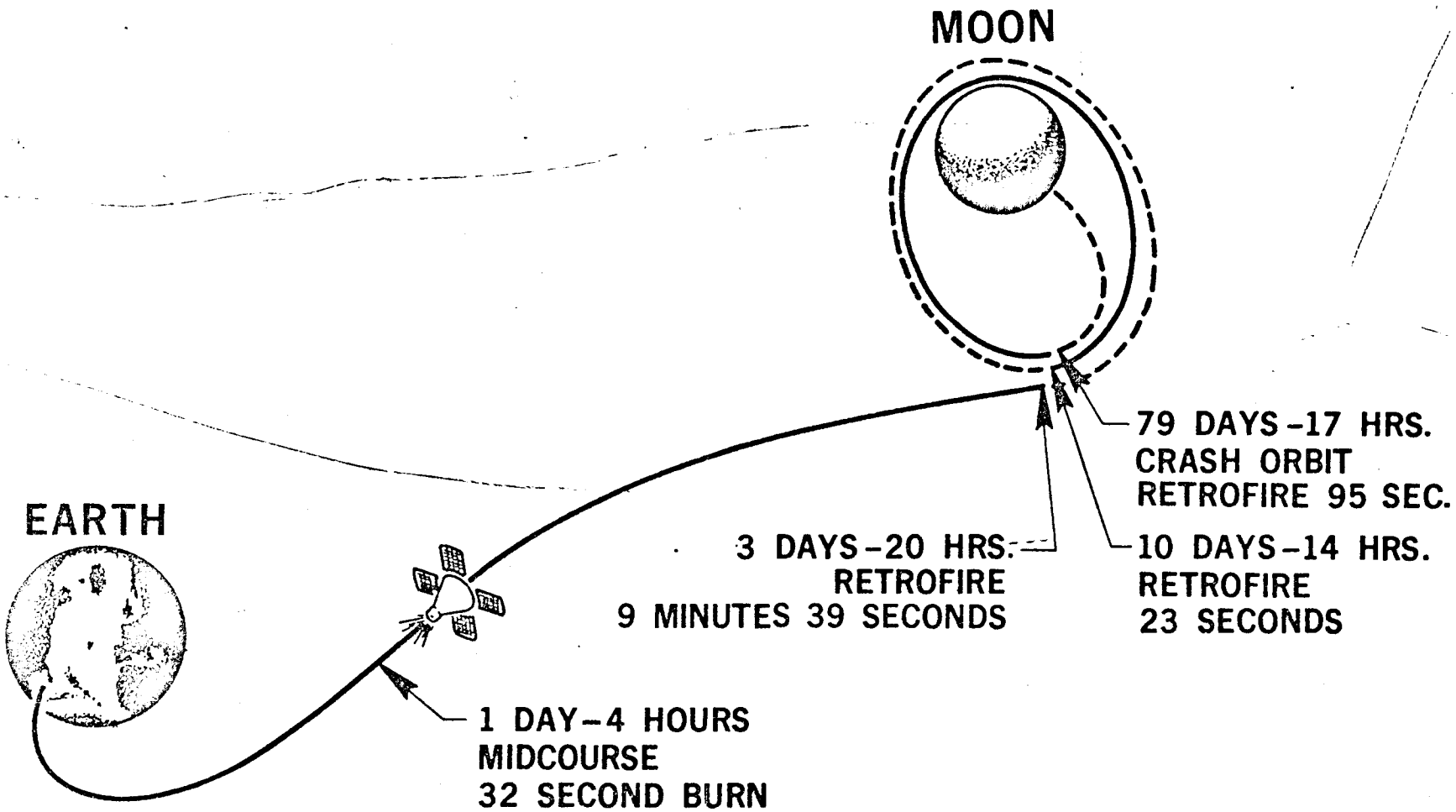

THE MARQUARDT CORPORATION

V5050-14

FIGURE 5

TABLE II

LUNAR ORBITER ENGINE FLIGHT LOG

	DATE		PACIFIC TIME	DAYS FROM LAUNCH	EVENT	BURN TIME (SEC)
LUNAR ORBITER I	10 AUG	1966	1226	0	LAUNCH	---
	11 AUG	1966	1700	1.2	MIDCOURSE CORRECTION	32.1
	14 AUG	1966	0835	3.8	DEBOOST TO LUNAR ORBIT	578.7
	21 AUG	1966	0242	10.6	TRANSFER TO LOW PHOTO ORBIT	22.4
	25 AUG	1966	0901	14.9	ADJUST ORBIT TO LOWER PERILUNE	3.0
	29 OCT	1966	0525	79.7	TRANSFER TO MOON CRASHING ORBIT	94.4
			TOTALS	79.7		730.6
LUNAR ORBITER II	6 NOV	1966	1521	0	LAUNCH	---
	8 NOV	1966	1130	1.8	MIDCOURSE CORRECTION	18.1
	10 NOV	1966	1226	3.9	DEBOOST TO LUNAR ORBIT	611.6*
	15 NOV	1966	1450	9.0	TRANSFER TO LOW PHOTO ORBIT	17.4
	8 DEC	1966	1236	31.9	ORBIT PLANE CHANGE	61.3
	14 APR	1967	0101	158.4 *	ADJUST ORBIT FOR LUNAR ECLIPSE	3.2
	26 JUN	1967	2400	232.3	RAISE PERILUNE TO EXTEND ORBIT LIFE	4.6
	10 OCT	1967	2255	338.3	TRANSFER TO MOON CRASHING ORBIT	36.0
			TOTALS	338.3*		752.2*
LUNAR ORBITER III	4 FEB	1967	1717	0	LAUNCH	---
	6 FEB	1967	0700	1.6	MIDCOURSE CORRECTION	4.3
	8 FEB	1967	1354	3.9	DEBOOST TO LUNAR ORBIT	542.5
	12 FEB	1967	1013	7.7	TRANSFER TO LOW PHOTO ORBIT	33.3
	12 APR	1967	0900	66.7	ADJUST ORBIT FOR LUNAR ECLIPSE	3.5
	16 JUL	1967	1822	162.0	RAISE PERILUNE TO EXTEND ORBIT LIFE	8.9
	30 AUG	1967	1239	206.6	REDUCE APOLUNE	127.1
	9 OCT	1967	0233	243.4	TRANSFER TO MOON CRASHING ORBIT	32.0
			TOTALS	243.4		751.6
LUNAR ORBITER IV	4 MAY	1967	1525	0	LAUNCH	---
	5 MAY	1967	0945	0.8	MIDCOURSE CORRECTION	52.7
	8 MAY	1967	0809	3.7	DEBOOST TO LUNAR POLAR ORBIT	501.7
	5 JUN	1967	1516	32.0	REDUCE PERILUNE	117.9
	8 JUN	1967	1439	35.0	REDUCE APOLUNE	42.8
	27 OCT	1967	---	176.0	MOON CRASH	
			TOTALS	176.0		715.1
LUNAR ORBITER V	1 AUG	1967	1533	0	LAUNCH	---
	2 AUG	1967	2300	1.3	MIDCOURSE CORRECTION	26.1
	5 AUG	1967	0949	3.8	DEBOOST TO LUNAR POLAR ORBIT	498.1
	7 AUG	1967	0144	5.4	REDUCE PERILUNE	10.8
	8 AUG	1967	2208	7.3	REDUCE APOLUNE	152.9
	10 OCT	1967	1237	69.9	ADJUST ORBIT FOR LUNAR ECLIPSE	40.8
	28 JAN	1968	2213	180.3	TRANSFER TO MOON CRASHING ORBIT	18.9
			TOTALS	180.3		747.6

TOTAL ALL ORBITERS	1,017.7 DAYS	29	FIRINGS
		3697.1	SEC
MISSIONS COMPLETED		(61.6	MIN)

*BIPROPELLANT ROCKET SPACE ENGINE RECORDS:

1. SINGLE BURN DURATION — 10.2 MINUTES
2. TOTAL BURN TIME ON ONE ENGINE — 12.53 MINUTES
3. SPACE EXPOSURE TIME BETWEEN BURNS, ONE ENGINE — 127 DAYS
4. TOTAL SPACE EXPOSURE TIME, ONE ENGINE — 338 DAYS

7 FEBRUARY 1968

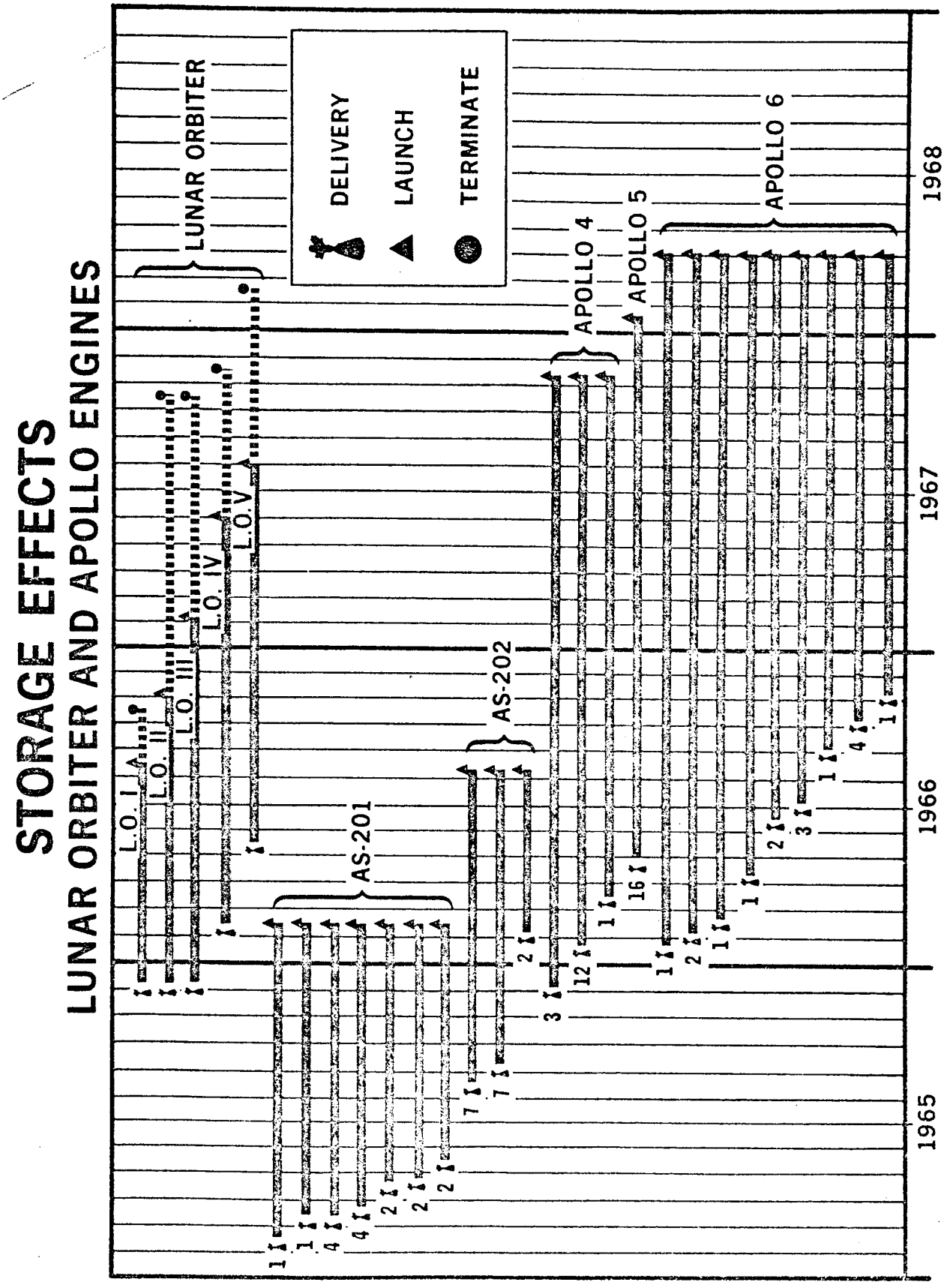
STORAGE EFFECTS
LUNAR ORBITER AND APOLLO ENGINES
LUNAR ORBITER
DELIVERY
LAUNCH
TERMINATE
L.O. I
L.O. II
L.O. III
L.O. IV
L.O. V
AS-201
AS-202
APOLLO 4
APOLLO 5
APOLLO 6
1965
1966
1967
1968

FIGURE 6

the elapsed time was from 12 months for Lunar Orbiter I to 23 months for Lunar Orbiter IV. Actual in-space exposure times (listed in Table II) varied from 80 days for Lunar Orbiter I to 338 days for Lunar Orbiter II.

During the space exposure times, data was returned which showed that the engine valves sealed after each usage. Even small leaks would have been detectable over such long time spans by one or both of two independent measurements. First, there was no decay of tank pressure during the flights whenever the engine was shut off and the GN_2 supply was shut off. For most of the time after the last photo orbit burn (the third burn usually) the GN_2 supply isolation valve leading to the propellant tanks was closed to conserve N_2 for the attitude control thrustors. Subsequent engine burns were made inthe blowdown mode. The tank pressure would vary with varying tank temperatures in a predictable and repeatable manner thereby confirming that the system was not leaking gas or propellant. The second method of confirming engine valve (and propulsion system) propellant sealing consists of comparing a computed total propellant usage at propellant exhaustion with the weight of loaded propellants. As will be shown later, the excellent agreement between propellant usage and loaded values would not permit propellant leakage of any significant quantity.

Thermal control of the propulsion subsystem was provided as follows:

1. Engine Heater - a 7 watt electrical heater was mounted directly on the engine injector head (see Figure 2) and electrical power was applied continuously. The engine was mounted in the shadow of the vehicle so the thrust chamber did not receive radiation from the sun.

2. Electrical Propellant Tank Heaters - these heaters were controlled from the ground and (typically for Lunar Orbiter III) were activated on 25 occasions for about 62 minutes each during the early part of the mission. The heaters were used to keep the propellants above 40°F.

3. Spacecraft Attitude - as the paint deteriorated on the spacecraft, the overall vehicle temperature increased. Excessively high temperatures were avoided by pitching the spacecraft 30 to 35 degrees off the sun line so that it presented a smaller profile to the sun.

Figure 7 presents temperatures as a function of mission time (plotted at 12 hour intervals) for the engine fuel valve, propellant tank deck and nitrogen tank. The engine valve body temperature is near that of the injector head and was between 70 and 80°F except after an engine firing. Peak valve temperatures occurred about 90 minutes after each engine burn with the maximum occurring after the longest burn which was the Lunar Orbit injection maneuver. Typically, the maximum was 110°F.

LUNAR ORBITER III

PROPULSION SYSTEM TEMPERATURES VS. MISSION TIME

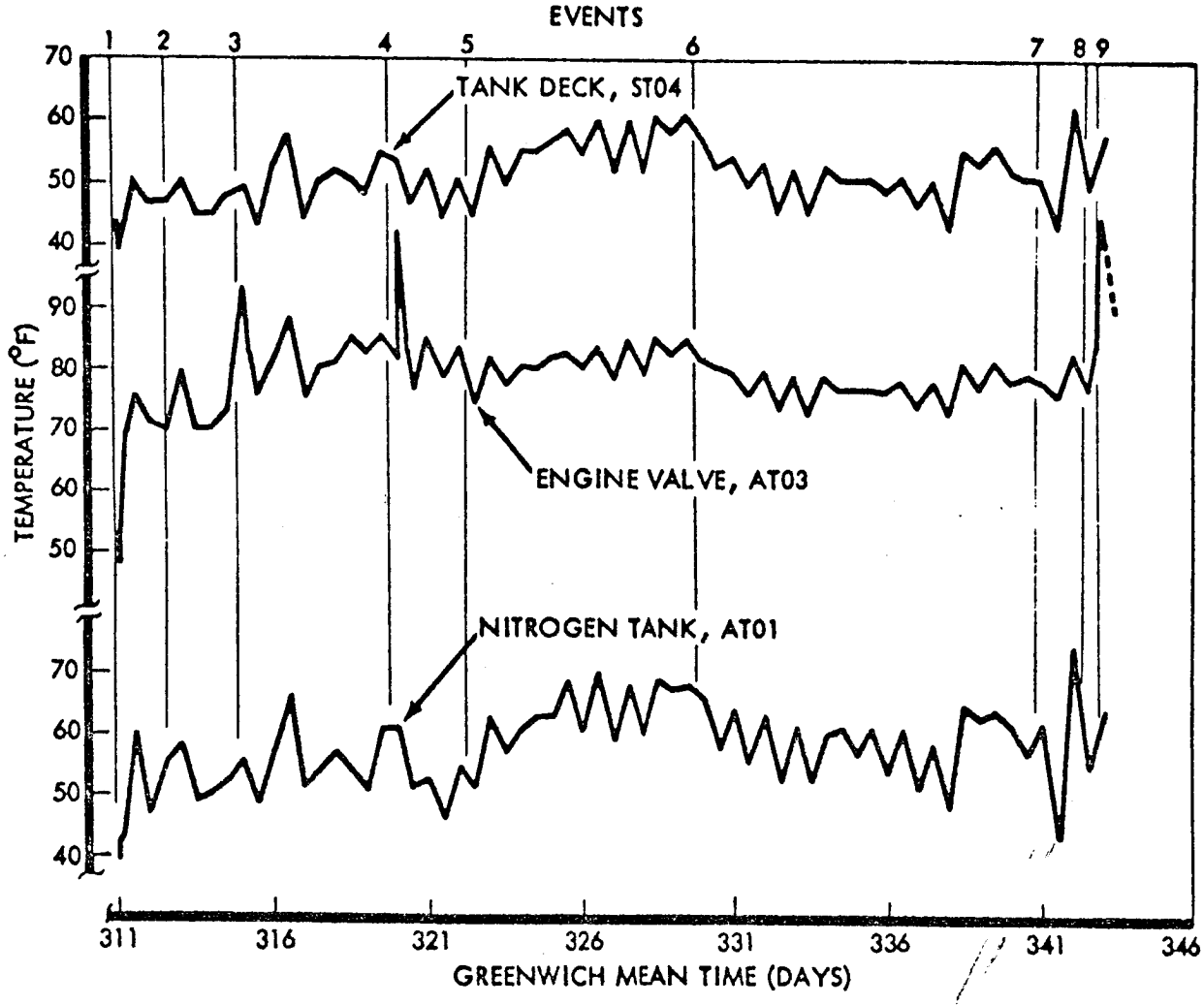

EVENTS:

1. LAUNCH
2. MIDCOURSE
3. INJECTION
4. ORBIT TRANSFER
5. START PHOTO
6. END PHOTO START READOUT
7. END READOUT
8. FIRE N_2 SHUTOFF SQUIB
9. INCLINATION CHANGE

NOTE: Temperature data returned at 12 hour intervals.

FIGURE 7

The gimbal mount and flexible hoses almost insulated the engine from the space craft. On other applications with solid engine mounts and propellant lines, the valves and injector temperatures should follow the spacecraft structure temperatures more closely.

For the total of 1,018 space exposure days for the five Orbiters, the engines remained in an operable condition. Except for Lunar Orbiter IV, engine firings were made at the termination of each flight to intentionally crash each vehicle onto the moon's surface. Through 25 July 1967 on the first four Lunar Orbiter flights, 11 micrometeorite hits had been recorded by the spacecraft detectors. Estimates of micrometeorite hit probability have indicated that the four engines should have been hit about 6 times; one or two of the hits should have been on the molybdenum chamber and the remainder on the L-605 bell. Since the engines were fired successfully after that time, it would appear that the Model R-4D engine can tolerate micrometeorites which are at least large enough to puncture the 0.001 inch thick beryllium copper skin of the micrometeorite detectors.

Engine Operating

As shown in Table II, 29 engine firings were made on the 5 Lunar Orbiters with burn times from a minimum of 3.0 seconds to a record maximum time of 10.2 minutes for the injection or deboost maneuver on Lunar Orbiter II. Each firing provided a precise velocity change in the desired direction which in turn provided orbit parameters in remarkable agreement with the predicted or planned values. For example, the desired and actual trajectories and velocity changes are compared for the Lunar Orbiter I flight in Table III. In general, subsequent flights provided even closer agreement between planned and actual trajectory values as the operators gained experience and more accurate lunar gravity constants were obtained.

Except during engine firings, vehicle attitude control was provided by GN_2 thrustors and these thrustors were used to point the vehicle in the desired direction prior to each engine firing. During an engine burn, attitude control was maintained by the Model R-4D engine gimbal system in pitch and yaw with the GN_2 thrustors maintaining roll control. Typical operation characteristics of the thrust vector control subsystem are shown in Figure 8 for the Lunar Orbiter II lunar-injection phase. The spacecraft attitude control limit, which was increased from $\pm$ 0.2 to $\pm$ 2.0 degrees during engine operation to reduce GN_2 thrustor operation and consequent gas wastage, was returned to $\pm$ 0.2 degrees following engine cutoff, and the spacecraft position error returned to less than $\pm$ 0.2 degrees.

Flight performance data are calculated results, since there is no measurement of engine chamber pressure or propellant flow rates. Knowing spacecraft weight (from "bookkeeping" operations on nitrogen and propellant expenditures) and determining engine operation time and spacecraft acceleration from telemetry data, the analytical approach is to assume values of specific impulse and calculate a thrust

TABLE III

TRAJECTORY CHANGE SUMMARY

LUNAR ORBITER I

	DESIRED TRAJECTORY	VELOCITY CHANGE (METERS PER SECOND)		ACTUAL TRAJECTORY
		DESIRED	ACTUAL	
Translunar Midcourse	AIM POINT 6509 KM	37.8	37.8	AIM POINT 6555 KM
Lunar Orbit Injection	Hp 199 KM Ha 1850 KM INCL 12.04 DEG	790.0	789.65	Hp 189 KM Ha 1867 KM INCL 12.15 DEG ± 0.05
Orbit Transfer	Hp 57.92 KM Ha 1855 KM INCL 12.04 DEG	40.2	40.15	Hp 56 KM Ha 1853 KM INCL 12.05 DEG ± 0.10
Orbit Trim	Hp 40.0 KM Ha 1824.0 KM INCL 12.03 DEG	5.43	5.42	Hp 40.5 KM Ha 1816.7 KM INCL 12.0 DEG ± 0.20

H_p - Perilune Altitude

H_a - Apolune Altitude

INCL - Orbit Inclination

TYPICAL THRUST VECTOR CONTROL

L.O. II LUNAR INJECTION MANEUVER

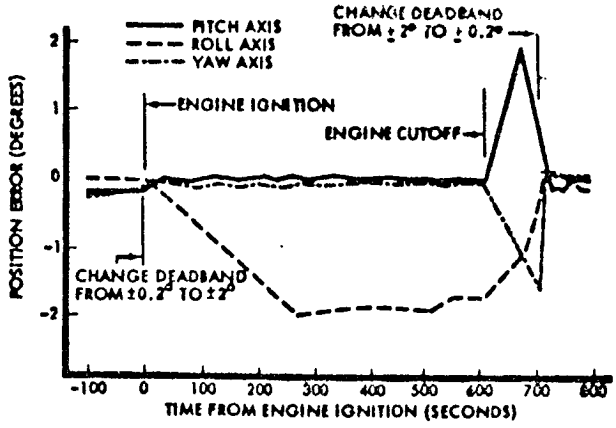

FIGURE 8

value that will match the acceleration profile. Iterations are performed to converge calculated and actual accelerations, thereby determining average values of thrust level and specific impulse. It is also possible to infer an average operating mixture ratio; this is accomplished by adjusting flight conditions with the proper influence coefficients, then comparing with acceptance data. Because of the long (10 minute) burn time and because over half the propellant load is used, the lunar orbit injection maneuver provided the most accurate measurement of flight performance. Flight specific impulse data was computed as above and corrected for propellant temperature to 70°F. This corrected Isp is compared with the ground acceptance test data in Figure 9. The excellent agreement is obvious. The minor differences (less than 1%) are expanded in Table IV where both flight Isp and thrust are compared with the acceptance test results.

On the final burns which lead to a crash into the moon's surface, Lunar Orbiter I and II's engine valves were held open to propellant exhaustion. On Orbiters III and V, the engines were shut off prior to the computed propellant exhaustion point. The computed propellant usage totals are compared with the useful amount of propellants loaded (assuming 99% expulsion efficiency) in the following table.

Lunar Orbiter	Actual Propellant Loaded, lbs.	Useful Propellant Loaded, lbs.	Computed Propellant Used, lbs.	Notes
I	276.8	274.0	274.4	Complete expulsion
II	277.0	274.2	275.8	Complete Expulsion
III	275.9	273.1	270.3	Propellant not completely expelled
IV	276.4	274.6	259.6	Propellant not completely expelled
V	276.2	273.4	273.2	Propellant not completely expelled

Since the computed usage very slightly exceeded the useful propellant loaded for Lunar Orbiter's I and II, it would appear that the expulsion was more complete than the 99% indicated by ground tests or else the actual engine flight Isp was very slightly higher than computed.

The thrust of the engines at the nominal inlet conditions of the acceptance tests varied only from 99.5 to 100.4 pounds (see Table IV). The actual flight thrusts varied over a wider range from 93 to 110 pounds. The highest

MODEL R-4D ROCKET ENGINE
COMPARISON OF FLIGHT AND ACCEPTANCE TEST PERFORMANCE

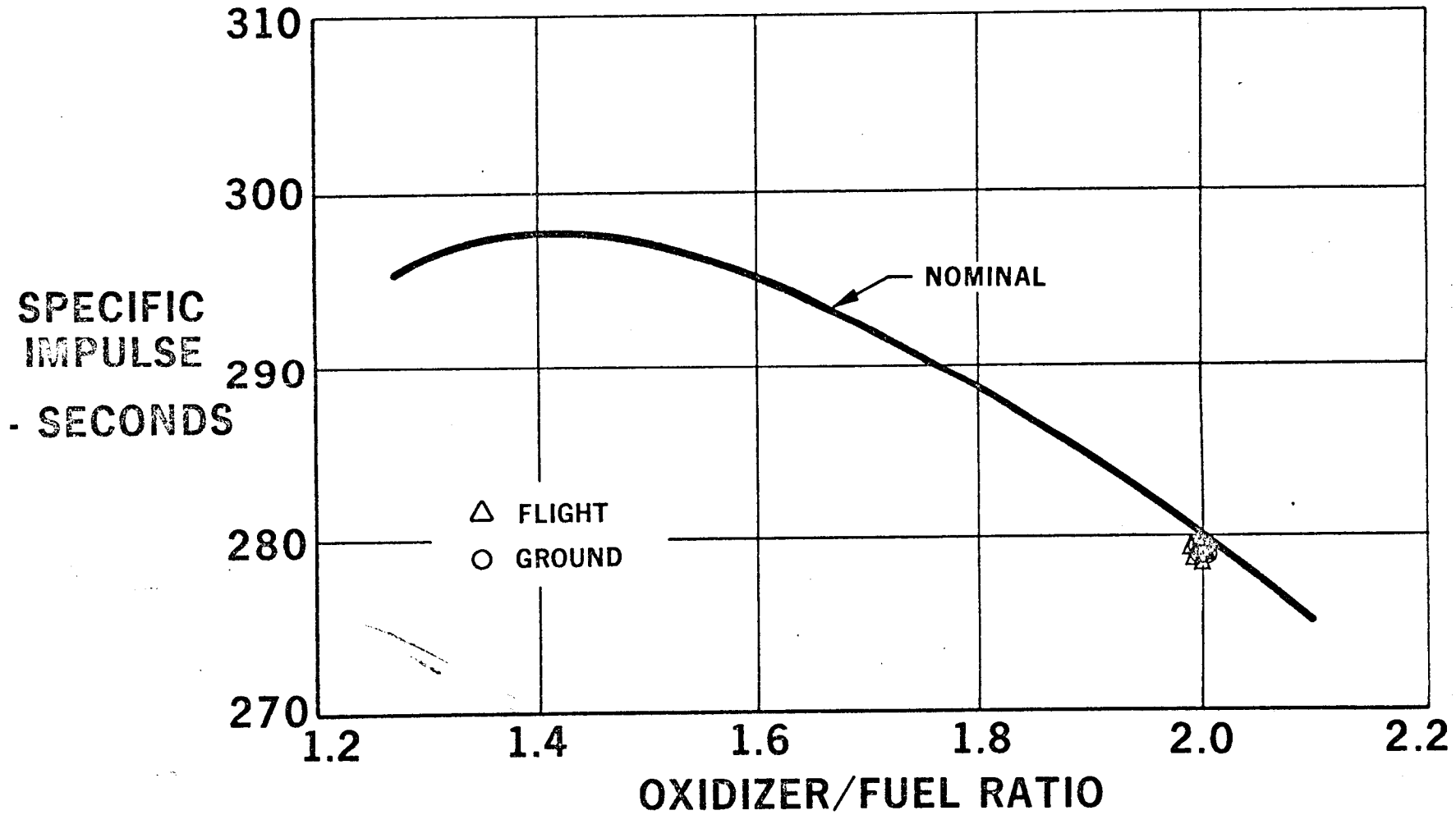

THE MARQUARDT CORPORATION

V5050-15 C

FIGURE 9

TABLE IV

COMPARISON OF FLIGHT AND ACCEPTANCE TEST PERFORMANCE

MODEL R-4D ROCKET ENGINE

PROPELLANT TEMP. - 70°F

PARAMETERS	LUNAR ORBITER I		LUNAR ORBITER II		LUNAR ORBITER III		LUNAR ORBITER IV		LUNAR ORBITER V	
	FLIGHT 579 SEC. BURN	ACCEPT TEST 70 SEC. BURN	FLIGHT 612 SEC. BURN	ACCEPT TEST 70 SEC. BURN	FLIGHT 542 SEC. BURN	ACCEPT TEST 70 SEC. BURN	FLIGHT 502 SEC. BURN	ACCEPT TEST 70 SEC. BURN	FLIGHT 498 SEC. BURN	ACCEPT TEST 70 SEC. BURN
AVERAGE SPECIFIC IMPULSE, SEC.	278.3	277.6	279.5	279.3	279.0	278.8	278.3	276.1	278.0	275.7
Δ Isp (FLIGHT - ACCEPT. TEST)	+0.3%		+0.1%		+0.1%		+0.8%		+0.8%	
AVERAGE THRUST, POUNDS	101.3*	100.4	101.0*	100.2	100.2*	99.7	100.0*	99.5	100.1*	99.6
ΔTHRUST (FLIGHT - ACCEPT. TEST)	+0.9%*		+0.8%*		+0.5%*		+0.5%*		+0.5%	

*ACTUAL THRUST NOT CORRECTED FOR TEMPERATURE - INCLUDES ERRORS FROM PRESSURE REGULATOR ADJUSTMENT AND LINE LOSS ESTIMATES

THE MARQUARDT CORPORATION

V5050-7C

thrust occurred on the final burn on Lunar Orbiter I which resulted from high tank pressures from a leaking N_2 regulator. The lowest thrust came at the end of the next to last engine firing on Lunar Orbiter III. Prior to this fairly long 127 second burn, the GN_2 supply isolation squib valve was closed so that the engine firing was in the blowdown mode from 106 to 93 pounds thrust. (A higher minimum thrust resulted from the final Lunar Orbiter III burn due to higher tank temperatures which increased the pressures). These blowdown operations were made after over 200 days in space and the engine operation was smooth and the performance was predictable. Apparently then, the aluminized bladder prevented nitrogen saturation of the propellants during the 200 plus days of exposure.

III. APOLLO SERVICE MODULE AND LUNAR MODULE FLIGHTS

Ten Apollo Spacecraft Flights have been completed including the successful manned landing on the moon. The number of engine starts, burn time, time in space for each of the ten flights are listed in Figure 1. During these ten flights, 373,389 engine firings have been made and all commaned vehicle maneuvers were successfully executed.

RCS Description

On the Service Module, four completely separate Reaction Control Subsystem Quads are used and each quad has four Model R-4D engines as shown in Figure 10. The schematic of a typical quad with instrumentation is presented in Figure 11. On the first flight (AS-201) 16 Model R-4C 95-lb. thrust PFRT engines were used for reaction control. On all other flights, 16 Model R-4D 100-lb. thrust Block I engines were used.

On the Lunar Module, the four quads each have four Model R-4D engines which are supplied from two independent propellant supply systems "A" and "B", as sketched in Figure 12 and shown schematically in Figure 13.

Apollo Flight Results

The R-4D reaction control engines on the Apollo Service Module and Lunar Module perform the following functions:

- Provides CSM/S-IVB Separation
- Provides docking attitudes in the LM and LM ejection maneuvers
- Provides attitude control during mid-course corrections
- Provides thrust for rotisserie temperature conditioning roll for passive thermal control

SERVICE MODULE REACTION CONTROL SUBSYSTEM, MISSION AS-201

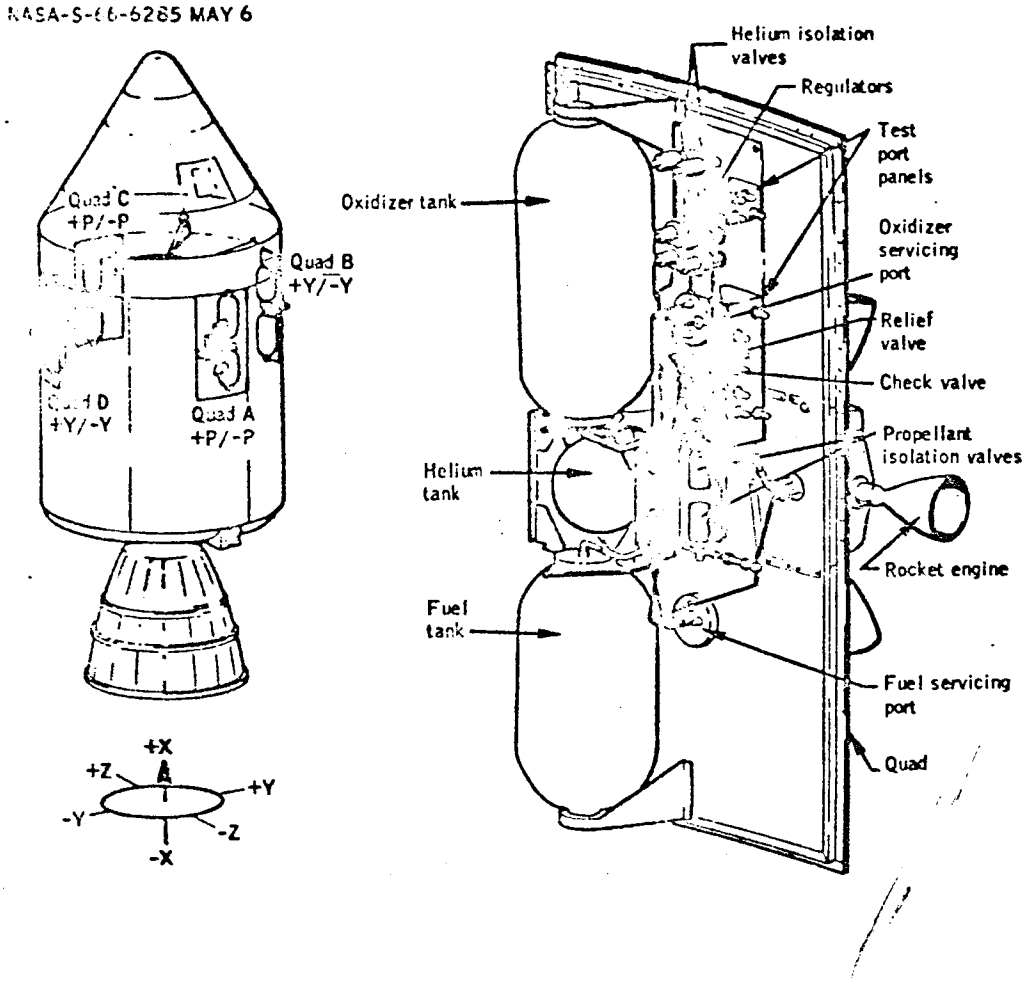

FIGURE 10

SCHEMATIC OF TYPICAL SM RCS QUAD, MISSION AS-201

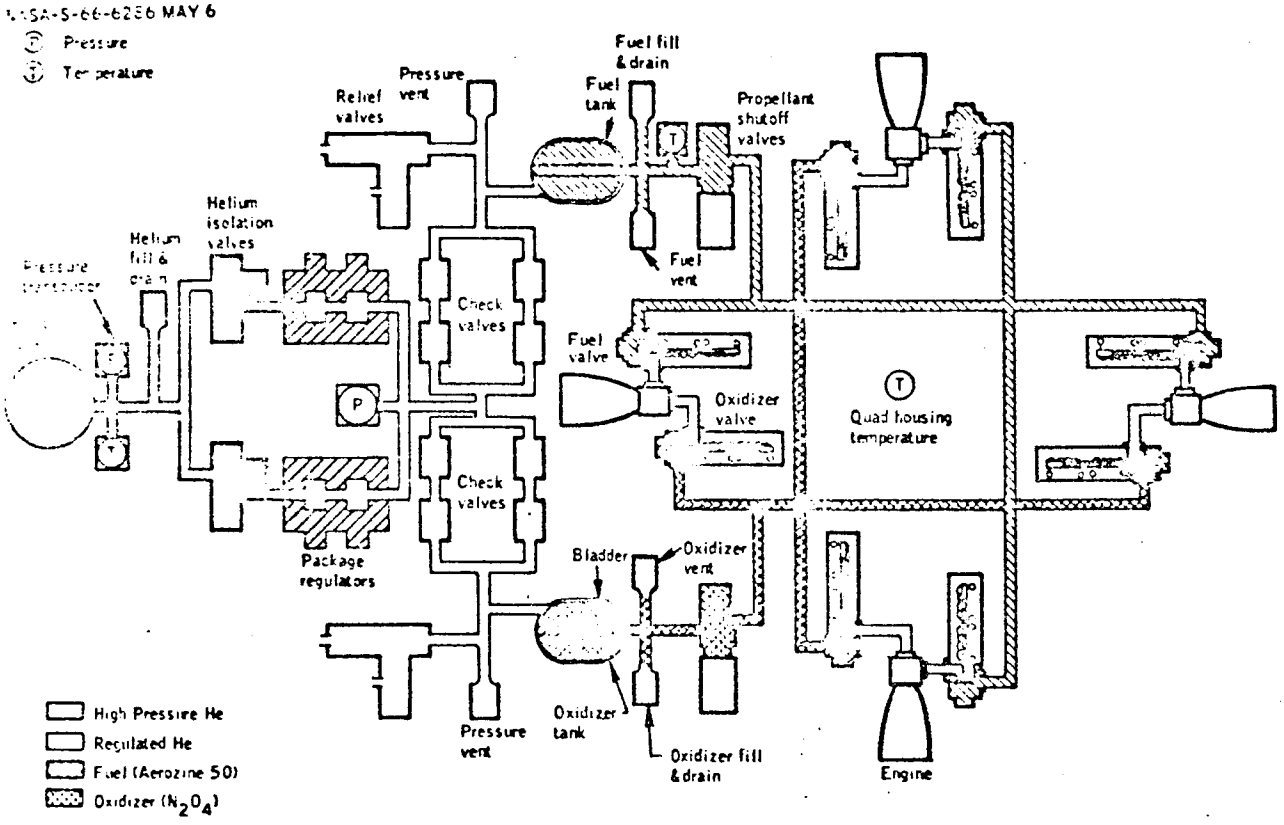

FIGURE 11

LUNAR MODULE RCS INSTALLATION

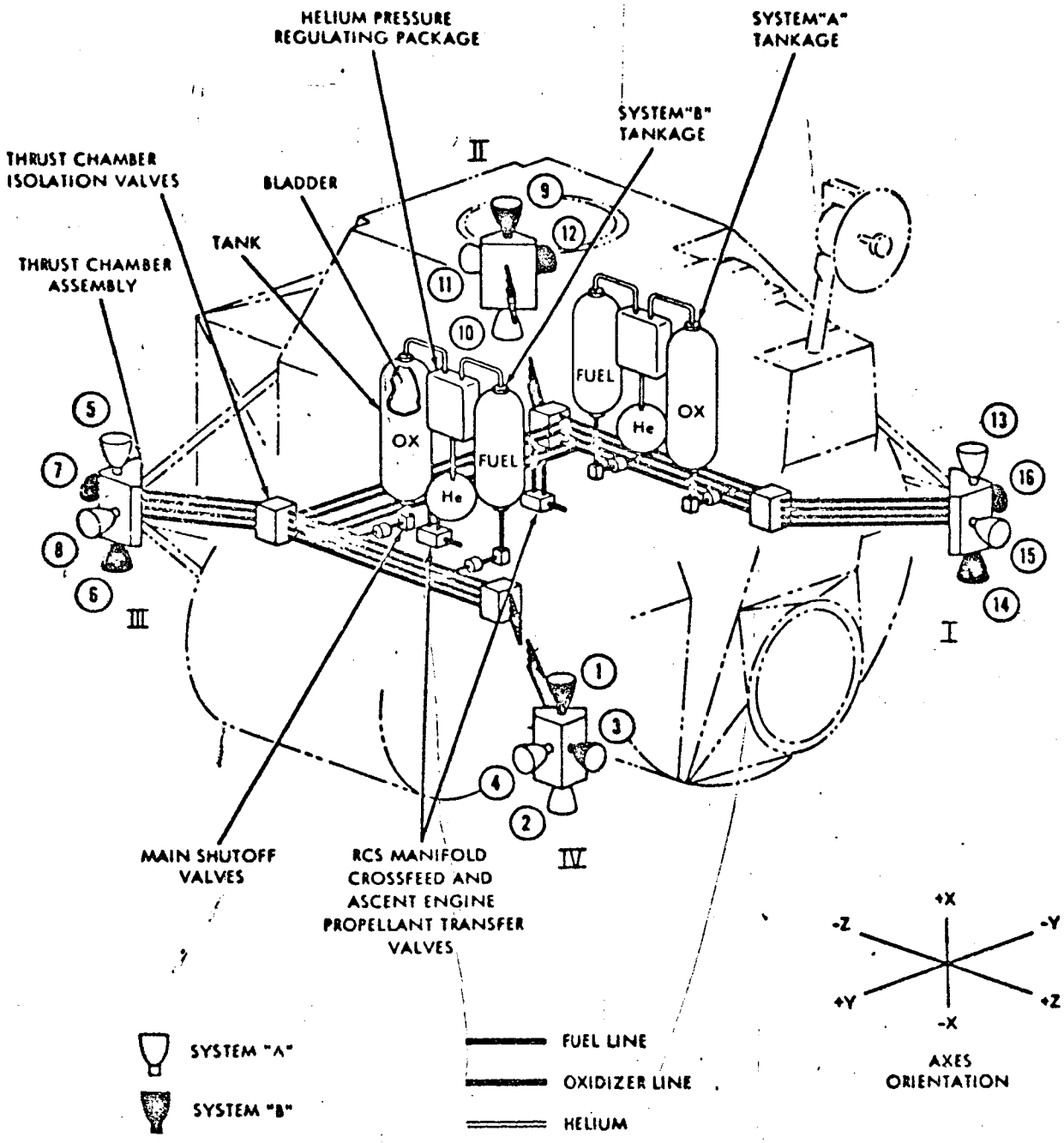

FIGURE 12

LUNAR MODULE REACTION CONTROL SUBSYSTEM SCHEMATIC

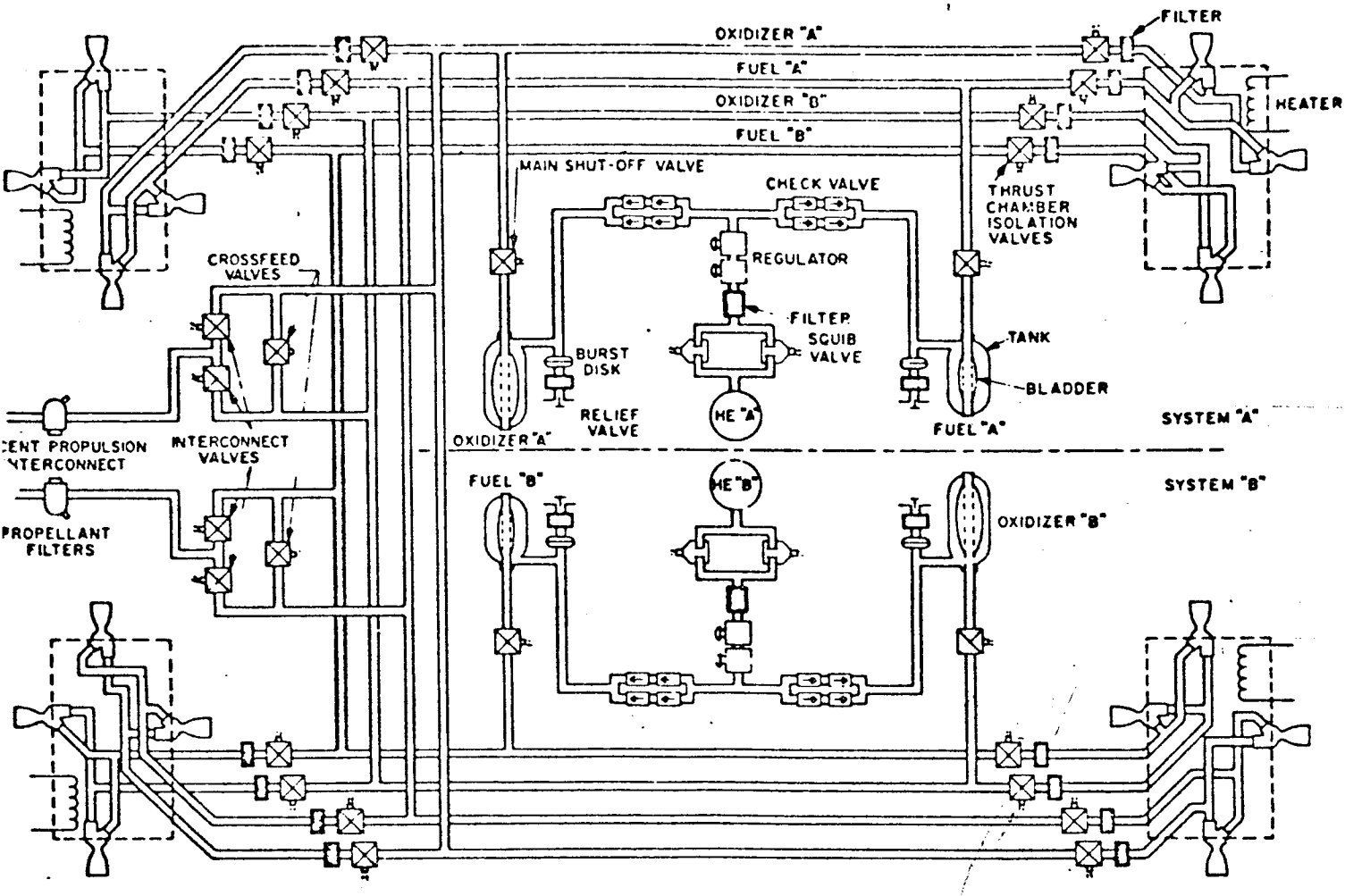

FIGURE 13

- Maintains attitude during translunar coast and navigational sightings.
- Small mid-course corrections
- Orients spacecraft for SPS burn during lunar orbit insertion
- Orients and maintains spacecraft during lunar orbit.
- Orients and maintains attitude during any SPS burn and provides ullage for SPS tank
- Provides attitude control and propulsion for CSM/LM undocking and separation maneuvers
- Provides attitude control for LM decent and lunar landing
- Provides attitude control for LM ascent
- Provides attitude control and thrust during LM orbit adjustments for CSM rendezvous.
- Provides attitude control and thrust during CSM-LM rendezvous
- Provides for LM jettison during CSM-LM separation maneuver.
- Orients and maintains attitude control during SPS burn and provides ullage for SPS tanks during trans-earth injection
- Provides attitude control and ΔV translation and maintains roll for passive thermal control during the return to earth.
- Provides attitude control and thermal for CM and SM separation.

In addition, during the Apollo 11 lunar landing, the engines were fired to translate the LM vehicle away from the rocky crater that was the initial landing site to the final landing site.

The performance of the RCS on the first five Apollo flights has been reviewed in some detail by NASA and Marquardt (References 5 to 8).

The five Apollo flights are sketched in Figure 14 and the flights included Marquardt R-4 RCS engine on four Service Modules (AS 201, 202 and Apollo 4 and 6) and one Lunar Module (Apollo 5). The primary interpretation of the in-flight operation of the Service Module RCS is obtained from Spacecraft Control System data (attitude rate, attitude error, and duty cycle data). From these data RCS operations can be inferred. Data obtained from RCS instrumentation consists of helium bottle and propellant tank temperatures and pressures, and temperatures on several engine injector heads. Telemetered data includes the time and length of the electrical on signal to each engine.

APOLLO FLIGHTS

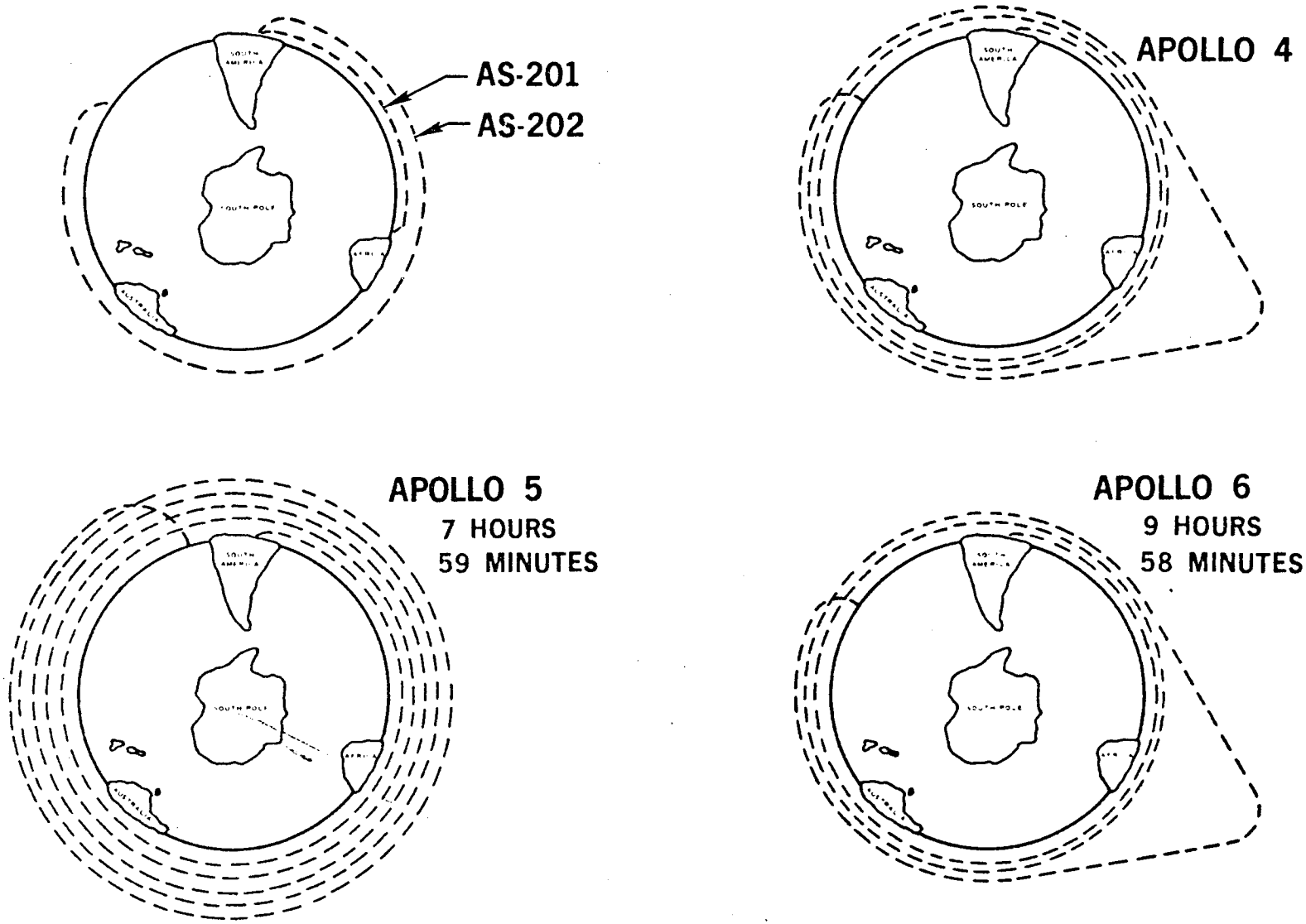

THE MARQUARDT CORPORATION

V6588-1

FIGURE 14

Flight AS-201

The maneuvers performed by the SM RCS engines were all successful and included S-IVB/SM separation, X translation ullage maneuvers, SM attitude control, attitude hold limit cycle control, and SM/CM separation. The engines used and their number of starts and total burn times are listed in Table V. As indicated on the table, the SM Quad A RCS did not fire throughout the flight. The use of helium tank pressure data, and Quad A engine temperature data (cooling) indicates that only one propellant (fuel) flowed through the Quad A engines. The only logical way to stop oxidizer flow to all four engines simultaneously is to close the oxidizer propellant isolation valve. Other occurrances (on the Command Module) of seized-closed oxidizer valves of this design were noted after 10 days exposure to oxidizer on the launch pad. The oxidizer valves were redesigned and requalified for all subsequent flights.

In addition to the Quad A valve problem, detailed analysis of available data indicates that the -Y/X Quad D (or Quad B) engine was not operating. The failure mode could not be determined due to lack of information and post flight analysis has led to no remedial action. The engine starts and burn times for the Quad A engines and the -Y/X Quad D engine have not been included in the total for the AS 201 flight.

Flight AS-202

All 16 Model R-4D engines of the SM/RCS performed as planned throughout the flight and totaled 7,040 engine starts and 727 seconds of burn time as listed in Table VI. No engine anomalies were discovered.

Flight Apollo 4

All 16 Model R-4D engines of the SM/RCS performed as planned throughout the flight and totaled 15,749 engine starts and 533.8 seconds of burn time as listed in Table VII. No engine anomalies were discovered.

Flight Apollo 5

For its first flight, the Lunar Module vehicle was separated from the S-IVB 54 minutes after launch and was placed in an orbit of 90 by 120 nautical miles. The Model R-4D engines on the LM RCS successfully performed all commanded maneuvers. The maneuvers performed and some RCS system anomalies are as follows:

TABLE V

SUMMARY OF STARTS AND BURN TIME FOR SC 009

Engine P/N	Engine P/N		Number of Starts	Total Burn Time (sec.)
227486	0014		185	45.5
227486	0012		*(22)	*(56.9)
227486	0005		*(19)	*(17.3)
227486	0007		185	44.1
227486	0023		153	38.5
227486	0019		44	66.7
227486	0009		21	2.7
227486	0021		**(173)	**(29.1)
227486	0017		194	7.2
227486	0022		216	8.3
227486	0026		194	7.2
227486	0018		216	8.3
227486	0001		*(194)	*(7.2)
227486	0011		216	8.3
227486	0003		194	7.2
227486	0020		*(216)	*(8.3)
		Total	1,818	244.0

NOTE: *Engines did not fire because the Ox isolation valve to Quad A did not open.

**This engine did not fire - Reason is unknown.

TABLE VI

SUMMARY OF STARTS AND BURN TIME FOR AFRM 11

Engine P/N	Engine P/N		Number of Starts	Total Burn Time (sec.)
228687	0018		204	15.660
228687	0023		208	69.300
228687	0021		645	20.405
228687	0111		666	21.960
228687	0020		167	66.965
228687	0012		165	9.525
228687	0014		645	20.405
228687	0011		666	21.960
228687	0003		216	61.075
228687	0107		218	14.955
228687	0001		666	21.960
228687	0008		645	20.405
228687	0010		310	59.115
228687	0004		308	16.935
228687	0019		666	21.960
228687	0006		645	20.405
		Totals	7,040	482.99

TABLE VII

SUMMARY OF STARTS & BURN TIME FOR APOLLO 4 FLIGHT

	ENGINE STARTS	TIME
QUAD A		
-Pitch	667	57.225
CCW	1324	25.995
+P	832	23.515
CW	1120	26.670
QUAD B		
-Yaw	809	65.840
CCW	1309	25.835
+Y	595	24.815
CW	1117	27.055
QUAD C		
-P	619	16.885
CCW	1311	25.795
+P	849	63.945
CW	1125	27.120
QUAD D		
-Y	928	33.450
CCW	1306	25.735
+Y	719	56.660
CW	1119	27.270
TOTAL	15,749	533.810

Orbit	Maneuver
1	Two +X translation maneuvers for separation of LM from S-IVB. Maintained attitude control in maximum deadband.
2	Maintained attitude control.
3	Adjusted attitude for LM descent propulsion system burn. Ullage burn. Attitude control.
4	Maintained attitude control in minimum deadband. Ullage burns for DPS firings 2 and 3. Because of a programming error, extremely high RCS usage began in an attempt to hold attitude control. This occurred after firing of the Ascent Propulsion System. The RCS "A" system main shut off propellant valves were closed during the high usage rates but the "B" system operated to propellant depletion.
5	High RCS usage rates continued when ascent propulsion system propellants were used to hold attitude control. Performed two ullage burns for APS burn and rate damping during APS burn. Maintained attitude control to shut-off of RCS.

Because of the programming error which commanded an excessive RCS impulse bit, the RCS consumed all of its Aerozine-50 and nitrogen tetroxide propellants and an additional 230 pounds more drawn from the ascent propulsion system through the interconnect. During part of orbits 4 and 5, the inlet pressures to the RCS engines covered a range from 40 psia to a normal 170 psia and included gas in the propellants. Engine operation continued at the off design conditions at reduced thrusts. The total number of starts and burn times for both on and off design inlet conditions are presented in Figure 1 and the values for each type are as follows:

Description	Starts	Burn Time (Minutes)
On-Design	8,540	32.2
Off-Design	7,737	13.1
Totals	16,277	45.3

After off design operation at an estimated 10# thrust level during the 5th orbit, the 4 up System B engine did not show any chamber pressure indications on subsequent attempted starts. In the system, the fuel had been depleted first and then the oxidizer. Later both propellants from the ascent propulsion system were brought to the engine. Ground tests with a one propellant purge and subsequent attempted starts have shown that such off design operations could cause thrust chamber and/or chamber pressure transducer failure. However, sufficient margin and redundancies exist in the Lunar Module RCS such that none of the anomalies that occurred during the flight interferred with the successful completion of the LM-1 mission.

Flight Apollo 6

Preliminary information received to date has indicated that the RCS function during the flight of Apollo 6, 4 April 1968, was entirely satisfactory. Approximately 400 pounds of propellant was used by the Service Module RCS in the six hours between command/service module separation from the S IVB and separation of the command module from the service module. During this time the service module RCS maintained the command/service module attitude so that the entire heat shield of the command module was cold soaked. The following is a preliminary breakdown of the RCS engine starts and propellant consumed during the flight:

Phase	Starts	Propellant Used (lb.)
CSM/SIVB Separation	4	30
Cold Soak		221
+ Pitch engines (2)	970	
- Pitch engines (2)	520	
+ Yaw engines (2)	620	
- Yaw engines (2)	710	
+ Roll engines (4)	7,900	
- Roll engines (4)	8,740	
CM/SM Separation	8	148
Totals	19,472	399

During the cold soak mission in which the command/service module reached an altitude of 12,000 nautical miles, the package temperatures of quads B and C reached 104 and 87°F respectively. The measured engine injector head temperatures were within 10°F of the package temperatures during the flight. The low package temperatures are attributed to Quads B and C being in the shade of the vehicle. Temperatures of Quads A and D, which faced obliquely toward the sun, cycled within the thermostat switching limits of 115 - 134°F.

REFERENCES

5-1 AIAA Paper No. 67-504 - The Lunar Orbiter Velocity Control System. Paper presented July 17-21, 1967 to AIAA Third Propulsion Joint Specialist Conference, Washington, D. C.

5-2 NASA CR-782 - Lunar Orbiter I Photographic Mission Summary prepared by The Boeing Company for NASA Langley, dated April 1967.

5-3 NASA CR-66437 - Lunar Orbiter II, Volume III - Mission System Performance prepared by The Boeing Company for NASA Langley, Contract NAS 1-38000, dated April 24, 1967. Boeing Document No. D2 100752-3, Volume III.

5-4 NASA CR-66437 - Lunar Orbiter III - Final Report dated August 11, 1967.

5-5 NAA Internal Letter 190-030-EA66-031 "Spacecraft 009 Flight Test - Reaction Control Systems" from R. R. Koppang to J. W. Gibb, dated 12 May 1966.

5-6 NAA Internal Letter "CSM RCS Propellant Utilization for SC 011", from F. C. Svenson to J. C. Griffiths.

5-7 Marquardt IOM 5022/153-41/868 - Weekly Status Report, Apollo IV Flight to H. McFarland, dated 28 December 1967.

5-8 Marquardt MIR 226 - Lunar Module - Reaction Control System Operation During Apollo V Mission.

CHAPTER 15

RELIABILITY PROVISIONS AND ASSESSMENT FOR THE APOLLO SM-LM RCS ENGINE DEVELOPMENT PROGRAM

BY

J. R. FRANKLIN

and

Q. R. CALL

TABLE OF CONTENTS

		PAGE
I.	INTRODUCTION	15-1
II.	RELIABILITY TASKS	15-1
	A. Reliability Analysis	15-1
	B. Failure Mode and Effect Analysis	15-2
	C. Control of Critical Items	15-2
	D. Design Review	15-6
	E. Failure Analysis and Corrective Action	15-7
	F. Test Planning and Monitoring	15-8
III.	RELIABILITY ASSESSMENT	15-8
	A. Reliability Requirement	15-8
	B. Qualitative Analysis	15-9
	C. Quantitative Assessment	15-10

LIST OF ILLUSTRATIONS

Figure Number	Title	Page
1	Failure Mode and Effects Analysis Form	15-3
2	Classification of Characteristics Valve Assembly Solenoid, Fuel	15-5

LIST OF TABLES

Table Number	Title	Page
I	Applicable Test Data for Reliability Assessment of the 100 Pound Thrust SM-LM RCS Engine	15-12
II	Summary of R-4D Engine Problems Experienced During Test Programs	15-15
III	Summary of R-4D Engine Problems Experienced During Acceptance Testing	15-18
IV	Summary of R-4D Engine Problems Experienced During Field Usage	15-20
V	Valve Leakage Failures Which Were Given Additional Consideration in the Reliability Assessment	15-24

I. INTRODUCTION

Reliability program provisions implemented during the Apollo SM-LM RCS engine development program were specifically intended to design reliability into the engine and prevent degradation of the reliability through controlled fabrication, acceptance test and handling procedures. The accomplishment of the above goal was achieved by effectively conducting six interrelated tasks: 1) Reliability analysis including reliability apportionment, math models, and reliability prediction, 2) failure mode and effect analysis, 3) control of critical items, 4) design review of engine parts and assemblies, and testing requirements, 5) failure analysis and corrective action, 6) test planning and monitoring.

The approach used by Marquardt Reliability for each of these disciplines is presented in the discussion. A summary of the method and data used for reliability assessment is also presented.

II. RELIABILITY TASKS

A. Reliability Analysis

Preparation of logic block diagrams and reliability apportionment of the reliability goal for the Apollo SM-LM RCS engine were conducted early in the development program. The method used for apportionment of the established engine goal was to subdivide the engine unreliability on the basis of subassembly weight factors derived through consideration of state-of-the-art, complexity, environments, and operating times.

The primary purpose of the apportionment was to outline the reliabilities required at subassembly levels in order to achieve the required assembly reliability requirement. These apportioned goals then serve as a basis for comparison with subassembly reliability predictions and assessments to point out major problem areas and to effectively monitor progress in achievement of required reliability objectives.

A reliability prediction was made for the engine based on failure rate information derived from in-house or industry-wide failure rate sources. The reliability predictions for the subassemblies were compared with the corresponding apportioned goal to reveal potential design deficiencies and to depict the extent and degree of development effort required to effectively substantiate achievement of the required reliability. Results of this analysis indicated that the propellant valves were the subassembly parts which needed improvement in reliability. Experience has borne out this conclusion and it became evident that the limiting capability of the RCS engine would be to seal against possible GN_2 leakage as was required by the procurement specification.

B. Failure Mode and Effect Analysis

A failure mode and effect analysis was prepared for the Apollo SM-LM RCS engine. This analysis started at the engine assembly and was carried down to the piece parts. The analysis determined the possible modes of failure and their causes whereby the RCS engine might fail to perform its intended functions as defined by all of the requirements of the procurement specification. In addition, the effect of each mode of failure was considered and compensating provisions to eliminate the effect of the failure or reduce the probability of occurrence were listed.

Figure 1 is a sample of the form used and the information presented. The completed analysis was released to Design Engineering and other affected groups associated with design and fabrication of the engine and component parts.

C. Control of Critical Items

Critical items for the RCS engine were identified by reliability review of the detail design, and by the failure mode and effect analysis. Components and parts within the engine were considered as critical items if failure of that item could result in a personnel hazard, a

FAILURE MODE & EFFECTS ANALYSIS FORM

FAILURE-MODE AND EFFECT ANALYSIS — Marquardt — PAGE OF

FAILURE CLASS.	FOR ANALYTICAL PURPOSES, THE EFFECTS OF A COMPONENT FAILURE ON THE END PRODUCT ARE CLASSIFIED AS SHOWN BELOW. CLASS I - CERTAIN LOSS CLASS III - POSSIBLE LOSS CLASS II - PROBABLE LOSS CLASS IV - NONE
PROB. OF FAILURE	NUMBER DEFINED BY DATA OF TESTS OF THE COMPONENT OR ITEM MODIFIED BY THE ENVIRONMENTAL OPERATING CONDITIONS REQUIRED. ALSO GENERIC FAILURE RATES AND ENGINEERING JUDGMENT SERVE TO SPECIFY THIS NUMBER.
REMARKS	APPROPRIATE REMARKS.
INHERENT COMPENSATING PROVISIONS	WHAT HAS (OR WILL) BE DONE TO MINIMIZE OR ELIMINATE THE MALEFFECTS TO THE SYSTEM AS A RESULT OF THE FAILURE (S), OR PREVENT THE FAILURES.
EFFECTS AND CONSEQUENCES	THE EFFECTS AND CONSEQUENCES OF THE LACK OF FUNCTION PERFORMANCE IN TERMS OF THE SUBSYSTEM AND SYSTEM OF WHICH THE COMPONENT IS A PART.
POSSIBLE CAUSES	THE POSSIBLE REASON FOR THE OCCURRENCE OF THE FAILURE.
ASSUMED FAILURE	THE FAILURE TYPE (S) OR FAILURE MODE (S) WHICH WOULD PREVENT OR HINDER THE SUCCESSFUL COMPLETION OF THE FUNCTION (S) AS STATED IN THE FUNCTIONS COLUMN.
FUNCTION	THE FUNCTION OR FUNCTIONS WHICH THE PART PERFORMS OR AIDS IN PERFORMING.
BLOCK DIAGRAM REF. NO.	MATH MODEL NUMBER AS IT APPEARS ON THE LOGIC BLOCK DIAGRAM.
ITEM NAME AND PART NUMBER	NAME AND NUMBER OF PART AS IT APPEARS ON PRODUCTION BLUEPRINT.

Figure 1

serious performance degradation or catastrophic failure of the engine.

A critical items list was prepared which listed the critical items, part numbers, areas of criticality, and traceability requirements.

For each critical item, the specific characteristics (the attributes of the part) that contribute to the criticality were identified. Classification of characteristics is a method to aid in producing and maintaining quality and reliability during manufacture, inspection, and throughout the useful life of the product. All characteristics are not given equal emphasis and in fact are not of equal importance. Without classification, each department or person uses independent judgement to determine the importance of a characteristic. The classification is a means of designating the relative importance and provide common criteria for all personnel involved.

A classification of characteristics was prepared for each engine part and assembly drawing and, along with the critical items list, released to Engineering, Manufacturing, and Quality Control. Figure 2 shows an example of a classification of characteristics for one of the parts.

Each drawing and applicable specification for all engine parts and assemblies were reviewed and approved by Reliability Engineering to ensure that proper definition of the necessary reliability performance parameters, the critical inspection parameters, and the traceability requirements were on the drawings or in the applicable specifications. All changes to these documents are also reviewed and approved by Reliability Engineering and the Change Control Board to ensure no degradation to the reliability of the hardware.

The requirements of the drawings, the special control specifications, and the critical items traceability and verification to ensure adequate control of the critical items are accomplished by manufacturing process procedures, fabrication planning, inspection planning, and acceptance test procedures. The classification of characteristics is used as a guide for assurance of reliable parts in that every critical characteristic

CLASSIFICATION OF CHARACTERISTICS

THE MARQUARDT CORPORATION
FORM TMC 1709 REV. 6-67

SHEET 1 OF 1

PROJECT	PART NAME	DRAWING NO.	CHG. LTR.	DATE OF ISSUE
279 (Apollo)	Valve Assembly - Solenoid, Fuel	228683	B	12-10-65

SUBSYSTEM	CLASSIFICATION IDENTIFICATION	SUPERSEDES CLASS. DATED
Solenoid Valve	C = CRITICAL M = MAJOR	8-25-65

CHARACTERISTICS	CLASSIFICATION	REMARKS
0.020/0.018 Stroke	M-A	Functional acceptance.
⊥ A 0.0005 of Surface "X"	M-A	Functional acceptance.
NOTE 1: Torque (90-100 in-lbs)	M-A	Functional acceptance.
NOTE 4: Cleanliness requirement per MPS 210	C	Possible contamination of valve may result in engine failure
NOTE 2: 2.75 ± .10 lbs. spring load	M-A	Functional acceptance.
⊥ .0005 of surface "Y"	M-A	Functional acceptance.
.020 of .010 + .010R in armature at surface "Y"	M-A	Functional acceptance.
NOTE 6: Functional test.		
6.3 Proof pressure test	C	Structural adequacy.
6.4 Leakage test	M-A	Functional acceptance.
MTS-0682 (B) Acceptance Test		
Par. 3.2: Cleanliness requirement	C	Possible contamination of valve may result in engine failure.
Par. 4.3: Pressure drop	M-A	Functional acceptance.
Valve response	M-A	Functional acceptance.
Pull-in current	M-A	Functional acceptance.
Drop-out current	C	Contractual requirement.
Leakage test	M-A	Functional acceptance.
.395/.392 diameter	M-A	Functional acceptance.
		All other characteristics are considered minor.

SAMPLE

PREPARED BY	DATE	REVISIONS						
[illegible]	7-14-65	CHG. LTR.	B					
RELIABILITY ENGINEERING [illegible]	8-25-65	APPROVED DATE	RL 12-10-65					
PROJECT ENGINEERING	DATE	APPROVED DATE						

Figure 2

must be verified on 100% of the parts. By this approach, failures due to fabrication defects have been held to a minimum.

D. Design Review

Design review on the Apollo SM-LM RCS engine has been in two forms. All drawings, specifications, and changes to these documents have been reviewed and approved by Reliability Engineering prior to release. Formal and informal design reviews have been conducted at significant phases of the program. Major design reviews were conducted early in the development program and shortly before the Qualification test program. These reviews included a detailed review of all aspects of the design and hardware fabrication and testing controls. Action items from both internal reviews and customer reviews were resolved. In addition, many special design reviews were held during the Development program and subsequent to the Qualification test program. These special reviews have been called whenever a problem is uncovered which indicated the need.

E. Failure Analysis and Corrective Action

During the Apollo SM-LM RCS engine development and production programs, a formal and controlled system was implemented at Marquardt for reporting, analysis, correction and data feedback of all failures and malfunctions that occurred throughout the fabrication, handling, test, checkout, and operation of the engine. This system has been complementary to, but not redundant with the quality assurance system for repetitive discrepancy control and material review.

The system provides for a formal and complete failure investigation under the direct cognizance of Reliability and Product Engineering for all cases where the engine, subassembly or component part failed to perform its required function within specified limits under specified conditions for a specified duration. Of primary concern was the failure analysis to determine the true cause of failure, and the evaluation of the failure to determine whether the failure cause was internal or external to the engine hardware. In all cases where the cause of failure could be considered assessable to the hardware reliability, necessary corrective action was defined in the failure report to maintain or improve the reliability of the hardware. When the cause of failure was found to be a hardware discrepancy or a malfunction which did not affect the reliability status of the hardware, corrective action was recommended or suggested. In these cases the quality assurance and material review corrective action system determined the required corrective action.

All failures which occurred during Qualification tests, the deliverable item final Acceptance tests, and any others which had significant impact upon the schedule commitments or cost considerations were reported to the customer within 24 hours. This verbal report was in addition to the formal report of the failure analysis and evaluation prepared at the completion of the failure investigation. In addition to customer notification of all significant failures, reports of all failures were distributed to the affected organizational groups within Marquardt.

Corrective action follow-up has been conducted by a formally established corrective action committee for all failures. In addition, Reliability Engineering has assured adequate corrective action for all failures affecting the reliability status of the hardware by review and approval of the design changes required.

F. Test Planning and Monitoring

Reliability has been an integral part of the formal test programs during the Apollo SM-LM RCS engine program. The Reliability group reviewed and approved each test plan associated with development, qualification, end-item acceptance, and ground test programs prior to testing. Test procedures were also reviewed to assure the inclusion of elements and data necessary for the assessment of achieved reliability.

During the conduct of the test programs, a member of Reliability was represented on the test committee and thus participated in all significant decisions during the conduct of the testing. By this method test monitoring was timely and effective.

III. RELIABILITY ASSESSMENT

A. Reliability Requirement

The reliability requirements of the TMC 100 pound thrust engine for the Apollo SM-LM reaction control systems are defined in the North American Rockwell Procurement Specification MC901-0004F.

The reliability design goal for the 100 pound thrust Apollo SM-LM RCS engine is 0.997 during a mission simulation cycle consisting of 5,518 pulses and 519.8 seconds burn time. This duty cycle is made up of pulse and steady state operation corresponding to engine utilization during a seven-day programmed lunar mission. The reliability assessment in this report, therefore, is based on this mission duty cycle.

The NAR procurement specification further specifies, that after Acceptance testing, the required engine reliable operating life without injurious deterioration is at least 1,000 seconds burn time and a minimum of 10,000 operational cycles for the environments specified for space operation.

B. Qualitative Analysis

The reliability of the TMC 100 pound thrust engine used for the Apollo SM-LM reaction control systems is a function of the propellant control, propellant sealing, propellant injection, combustion gas sealing, and thrust generation reliabilities. A review of the failure mode and effect analysis shows that the propellant sealing and valve attach hardware, the injector head assembly, the combustion gas sealing and attach hardware, and the thrust chamber have only structural or fluid flow functions. These are passive functioning components (no electrical or mechanical operation) with only structural failure modes except in the case of improper injector flow distribution and combustor coating wear out.

Based on TMC experience of testing and analysis, there is a very low probability of flow distribution problems due to self induced contamination or corrosion. Within the limits of the environments and propellant contamination levels tested, there is no experience to indicate that flow distribution might be affected in such a way as to cause a performance failure or a chamber burn out. As further protection against inadvertent or unexpected externally introduced contamination, a sediment strainer was added to the valve inlet to protect the engine.

The molybdenum disilicide coating degradation on the 100 pound thrust RCS engine combustor is negligible during the required pulsing operation duty cycle while operating in a hard vacuum. The deterioration of the combustor molybdenum disilicide protective layer of silica and the failure of the molybdenum is caused by the sublimation of the SiO_2 layer and the transformation of the $MoSi_2$ sublayer to Mo_5Si_3 which is oxidized by the combustion gases. The rates of this action is a

function of time and temperature in an environment of combustion gas products. Based on an analysis of the coating loss at various wall temperatures supported by experimental experience, the predicted coating life of this RCS engine combustor at the maximum combustor operating temperature of 2450°F (acceptance test data indicates temperatures of 1800°F to 2100°F) is in excess of 3,000 minutes. Comparison of 3,000 minutes to the Apollo S/M lunar mission duty cycle of 519.8 seconds (8.67 minutes) indicates a negligible probability of coating wear out for this application.

Probability of any structural failure within the specified environment is considered to be very small in view of the stress analysis results which show adequate margins of safety.

In addition to the stress analysis, the Qualification test has demonstrated that the engine will not fail structurally when subjected to the stress environments required. Also, all critical characteristics (materials, processes and dimensions) have been defined with special Quality Control care taken to verify compliance in these critical areas.

In view of the qualitative analysis presented above, it has been concluded that the reliability of the 100 pound thrust engine is, for practical purposes, dependent on the propellant control reliability. Therefore, the engine reliability assessment presented in the following section was based on valve cycle experience accumulated during the valve design substantiation testing and applicable engine testing. Table I presents a summary of this test data.

C. Quantitative Assessment

The quantitative reliability assessment for the TMC 100 pound thrust engine for the Apollo SM-LM Reaction Control Systems was established from applicable valve and engine test experience as shown in Table I.

As discussed in the qualitative analysis, it was concluded that engine reliability is primarily dependent on the reliability of the solenoid valves. The reliability assessment, therefore, was based on engine cycle operation rather than engine burn time.

The quantitative assessment of the engine was based on the assumption of reasonably random failure occurrences (constant failure rate system: $R = e^{-\lambda t}$). This method is recommended in "Reliability Assessment Guides for Apollo Suppliers" (NAR document SID 64-1447A) if twenty equivalent mission duty cycles of testing experience exist from data accumulated on at least five separate test units.

As recommended in the Reliability Assessment Guide, and as justified by the analysis approach, all test data prior to the qualification design was excluded from the assessment. Since the design changes which changed the PFRT design to the Qual design directly affected the valve reliability, both the failures and successes prior to these design changes were eliminated except as back up for the qualitative assessment presented in the preceeding section.

Each of the failure investigations referenced in Table I are summarized in Tables II and III. Also, all of the indicated failures which have occurred during customer field usage are summarized in Table IV. Based on careful evaluation of each of the failures which have been experienced during acceptance testing, TMC test programs and customer usage, it was concluded that all of the failures should be excluded for calculation of the reliability of the engine to complete its intended mission. Therefore, the reliability calculation is as follows:

TABLE I

APPLICABLE TEST DATA FOR RELIABILITY ASSESSMENT
OF THE 100 POUND THRUST SM-LM RCS ENGINE

TEST DATE	TEST DESCRIPTION	ENGINES TESTED	BURN TIME-SEC.	ENGINE CYCLES	REMARKS
7-65	Valve Design Verification (DST)	9 valves	-	102,500	205,000 valve cycles were completed at various environmental conditions.
7-65/8-65	Pre-Qualification	2	2,931	32,495	
8-65/12-65	Qualification	6	7,712	85,818	FMR's 279-107, 110, and 114
10-65/3-66	LM Low Voltage	2	2,455	32,950	
10-65/3-66	LM Transducer Evaluation	1	731	23,820	
3-66/4-66	LM Production Cluster	5	1,952	9,425	FMR's 329-045, and 083
11-65/12-65	IR&D	2	12,490	106,964	
1-66/3-66	Off-Limits	4 of the Qual. Engines	6,238	16,158	FMR 279-117
8-66/11-66	LM Production System	16	8,256	56,467	FMR's 329-054, 057, 077, and 078
8-66/9-66	SM Structural Adequacy Proof Test	3	76	5,992	FMR 279-118
9-66	LM Design Verification Engine Ignition Testing	3	104	8,187	
10-66/11-66	SM Supplemental Qualification	3	2,136	26,864	
12-66-1-67	R-4D-1 Design Verification	1	2,686	16,683	
11-66/1-67	LM Supplemental Qualification	2	1,277	17,616	FMR 329-080
2-67/3-67	LM DVT System	17	3,767	24,469	FMR 329-094, 098, 102, 103, and 104
6-67/5-68	SM Product Improvement Program	7	8,075	28,741	

The size of contamination which will cause valve leakage is a very difficult criteria to establish. To protect the valve and injector flow passages against large external contamination, a 160 micron sediment strainer has been put in the inlet of each valve as a retrofit program. Contamination control procedures during engine fabrication, test, and usage have been carefully established and improved to give maximum protection to the engine.

Because of the many variables which control the test programs and conditions found in each of the valve leakage failures summarized in Table V, none of these failures has been proven to be assessable against the engine design. Also, whether or not GN_2 valve leakage or minor propellant leakage (as experienced in some cases or might result in some cases of large GN_2 leakage) would cause actual engine failure during mission operation is doubtful. Therefore, reliability assessment for the engine to complete its intended mission was made, excluding all of these failures.

TABLE I (continued)

APPLICABLE TEST DATA FOR RELIABILITY ASSESSMENT
OF THE 100 POUND THRUST SM-LM RCS ENGINE

TEST DATE	TEST DESCRIPTION	ENGINES TESTED	BURN TIME-SEC.	ENGINE CYCLES	REMARKS
10-67	LM Priming and Off Limits Contamination	2	790	11,078	
7-67	LM Short Electrical Pulse Width Engine Test	1	99	371	
2-68/5-68	LM Heater Integration Test	2	129	7,468	FMR 329-116
5-68/6-68	LM RCS Integration Test	4	194	10,291	FMR 329-116 FMR 329/M-224
5-68/6-68	LM Attitude Control Engine Performance Evaluation at O/F = 1.3	2	10,340	12,071	
1-68/2-68	Monopropellant - 75 Pound Thrust Evaluation (Valves Identical to Apollo 100 Pound Thrust RCS Engine)	1	81	733	
5-67/3-68	Monopropellant - 5 Pound Thrust Evaluation (Valves Identical to Apollo 100 Pound Thrust RCS Engine)	12	52,264	287,167	574,334 cycles were completed, however, each engine had only one valve.
8-67/12-67	MOL High Thrustor Demonstration Test	2	16,432	2,256	
7-65/9-68	Acceptance Tests (Est. 400 Cycles and 70 Sec./Engine	650	45,500	260,000	See Table III for summary of FMR's.
to 4-1-69	Model R-4D Space Firing Summary	149	14,940	226,218	See next page for more detailed summary.
	TOTALS		201,655	1,412,802	All failures are considered to be nonassessable to mission success.

TABLE I (CONTINUED)

MODEL R-4D SPACE FIRING SUMMARY

APRIL 1, 1969

LUNAR ORBITER PROGRAM (FIVE FLIGHTS)

SPACECRAFT IDENTIFICATION	TOTAL ENGINE STARTS	TOTAL BURN TIME	SPACECRAFT TIME IN SPACE	ENGINE TIME IN SPACE (ENGINE DAYS)	NO. OF ENGINES
L. O. I	5	12.2 MIN.	80 DAYS	80 DAYS	1
L. O. II	7	12.5 MIN.	338 DAYS	338 DAYS	1
L. O. III	7	12.5 MIN.	243 DAYS	243 DAYS	1
L. O. IV	4	11.9 MIN.	176 DAYS	176 DAYS	1
L. O. V	6	12.5 MIN.	180 DAYS	180 DAYS	1
TOTAL TIME HISTORY FOR LUNAR ORBITERS	29	1.03 HOURS	2.79 YEARS	2.79 YEARS	5

APOLLO SPACECRAFT PROGRAM (EIGHT FLIGHTS)

MISSION IDENTIFICATION	SPACECRAFT IDENTIFICATION	TOTAL ENGINE STARTS	TOTAL BURN TIME	SPACECRAFT TIME IN SPACE	ENGINE TIME IN SPACE (ENGINE DAYS)	NO. OF ENGINES
APOLLO (AS201)	SC 009	1,818	4.1 MIN	0.5 HRS.	0.3 DAYS	16
APOLLO (AS202)	SC 011	7,040	8.0 MIN.	1.5 HRS.	1.0 DAYS	16
APOLLO 4	SC 017	15,749	9.3 MIN.	8.5 HRS.	5.7 DAYS	16
APOLLO 5	LM 1	8,540	36.5 MIN.	8.0 HRS.	5.3 DAYS	16
APOLLO 6	SC 020	19,472	17.5 MIN.	9.6 HRS.	6.4 DAYS	16
APOLLO 7	SC 101	61,000	41.5 MIN.	10.8 DAYS	172.8 DAYS	16
APOLLO 8	SC 103	46,240	27.3 MIN.	6.0 DAYS	96.0 DAYS	16
APOLLO 9	SC 104	41,100	25.8 MIN.	10.0 DAYS	160.0 DAYS	16
	LM 3	25,230	17.4 MIN.	4.2 DAYS	67.2 DAYS	16
TOTAL TIME HISTORY FOR APOLLO R.C.S. ENGINES		226,189	3.12 HOURS	32.2 DAYS	514.7 DAYS	144

TOTAL SPACE FIRING TIME HISTORY FOR R-4D ENGINES USED ON APOLLO AND LUNAR ORBITER SPACECRAFT

ENGINE STARTS	TOTAL BURN TIME	SPACECRAFT TIME IN SPACE	ENGINE TIME IN SPACE	NO. OF ENGINES
226,218	4.15 HOURS	2.88 YEARS	4.2 YEARS	149

TABLE II

SUMMARY OF R-4D ENGINE PROBLEMS EXPERIENCED DURING TEST PROGRAMS

FMR NO. DATE OF FAILURE	P/N S/N	FAILURE MODE	CAUSE OF FAILURE	REMARKS
279-110 9-17-65	228687 S/N 0009	Excessive oxidizer leakage with subsequent explosion resulting in a broken combustor during Qual testing.	Valve seat damage was caused by an explosion in the oxidizer manifold. This explosion was concluded to have been caused by residual fuel in the oxidizer manifold from pulse shut down. Low injector temperatures and cell pressure above 0.05 psia were environments which allowed this condition.	This failure mode was catastrophic but the failure was considered to be nonassessable to the engine reliability for space operation within the requirements of the existing spec. temperatures. However, it was necessary to restrict the ambient pressure requirements to 0.03 psia or less when test conditions require an injector head temperature of less than 60°F.
279-107 11-4-65	228687 S/N 0017	High O/F ratio and Low ISP during Qual. testing.	Improper acceptance test calibration due to instrumentation problems.	
279-114 1-10-66	228687 S/N 0002	Slow thrust decay rate for hot pulse operation during Qual. testing.	Design capability not compatible with the spec. requirements.	The customer's specification was changed.
279-117 3-31-66	228687 S/N 0002	Oxidizer valve GN_2 leakage during tear down evaluation subsequent to Qual and off limits testing.	Leakage was caused by Teflon seal surface defects probably due to entrapped contamination between the armature pintle and the valve seat.	This valve completed almost 30,000 cycles without indication of leakage.
279-118 8-12-66	228686-501 S/N 0234	Fuel valve GN_2 leakage during reacceptance testing following SM RCS structural adequacy proof test program.	Teflon seal surface defects probably caused by entrapped contamination.	This engine was tested without protective filters between the pulse tanks and the engine. It has subsequently been established that out-of-spec. contamination existed in the Pad-G environmental facility.
329-045 4-27-66	227894 S/N 1010	Broken combustor during LM Production Cluster Testing.	Failure was caused by an ignition spike. This spike resulted from accumulation of residual propellant products in conjunction with poor or no preigniter operation probably due to oxidizer lead resulting from trapped bubbles in the gas saturated fuel.	This failure mode is catastrophic and assignment of nonassessability to the engine reliability required changes to the customer's requirements including limitation of the minimum engine flange temperatures to about 120°F or using MMH fuel with the minimum engine flange temperature limited to about 50°F. Operation with saturated propellants was previously outside the specification requirements.
329-054 9-6-66	227895 S/N 1040	Minor fuel leakage during LM Production system testing	The leakage stopped without actuating the valve. Probable cause was contamination that held the valve pintle away from the teflon seat.	
329-056 10-8-66	227895 S/N 1033	Fuel valve GN_2 leakage during LM Production cluster vibration testing.	Leakage was caused by entrapped Braycote and/or metal particle contamination.	Test lines were attached to the valve inlet several times in an uncontrolled area using Braycote lubrication. There was no filter on the valve inlet.
329-057 10-11-66	228745 S/N 1001	Minor oxidizer-leakage during LM Production system testing. The leakage stopped after valve cycling. GN_2 leakage recurred at post-burn test following completion of the LM Production system testing.	Leakage was caused by teflon seal surface defects probably resulting from entrapped contamination between the armature pintle and the valve seat.	This valve completed about 21,000 cycles without indication of leakage.

TABLE II (continued)

SUMMARY OF R-4D ENGINE PROBLEMS EXPERIENCED DURING TEST PROGRAMS

FMR NO. DATE OF FAILURE	P/N S/N	FAILURE MODE	CAUSE OF FAILURE	REMARKS
329-062 10-12-66	227895 S/N 1032 and 1034	Fuel valve GN_2 leakage during LM Production cluster shock testing.	Teflon and metal contamination on the valve seat due to excessive dry vibration and Braycote contamination.	These failures are not considered to be assessable to the engine reliability since these engines were handled as in FMR 329-056 above. Also, the dry vibration was abnormal to engine capability.
329-067 10-14-66	227895 S/N 1031			
329-076 11-29-66	227895 S/N 1033	Ox. valve GN_2 leakage during LM Production cluster passive overstress testing.		
329-077 12-7-66	227895 S/N 1002	Oxidizer valve GN_2 leakage during postburn check following LM Production System Testing.	Leakage was caused by an inadequate teflon sealing surface such that a seal was not effected around the entire circumference.	This valve had completed over 12,000 cycles without indication of leakage.
329-078 12-7-66	227895 S/N 1012	Oxidizer valve GN_2 leakage during postburn check following LM Production System Testing.	Leakage was probably caused by entrapped Teflon particles between the armature pintle and the seat. Braycote thread lubricant may have been the source of the Teflon.	The use of Braycote as a lubricant on the threads in the valve was replaced with an oil which has particles in it. This valve had completed over 5,000 cycles subsequent to assembly without indication of leakage.
329-080 12-15-66	228686-501 S/N 0261	Fuel valve GN_2 leakage during postburn checkout following LM supplemental Qual testing in RRL-Pad-G.	Leakage was caused by damage to the Teflon surface probably from facility introduced contamination.	The test program in RRL Pad-G was being conducted without test filters to protect the engines.
329-083 1-6-67	227894 S/N 1008	Oxidizer valve GN_2 leakage during postburn check following LM Production cluster testing.	Leakage was caused by surface defects in the Teflon seal probably due to entrapped contamination between the armature pintle and the valve seat.	This engine experienced a significant amount of corrosion due to uncontrolled storage environments and may have caused the valve leakage. This valve had completed 2,229 cycles without indication of leakage.
329-094 3-3-67	228745 S/N 1002	Oxidizer leakage during LM DVT system testing.	Leakage was caused by a loose retainer in the valve seat probably due to explosion of residual propellants in the injector assembly.	Inadequate purging methods employed in the test program allowed the residual propellants in the injector. Therefore, the engine reliability is not affected.
329-098 3-6-67	228686-501 S/N 0324	Minor oxidizer leakage during LM DVT system testing.	The leakage stopped without actuating the valve. Probable cause was contamination that held the pintle away from the teflon seat.	
329-102 3-22-67	227895 S/N 1013	Fuel valve GN_2 leakage during LM DVT system testing.	Same as FMR 329-094 above.	Same as FMR 329-094 above.
329-103 3-22-67	227895 S/N 1004	Fuel valve GN_2 leakage during check at completion of LM DVT system testing.	Leakage was caused by a cellulose filter fiber entrapped between the armature pintle and the valve seat.	The contamination was probably introduced into the valve prior to engine testing. This valve had completed over 10,000 cycles without indication of leakage.
329-104 4-7-67	227895 S/N 1037	Increase in water flow rate after completion of LM DVT system testing.	The increase in flow rate was probably due to flushing some type of contaminate from the injector head during the engine firing tests.	The shift to water flow was a failure to Acceptance test requirements

TABLE II (continued)

SUMMARY OF R-4D ENGINE PROBLEMS EXPERIENCED DURING TEST PROGRAMS

FMR NO. DATE OF FAILURE	P/N S/N	FAILURE MODE	CAUSE OF FAILURE	REMARKS
329-116 2-19-68	228686-501 S/N 0261 S/N 1088 S/N 1100	Broken combustors on engine S/N 0261 during LM heater integration testing and on engines S/N 1088 and 1100 during LM RCS integration testing.	The combustors were damaged by large ignition overpressures caused by an accumulation of explosive combustion residue.	The testing which broke these combustors was conducted with aerozine 50 fuel at engine flange temperatures below 95°F while firing continuous minimum impulse bit pulse mode operation. These conditions are outside the safe operating environment for the engine and the engine specification requirements.
329/M-224 3-7-68	228686-501 S/N 1100	Oxidizer valve GN_2 leakage during failure investigation 329-116.	Leakage was caused by an inadequate teflon sealing surface such that a seal was not effected around the entire surface.	This valve completed 3099 cycles without indication of leakage.

TABLE III

SUMMARY OF R-4D ENGINE PROBLEMS EXPERIENCED DURING ACCEPTANCE TESTING
(ONLY FAILURES OF PREVIOUSLY ACCEPTABLE FUNCTIONS ARE INCLUDED)

FMR NO. DATE OF FAILURE	P/N S/N	FAILURE MODE	CAUSE OF FAILURE	REMARKS
279-099 7-26-65	228687 S/N 0002	Low insulation resistance at postburn Acceptance testing.	Fabrication procedures allowed insulation defects in conjunction with moisture forced into the valve winding during burn test shutdown procedures caused the indicated low insulation resistance. The insulation was acceptable when the valve was dry.	The introduction of moisture from burn test shut down procedures is considered to be an out-of-spec. environment since moisture can be forced into the valve windings under vacuum conditions.
279-102 8-8-65	228687 S/N 0007			
279-108 11-22-65	228687 S/N 0057	Fuel valve GN_2 leakage during postburn acceptance testing.	Leakage was caused by a scratch on the Teflon seal which existe at assembly.	This problem is not considered a failure since the level of leakage (14.5 cc/hr.) is within the existing specification limits (15 cc/hr. max.). Also, this valve problem was previously found during valve acceptance testing (279-101).
279-112 12-16-65	228685 S/N 085	Fuel valve GN_2 leakage during preburn acceptance testing.	Leakage was caused by surface defects in the Teflon valve seal. The defects were probably caused by entrapped contamination.	
279-113 12-8-65	228687 S/N 0069	Fuel valve closing response on automatic coil was slow at postburn acceptance testing.	Postburn test tolerances were not compatible with design tolerances and test instrumentation variations.	Postburn tolerances were increased.
279/M-052 1-18-66	228687 S/N 0083	Combustor seal leakage at postburn acceptance testing.	Not established, as leakage could not be repeated.	It was concluded that this problem was a malfunction of the test.
8417-005 4-25-66	228687 S/N 0142	Combustor seal leakage at postburn acceptance testing.	Leakage was caused by Vibroetch bolt hole identification marks on the attach ring in the area of the bolt head bearing surface.	Other parts with the same problem would be found at postburn acceptance testing. Also the low leakage level is a non-critical problem.
8417/M-088 8417/M-099 4-28-66	228685 S/N 178	Oxidizer valve GN_2 leakage during preburn acceptance testing.	Leakage was caused by an inadequate teflon sealing surface such that a seal was not effected around the entire circumference.	Although the valve passed the leakage test as a valve, the defect was detected during the preburn acceptance testing.
8417/M-092 8417/M-124 5-18-66	228685 S/N 1062	Valve mismatch due to a shift in the oxidizer valve opening response characteristics, and oxidizer valve GN_2 leakage during preburn acceptance testing.	The shift in valve response and the valve leakage were caused by lack of contact between the pintle and the teflon seal around the entire circumference. A depression on the pintle sealing surface may have contributed to the leakage.	This valve was acceptance tested and then used in a valve low voltage test program. The problem was detected during subsequent preburn acceptance testing after assembly of the valve to the engine. The valve completed 1200 cycles without indication of leakage.

TABLE III (continued)

SUMMARY OF R-4D ENGINE PROBLEMS EXPERIENCED DURING ACCEPTANCE TESTING
(ONLY FAILURES OF PREVIOUSLY ACCEPTABLE FUNCTIONS ARE INCLUDED)

FMR NO. DATE OF FAILURE	P/N S/N	FAILURE MODE	CAUSE OF FAILURE	REMARKS
8417-009 9-21-66	228687 S/N 0299	Low water flow through the oxidizer injector system during postburn acceptance testing.	Flow restriction was caused by Braycote contamination.	Failure to pass the water flow acceptance test requirement is not assessable to engine reliability since the burn O/F ratio was acceptable. Braycote has been replaced with a less contaminating lubricant for most engine requirements.
8417-012 1-17-67	228687 S/N 0436	Oxidizer valve GN_2 leakage during postburn acceptance testing.	Leakage was caused by surface defects in the Teflon valve seal. The defects were made by metal slivers entrapped between the armature pintle and valve seat. The slivers came from the seat retainer due to abnormal armature-retainer contact.	An adverse stack-up of print tolerances, in conjunction with a .001 dimensional error on the retainer, allowed the abnormal armature-retainer contact.
8417-013 1-31-67	228687 S/N 0447	A combustor attach bolt was found broken at postburn acceptance test.	The combustor attach bolt broke during heat soak-back after the 50 second engine acceptance test burn run due to an internal crack in the bolt. The crack was caused by overrolling during bolt fabrication.	X-ray was added to the bolt inspection to detect other possible similar defects. The acceptance test 50 second burn run represents the most severe stress condition the combustor attach will see in service after installation. Also, one combustor attach bolt failure will not result in engine failure.
8417-014 3-2-67	228687 S/N 0468	Low water flow through the oxidizer injector system during postburn acceptance testing.	Flow restriction was caused by Braycote contamination.	Failure to pass the water flow acceptance test requirement is not assessable to engine reliability since the burn O/F ratio was acceptable. Braycote has been replaced with a less contaminating lubricant for most engine requirements.
329-109 11-27-67	228687-519 S/N 1099	Low water flow through the oxidizer injector system during retest subsequent to acceptance test after sediment strainer retrofit of this engine.	Decrease in flow was caused by rotation of the sediment strainer. Installation of sediment strainers in the engines caused a slight increase in the total variability of flow rates.	
8428-016 8-7-68	228687-517 S/N 1317	Oxidizer valve GN_2 leakage during thrust stand build-up prior to the burn acceptance test.	Leakage was caused by entrapment of a large metal particle between the armature pintle and the valve seat. The source of the particle was not found but it was established to be foreign to the engine.	

TABLE IV

SUMMARY OF R-4D ENGINE PROBLEMS EXPERIENCED DURING FIELD USAGE

FMR NO. DATE OF FAILURE	P/N S/N	FAILURE MODE	CAUSE OF FAILURE	REMARKS
CR-056 8-15-66	228687 S/N 0055	Low flow through fuel injector system during customer checkout at Cape Kennedy.	Low flow was caused by a piece of nylon plastic contamination caught in the injector preigniter tube.	
CR-057 9-11-66	227895 S/N 1025	Suspected fuel valve response failure during customer testing at White Sands.	The failure was not repeated and the indication of failure was probably a malfunction of instrumentation or set-up.	
CR-072 2-1-67	227889 S/N 1007	Fuel valve GN_2 leakage during customer checkout at GAEC.	The cause of leakage was not established but was probably minor surface defects in the Teflon seal or contamination.	The valve leakage was within specification limits when investigated.
CR-073 2-1-67	227889 S/N 1018	Oxidizer valve GN_2 leakage during customer checkout at GAEC.	The cause of leakage was not established but was probably minor surface defects in the Teflon seal or contamination.	The valve leakage was within specification limits when investigated.
CR-075 12-4-67	228687 S/N 0083	Fuel valve GN_2 leakage during customer checkout at KSC, Florida on spacecraft 020.	The valve leakage was caused by the entrapment of white "torque striping" paint between the armature pintle and the valve seat.	
CR-076 1-8-68	228687-519 S/N 1081	Broken oxidizer valve mounting screw was found during customer assembly of a propellant line to the engine at GAEC.	The broken screw was found to be a defective part in that the pilot hole for the internal wrenching hex in the screw head had been drilled too deep.	To insure that the reliability status of other existing engines was not affected, a reinspection of the hex pilot-hole depth in the oxidizer valve screws of all engines was conducted. Also, this characteristic was redefined as critical requiring 100% inspection for subsequently fabricated parts.
CR-078 3-6-68	228687-519 S/N 1089	Low fuel preigniter flow was indicated during customer checkout at GAEC.	The indicated low flow was caused by an averse dimensional stackup of the engine relative to flow sensor unit. This design incompatibility allowed improper positioning of the flow sensor probe relative to the preigniter doublet exit face.	
CR-079 6-5-68	228687 S/N 0137	During the tear down inspection for refurbishment of the engine, a flat metal stringer was found attached to the oxidizer valve seat-retainer.	This discrepancy occurred during radiusing of the sharp edge on the retainer at the original fabrication.	No functional problem resulted due to this discrepancy. It was considered only as a potential failure mechanism.
CR-080 6-13-68	228687 S/N 0341	During the tear down inspection for refurbishment of the engine, a 44 micron glass bead was found embedded in the fuel valve seat teflon seal.	The glass bead contamination may have been introduced from either TMC or NR/SD operations. It was concluded that this glass bead was not detrimental to the valve function.	Both TMC and NR/SD have discontinued the use of glass beads in the processing of parts for the Service Module Reaction Control System.

TABLE IV (continued)

SUMMARY OF R-4D ENGINE PROBLEMS EXPERIENCED DURING FIELD USAGE

FMR NO. DATE OF FAILURE	P/N S/N	FAILURE MODE	CAUSE OF FAILURE	REMARKS
CR-081 10-15-68	228687-519 S/N 1117	Engine was rejected from a LM 4 cluster due to a small pimple observed on the inside of the combustion chamber.	The pimple was a minor anomaly in the disilicide coating about .020" x .025" x .003" above the surface. The coating pimple resulted from a small surface indentation or pit in the parent metal.	The anomaly in question was known to exist during fabrication and was considered acceptable. reevaluation of the condition resulted in the same conclusion.
CR-082 11-1-68	228687-517 S/N 0415	During check out prior to retrofit, the insulation resistance test indicated an intermittent short in the fuel valve direct coil to case.	A hole was found in the insulation on the black lead to the fuel valve. Repeated high voltage tests had caused a leak path recorded at 28,000 ohms.	No functional degradation would result with the 28,000 ohm leakage path. The postburn test prior to shipment verified that the valve was acceptable at that time and would not have had below spec. insulation resistance except for subsequent checks.
CR-083 10-7-68	228687-517 S/N 1053	The fuel valve closing response was slightly slow during check out after return of the engine for strainer retrofit.	The cause of the indicated slow response could not be established. The condition occurred only once and could not be repeated.	The slight out of specification closing response indicated was not significant relative to engine performance.
CR-084 10-14-68	228687-517 S/N 0380	The fuel valve closing response was slightly slow during check out after return of the engine for strainer retrofit.	The slow response was caused by scored surfaces on the armature flutes and the internal diameter of the valve spool body. The scoring was probably caused by contamination.	The slight out of specification closing response was not significant relative to engine performance.
CR-085 1-8-69	228687-519 S/N 1046	The oxidizer valve closing response was slightly slow during checkout at GAEC test facility.	The cause of the indicated slow response could not be established. The condition could not be duplicated at TMC or GAEC and investigation revealed no discrepant conditions in the valve.	The slight out of specification closing response was not significant relative to engine performance.

$$R_{\gamma} = e^{-t/M_{\gamma}}$$

where: R_{γ} = lower γ confidence level of engine reliability

t = mission duty cycle = 5,518 cycles

$M_{\gamma} = 2T/X^2_{1-\gamma,2r+2}$ and is the lower γ confidence limit on MTBF

T = cumulated engine cycles = 1,412,802

γ = confidence level

r = number of assessable failures - assume zero

$X^2_{1-\gamma,2r+2}$ = Chi Square value exceeded with $1-\gamma$ probability for 2r+2 degrees of freedom (obtained from tables of the Chi Square distribution).

Reliability = 0.9973 at 50% confidence

Reliability = 0.9910 at 90% confidence

Reliable engine operating life of 1,000 seconds burn time and 10,000 operational cycles was successfully demonstrated during the Qualification Test Program. Each of the five engines completed more than 1,000 seconds burn time and more than 10,000 operational cycles after Acceptance testing. The average operation for these engines was 1,462 seconds and 15,724 cycles. In addition, some engines and valves have been cycled in propellants over 100,000 times without indication of degradation. Lunar Orbiter and Apollo flight successes as shown in Table I adds considerable confidence to engine reliability.

Of all the failures summarized in Tables II, III, and IV, there are several cases of valve leakage where nonassessability to engine reliability cannot be proven.

These valve leakage problems were caused by two basic conditions. Particulate contamination causes valve leakage by holding the valve pintle away from the Teflon seal when contamination is entrapped or by making slight surface defects in the form of scratches, gouges or depressions. A condition of wear or seat fabrication variations may cause limited contact between the pintle and the Teflon seat. Subsequent minor surface defects described above may result in leakage.

TABLE V

VALVE LEAKAGE FAILURES WHICH WERE GIVEN ADDITIONAL CONSIDERATION IN THE RELIABILITY ASSESSMENT

DATE OF FAILURE	FMR NUMBER	GN_2 LEAKAGE RATE CC/HR	VALVE CYCLES AT FAILURE	TYPE OF USAGE
12-16-65	279-112	6,000	308	Acceptance Test
3-31-66	279-117	850	30,612	TMC Test Program
4-28-66	8417/M-088	Large(not recorded)	336	Acceptance Test
5-18-66	8417/M-092	180	1,263	Acceptance Test
9-6-66	329-054	Minor Fuel Leakage	3,843	TMC Test Program
10-11-66	329-057	Minor Ox. Leakage	21,565	TMC Test Program
12-7-66	329-077	1,200	12,818	TMC Test Program
12-7-66	329-078	2,400	5,137	TMC Test Program
1-6-67	329-083	252	2,229	TMC Test Program
1-17-67	8417-012	18	51	Acceptance Test
3-6-67	329-098	Minor Ox. Leakage	320	TMC Test Program
3-22-67	329-103	133	10,899	TMC Test Program
3-7-68	329/M-224	720	3,099	TMC Test Program
2-1-67	CR-072	480	1,190	Customer Checkout
2-1-67	CR-073	510	1,541	Customer Checkout